

University of Nebraska - Lincoln

DigitalCommons@University of Nebraska - Lincoln

Theses, Dissertations, and Student Research from
Electrical & Computer Engineering

Electrical & Computer Engineering, Department of

7-2014

RELIABILITY MODELING AND EVALUATION OF DISTRIBUTED ENERGY RESOURCES AND SMART POWER DISTRIBUTION SYSTEMS

Salman Kahrobaee

University of Nebraska-Lincoln, skahrobaee@huskers.unl.edu

Follow this and additional works at: <http://digitalcommons.unl.edu/elecengtheses>

Kahrobaee, Salman, "RELIABILITY MODELING AND EVALUATION OF DISTRIBUTED ENERGY RESOURCES AND SMART POWER DISTRIBUTION SYSTEMS" (2014). *Theses, Dissertations, and Student Research from Electrical & Computer Engineering*. 54.

<http://digitalcommons.unl.edu/elecengtheses/54>

This Article is brought to you for free and open access by the Electrical & Computer Engineering, Department of at DigitalCommons@University of Nebraska - Lincoln. It has been accepted for inclusion in Theses, Dissertations, and Student Research from Electrical & Computer Engineering by an authorized administrator of DigitalCommons@University of Nebraska - Lincoln.

RELIABILITY MODELING AND EVALUATION OF DISTRIBUTED ENERGY
RESOURCES AND SMART POWER DISTRIBUTION SYSTEMS

by

Salman Kahrobaee

A DISSERTATION

Presented to the Faculty of
The Graduate College at the University of Nebraska
In Partial Fulfillment of Requirements
For the Degree of Doctor of Philosophy

Major:

Electrical Engineering

Under the Supervision of Professor Sohrab Asgarpoor

Lincoln, Nebraska

July, 2014

RELIABILITY OF DISTRIBUTED ENERGY RESOURCES AND
SMART POWER DISTRIBUTION SYSTEMS

Salman Kahrobaee, Ph.D.

University of Nebraska, 2014

Adviser: Sohrab Asgarpoor

From the date of the very first electrical network until now, power system engineers have always been concerned with supplying electricity to the loads reliably. A reliable power system may be realized as an art of determining a balance between the customer satisfaction and the associated expenses. As power systems are being upgraded with today's communication and control technologies and additional uncertainties are introduced through integration of intermittent generation units, it is critical to develop new models, methods, and indices to evaluate and improve the future power system reliability.

This dissertation has a twofold objective. First, the reliability of distributed and renewable energy resources as an expanding and critical contributor to the future power system is analyzed. The power generated from renewable generation units, such as wind turbines, is stochastic and difficult to predict. Therefore, a number of analytical, simulation, and hybrid methods are proposed for modeling and reliability assessment of renewable generation in different operation conditions, considering aging of the equipment, maintenance, etc. The second objective of this dissertation considers a bigger

scope of future power distribution systems and oversees the urge for improving the reliability and availability of electricity supplied to the customers.

Thus, three simulation models of a smart power distribution system have been developed using Multiagent systems, Monte Carlo simulation, and power system software. These models include the impact of several components, such as renewable generation, energy storage, customer power interactions, demand side management, etc., and are used to evaluate and improve power system reliability. The reliability of the power system is evaluated using typical system-perspective indices as well as a number of newly defined indices from the customers' perspective. In addition, these models are used to determine the optimum capacities of renewable generation and storage system in order to supply electricity reliably. The work in this dissertation can be expanded to incorporate communication and control system reliability as well as cyber security for future power system studies.

To My Love,

Tarlan

ACKNOWLEDGEMENT

I would like to express my sincere gratitude to my advisor, Dr. Sohrab Asgarpoor for all his support and care about my academic progress and personal life. In the course of this dissertation, Dr. Asgarpoor helped me to learn more and guided me to develop critical thinking skills. He gave me an insight into power system reliability, and encouraged me to look for research and internship opportunities and take courses from Computer Science and Industrial Engineering departments which expanded my horizon and assisted me gain knowledge about different aspects of future power systems. Not only was Dr. Asgarpoor my academic mentor, but he and his lovely wife, Dr. Jena Shafai, were also our great friends, family, and so hospitable that my wife and I barely felt living far away from our families.

I am also grateful to my committee members, Dr. Hudgins, Dr. Qiao, Dr. Soh, and Dr. Vuran, for their support and guidance. I had a privilege to take the *Wind Energy* course with Dr. Hudgins and the *Computational Intelligence* course with Dr. Qiao. The content of these courses were valuable in model development and studies provided in this dissertation. In addition, taking the *Sensor Networks* course instructed by Dr. Vuran assisted me to realize the wide range of applications for communication networks and network of sensory devices, e.g. in the smart grid. Besides, I learned a lot about multiagent systems from Dr. Soh, whose practical course and inspiring personality were my main drivers to work on the current subject for this dissertation. Next, I would like to

thank the staff of the Department of Electrical Engineering, specifically Cheryl Wemhoff who has always been caring and helpful to all graduate students, including me.

I appreciate all the guidance, funding and research opportunities Dr. Algrain provided during my study. In addition, I am thankful to Nebraska Center for Energy Sciences Research for providing assistantship through research projects.

In the end, I can't find words to express my appreciation to my best friend, my companion, and my soulmate, Tarlan Razzaghi; thank you for being a perfect spouse. My heartfelt thanks go to my parents-in-law, Dr. Adel Razzaghi and Soosan Saadati, who have always supported and encouraged us from the first day of this journey. I am also thankful to my parents Marzyeh Shahhosseini, and Firooz Kahrobaee for their prayers, and my friend, Ali Rajabzadeh, for his assistance. Last, I extend a special thanks to all our Persian friends we met in Lincoln, and will always remember all the enjoyable moments we shared together.

TABLE OF CONTENTS

ACKNOWLEDGEMENT	IV
TABLE OF CONTENTS	VI
LIST OF FIGURES	X
LIST OF TABLES	ERROR! BOOKMARK NOT DEFINED.
1. INTRODUCTION	1
1.1 Transitioning Toward an Advanced Power System	2
1.2 Reliability of Renewable Generation	5
1.3 Reliability of the Future Power System	7
1.4 Publications	11
1.5 Overview of the Dissertation.....	13
2. RELIABILITY OVERVIEW	15
2.1 Reliability Concept in Power System.....	16
2.2 Reliability Evaluation Methods.....	21
2.2.1 Fault Tree Analysis (FTA)	22
2.2.2 Failure Mode, Effect, and Criticality Analysis (FMECA)	22
2.2.3 Markov Processes.....	24
2.2.4 Other Analytical Methods	25
2.2.5 Monte Carlo Simulation	26
3. RELIABILITY OF	
DISTRIBUTED ENERGY RESOURCES	28
3.1 Introduction to Distributed Energy Resources (DER)	29
3.2 DER Reliability Assessment (e.g. wind turbines).....	31
3.2.1 Fault Tree Analysis	35
3.2.2 Failure Mode, Effect, and Criticality Analysis (FMECA)	37

3.2.2.1	Proposed RB-FMEA Process	39
3.2.2.2	RB-FMEA for Wind Turbines	40
3.2.3	Markov Processes.....	45
3.2.3.1	Short-term study.....	51
3.2.3.2	Long-term study	52
3.2.4	Monte Carlo simulation.....	54
3.2.5	Hybrid analytical-simulation approach	57
3.2.5.1	Analytical approach.....	61
3.2.5.2	Simulation approach.....	64
4.	RELIABILITY OF	
	SMART POWER DISTRIBUTION SYSTEM.....	66
4.1	Introduction to Smart Power Distribution Systems.....	67
4.2	Modeling of Smart Distribution Systems (SDS).....	68
4.2.1	SDS model-I.....	69
4.2.1.1	Electrical grid and electricity rate	71
4.2.1.2	Customers.....	72
4.2.1.3	Renewable generation and storage system.....	74
4.2.1.4	Demand side management (DSM)	75
4.2.2	SDS model-II.....	83
4.2.2.1	Electrical grid and electricity rate	84
4.2.2.2	Customers.....	86
4.2.2.3	Renewable generation and storage system.....	87
4.2.2.4	Demand side management (DSM)	89
4.2.3	SDS model-III	93
4.2.3.1	Electrical grid	93
4.2.3.2	Customers.....	94
4.2.3.3	Demand side management (DSM)	95
4.3	SDS Reliability with Demand Side Management	96
4.4	SDS Reliability with Energy Storage System	99
4.5	Optimum DER Capacity for Reliable SDS	103
4.6	SDS Reliability with Active Customer Interactions	110
4.6.1	Outage Response	111

4.6.2	Reliability Assessment Method.....	114
4.6.3	Reliability Evaluation Indices	115
4.7	Summary of the models and proposed studies	116
5.	SYSTEM STUDIES.....	118
5.1	Reliability of Distributed Energy Resources (Case study: wind turbines) 119	
5.1.1	Fault Tree Analysis	119
5.1.2	Failure Mode, Effect, and Criticality Analysis (FMECA)	120
5.1.2.1	Sensitivity Analysis.....	123
5.1.3	Markov Processes.....	125
5.1.3.1	Short-term study.....	125
5.1.3.2	Long-term study	126
5.1.4	Monte Carlo simulation.....	128
5.1.5	Hybrid analytical-simulation approach	130
5.1.5.1	Analytical approach.....	132
5.1.5.2	Simulation approach.....	134
5.2	Reliability of Smart Power Distribution System.....	138
5.2.1	SDS reliability with demand side management	138
5.2.1.1	Base case reliability.....	140
5.2.1.2	Reliability with energy conservation.....	140
5.2.1.3	Reliability with load shifting.....	141
5.2.1.4	Sensitivity analysis.....	141
5.2.2	SDS reliability with energy storage system	144
5.2.2.1	Base case reliability.....	147
5.2.2.2	Sensitivity Analysis.....	148
5.2.2.3	Reliability-based sizing of energy storage system	149
5.2.3	Optimum DER capacity for reliable SDS.....	151
5.2.3.1	Sensitivity to the cost of DER.....	152
5.2.3.2	Sensitivity to electricity purchase rate	154
5.2.4	SDS reliability with active customer interactions	155
5.2.4.1	Reliability analysis with residential customers	157
5.2.4.2	Reliability analysis with residential, commercial, and industrial customers.....	159
5.2.4.3	Sensitivity analysis with wind and PV generation	161

6. CONCLUSION AND FUTURE WORK	165
6.1 Conclusion.....	166
6.2 Recommendation for the Future Work.....	170
REFERENCE	173

LIST OF FIGURES

Figure 1.1 Power flow among sectors of a conventional power system.....	2
Figure 1.2 Power flow among sectors of a smart grid	4
Figure 2.1 Reliability concept from different perspectives.	18
Figure 2.2 Hierarchical levels for power system reliability assessment.	19
Figure 3.1 Failure rate and downtime for different parts of wind turbine	34
Figure 3.2 Fault Tree for a typical wind turbine	36
Figure 3.3 FMECA process for a typical wind turbine.....	38
Figure 3.4 Study steps of RB-FMEA for a wind turbine	41
Figure 3.5 Wind turbine hierarchy for RB-FMECA.....	42
Figure 3.6 Rate diagram for the wind farm Markov model.....	46
Figure 3.7 Power curve of a 1500kW wind turbine.....	48
Figure 3.8 Power system model for reliability study of the wind farm	48
Figure 3.9 Procedure of wind farm reliability calculation using Markov Processes	50
Figure 3.10 Wind turbine model for output power estimation in Arena software.....	55
Figure 3.11 Failure and repair model of main subassemblies of a wind turbine in Arena	57
Figure 3.12 State transition diagram for SMDP study of deteriorating equipment	62
Figure 3.13 State transition diagram for MCS-based modeling of deteriorating equipment	65
Figure 4.1 Different entities of SDS model-I.....	71
Figure 4.2 The features of an active customer agent in SDS model-I.	73
Figure 4.3 Illustration of the <i>Utility based method</i> for DSM.....	81
Figure 4.4 Illustration of the <i>Average Deficit method</i> for DSM.....	81

Figure 4.5 Flowchart of the proposed <i>Average Deficit method</i> for DSM.....	83
Figure 4.6 Mean EPR and 90% confidence interval for the fitted probability distributions	85
Figure 4.7 Mean base load and 90% confidence interval for the fitted normal distributions	87
Figure 4.8 Mean wind speed and 90% confidence interval for the fitted Weibull distributions.....	88
Figure 4.9 Flowchart of the rule-based DSM	91
Figure 4.10 Typical variables determined and used by the DSM within a day	92
Figure 4.11 One-line diagram of a power distribution system model in DIgSILENT	94
Figure 4.12 A typical load curve in SDS model-III.....	95
Figure 4.13 Load profiles with different levels of energy conservation.....	95
Figure 4.14 Load profiles with different levels of load shifting.....	96
Figure 4.15 Flowchart of the study to determine the optimum storage capacity.....	102
Figure 4.16 The optimization process incorporating the rule-based DSM of SDS model-II	107
Figure 4.17 Main entities of an SDS model used for reliability evaluation impacted by instances of contingencies A, B, and C.....	111
Figure 4.18 Potential sequential requests of a customer agent from its neighbors during an outage.....	112
Figure 5.1 Change in reliability of the wind turbine within a week	120
Figure 5.2 Snapshot of the spreadsheet for RB-FMEA Analysis	121
Figure 5.3 RPN and CPN for major parts of the study wind turbine.....	122
Figure 5.4 AFC and CPN for major parts of the wind turbine	122
Figure 5.5 Sensitivity of the turbine AFC to the additional imposed delay	123
Figure 5.6 Sensitivity of the turbine AFC to the EPR and CF.....	124
Figure 5.7 Failure cost with 10% improvement in the turbine's fault detection	124

Figure 5.8 Hourly wind farm power production vs. load demand with 7 (a) and 3 (b) initially available wind turbines	126
Figure 5.9 Long-run availability of the wind farm	127
Figure 5.10 Probability distribution of the wind turbine output power states	127
Figure 5.11 Optimum maintenance decisions at different operating states: a) <i>D1</i> , b) <i>D2</i> and c) <i>D3</i> using SMDP. d) Wind turbine availability and total system gain with various maintenance frequencies	133
Figure 5.12 Expected gain of the wind turbine with different maintenance policies.	135
Figure 5.13 Expected availability of the wind turbine with different maintenance policies.	135
Figure 5.14 Expected availability of the wind turbine with different durations of maintenance.....	136
Figure 5.15 Expected wait time before repair with different numbers of turbines on a wind farm.	137
Figure 5.16 Expected availability of the wind turbine based on the number of turbines on the wind farm.	137
Figure 5.17 Loadings of power lines and transformers with different capacities at the peak load.	142
Figure 5.18 SAIFI with different percentage of load shifting and system capacity increments.	143
Figure 5.19 SAIDI with different percentage of load shifting and system capacity increments.	143
Figure 5.20 Single line diagram of the case study with four integrated DERs.....	144
Figure 5.21 Cumulative percentage of LP1 active and reactive power binned to define load states, with DER in the system (base case).	145
Figure 5.22 Load interruption cost function for the customers.	146
Figure 5.23 Cost analysis with different capacities of standby storage at LP1.	148
Figure 5.24 Cost analysis with different capacities of standby storage at all the DER-integrated load points.	149

Figure 5.25 Optimum standby storage capacities at all of the DER-integrated load points.	150
Figure 5.26 Optimum size of battery (a) and wind generation (b), with different levelized costs of wind generation and battery.....	153
Figure 5.27 Minimum electricity cost of the household with different levelized costs of wind generation and battery.....	153
Figure 5.28 Sensitivity of wind generation-battery capacities (top) and the electricity cost of the home (bottom) to the change of average EPR.	154
Figure 5.29 Average load profiles for residential, commercial, and industrial loads.	156
Figure 5.30 Typical average PV and wind generation profiles.	157
Figure 5.31 SDS-perspective reliability indices with different percentages of residential customers owning generation-battery systems and neighborhood electricity trading option.	158
Figure 5.32 SDS-perspective reliability indices with different percentages of residential/commercial/industrial customers owning generation-battery systems and neighborhood electricity trading option.	159
Figure 5.33 SAIDI of the SDS impacted by different capacities of renewable generation-storage and generation technologies.	162
Figure 5.34 SAIFI of the SDS impacted by different capacities of renewable generation-storage and generation technologies.	163
Figure 5.35 Comparison of wind and PV impact on VOLL in load sectors.....	164

LIST OF TABLES

Table 3.1 Different types of wind generation systems.....	33
Table 3.2 General set of Wind turbine sub-assemblies and main parts	43
Table 3.3 Root causes of the wind turbine failure modes.....	44
Table 3.4 Major detection methods of the wind turbine failure modes	45
Table 4.1 Models developed and their features for different types of SDS studies.....	117
Table 5.1 Failure rates for main subassemblies of a wind turbine.....	119
Table 5.2 Wind farm availability with respect to initial conditions and time.....	125
Table 5.3 LOLP, LOEE and ESWE within a week	126
Table 5.4 Steady state probabilities of the wind farm model	126
Table 5.5 LOLP, LOEE and ESWE for one year	128
Table 5.6 Average outage duration of a wind turbine’s subassemblies.....	129
Table 5.7 Average outage duration of 7turbines’ subassemblies	130
Table 5.8 Expected reward/penalty of being in each state.....	131
Table 5.9 Transition probabilities after maintenance	131
Table 5.10 Transition rates among the states.....	132
Table 5.11 Distribution System Components	139
Table 5.12 Input failure and repair data for the reliability analysis.....	139
Table 5.13 Reliability indices for the base case study	140
Table 5.14 Reliability indices with different load scaling factors	140
Table 5.15 Reliability indices with different percentages of load shifting.....	141
Table 5.16 Distribution system statistics	145
Table 5.17 Load flow results of the distribution system.....	146

Table 5.18 Input data for the reliability analysis	146
Table 5.19 System reliability results for the base case study	147
Table 5.20 Load point reliability results for the base case	147
Table 5.21 Load point reliability results with integraiton of the optimum standby energy storage systems	150
Table 5.22 L2 Loads considered for the case study.....	151
Table 5.23 Input parameters of the base case study.....	152
Table 5.24 Parameters used for the case studies.....	156
Table 5.25 Customer perspective reliability with different percentages of them owning generation-battery systems, and neighborhood electricity trading option.	159
Table 5.26 Reliability of the residential/commercial/industrial customers with different percentages of owning generation-battery systems, and neighborhood trading options.	160

CHAPTER 1

INTRODUCTION

1.1 Transitioning Toward an Advanced Power System

1.2 Reliability of Renewable Generation

1.3 Reliability of the Future Power System

1.5 Publications

1.4 Overview of the Dissertation

1.1 Transitioning Toward an Advanced Power System

As a critical infrastructure, the power grid system needs continuous adoption of technological advancements for higher efficiency in terms of operation, reliability, and cost. However, due to the sheer size of the power system, the transition towards adopting new innovations and state of the art technologies has been slow. The operation of power systems with the conventional infrastructure would result in higher complexity, less efficiency, and difficulty to sustain the future system demand. A North American Electric Reliability Corporation (NERC) study showed that forecasted demand for electricity might exceed projected available capacity in the U.S. without a major action [1]. As the electricity demand keeps growing and the system is more pushed toward its boundary operation, system reliability has also become a critical concern.

In fact, a conventional power system is centralized in terms of control and transmission of electricity, in a sense that, the energy produced by the generators in power plants flows over the grid from transmission and distribution system down to the consumers.

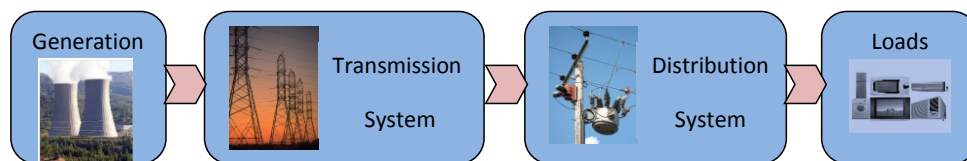


Figure 1.1 Power flow among sectors of a conventional power system

Therefore, a failure or an incident in any of these segments, as well as operation, and control of a conventional power system, could impact a large number of end users and assets, and cost a large amount of money. In fact, interruptions in the electricity

supply directly or indirectly cost American consumers an estimated \$150 billion a year [2]. There have been five massive blackouts over the past 40 years, three of which have occurred in the past decade. More blackouts and brownouts are occurring due to the slow response times of mechanical switches, lack of automated analytics, and lack of situational awareness [2], [3]. On the other hand, distributed generation, management, and control may contribute to mitigate these effects by allowing higher redundancy and faster control over the energy generated and consumed in the network.

The concept of the smart grid, as an advanced power system, is generally accepted to indicate the integration of communication, computing, control, and information technologies to enhance the reliability, flexibility, efficiency, and sustainability of the electricity grid [4]. Restrictions of energy resources, aging infrastructure, environmental concerns, and increasing expectations of customers are some of the drivers of the transition toward a smarter electrical grid [5]. The advent of the smart grid will influence planning, operation, and maintenance of the power system, which is expected to become more adaptive, predictive, and distributed. Achieving this will require new infrastructure enabling the participation of active customers, accommodation of distributed generation and storage options, and incorporation of new products and intelligent control strategies [6]. The concept of intelligence in today's power systems is centered on the idea of pushing sensory and analytic capabilities further down the system hierarchy. In a smart grid, more can be done locally at the substation or even device level, allowing operators and computing resources in the control center to be more effectively utilized.

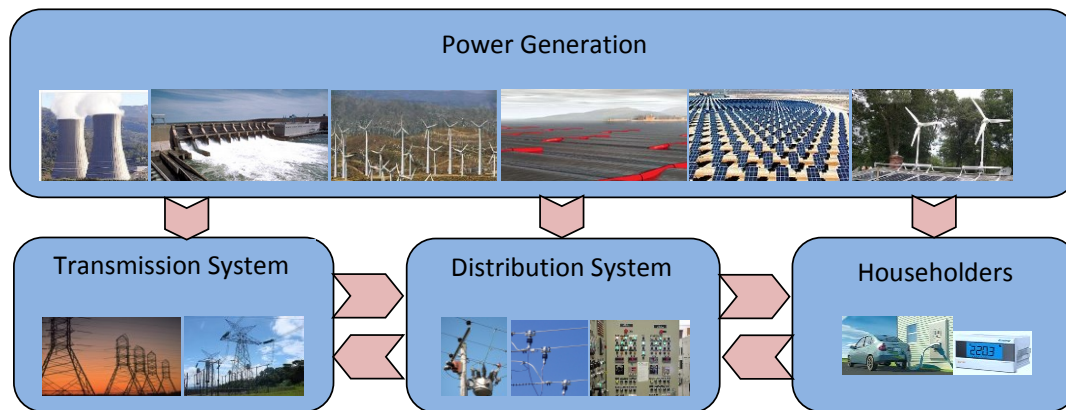


Figure 1.2 Power flow among sectors of a smart grid

In contrast to a conventional power system, electrical power may flow in different directions among assorted sectors of a smart grid. Renewable power generation, from a small rooftop photovoltaic system supplying a single residential property up to megawatt wind farms connected to the medium voltage system, can be integrated into this power grid. Incorporation of bidirectional communication and power flow in a smart grid provides an opportunity for both the electricity providers and customers to efficiently use their assets and cut down on their costs through demand side management [7], real-time pricing [8], power sell-back opportunities [9], etc. Indeed, electricity customers of the smart power distribution systems may no longer be perceived as passive loads. Installation of distributed energy resource-based generation, storage devices, and smart appliances will enable customers to function as integrated entities who provide support to the grid by contributing to peak-load shaving, ancillary services, reliability improvement, and investment postponement [10].

Meanwhile, regardless of all the changes and restructuring required for the transition toward a smarter grid, the main concern and key goal of power systems remain untouched, which is to provide electricity to the customers reliably and economically.

1.2 Reliability of Renewable Generation

The advent of intelligent electrical networks to allow efficient use of energy resources, reduce carbon emissions and increase sustainability is a key feature of the smart grid and promise of a greener future [11]. Due to the limited resources of the fossil fuels, the renewable resources, such as wind and solar energy, have been the subject of research and experiment from a long time ago [12]. Although the current grid still relies heavily on traditional fossil fuels for power generation, the environmental concerns and their associated cost penalties [13], as well as technological advances and device cost reduction in the past decade, have enabled a great potential for the substantial growth in utilizing renewable energy resources [14]. One of the main issues regarding integration of large capacity of renewable generations, such as wind generation and photovoltaic system, is their impact on reliability and availability of the power system [15], [16].

In general, Reliability is defined as the probability that a component or system will perform a required function, for a given period of time, when used under stated operating conditions. In power industry, there are various indices used to measure the reliability of systems. As an important index of reliability, Availability is the probability that a system or component is performing its required function at a given point in time when operated and maintained in a prescribed manner [17].

As the percentage of renewable generation capacity is rising, new reliability challenges are introduced in the smart grid. In evaluating the reliability of wind generation, for example, the first concern is about wind turbines themselves which consist of many moving and rotating subassemblies installed at a high elevation. These equipment include blades, rotor, gears and generator which bear more tension and wear during operation compared with conventional generation [15]. In addition, wind turbines may be exposed to the changes in weather as well as extreme weather conditions. Variability of wind speed and direction not only increases the chance of failure due to additional imposing stress on wind turbines' parts but also affects the availability of their output power generation [18]. These effects necessitate probabilistic modeling of wind turbines' operation to include both the turbines and wind speed states. Major factors contributing to the total failure of the turbines have been studied through individual wind turbine reliability modeling [19].

As another example, the reliability of a PV system is also affected by a variety of factors, such as failure of the components, system configuration, the ambient conditions, etc. [20]. Some of these factors may not be the cause for a total failure, but still have a derating impact on the output of a PV system [21]. In fact, any parameter that impacts the output power of a PV system causes a de-rating in its nominal generation, and can potentially degrade its capability to supply the load, and that leads to a reliability issue.

The main parts of a PV system subject to failure are PV modules, inverter, and energy storage system; where, the inverters are the most vulnerable equipment [22]. Moreover, the ambient parameters as the de-rating factors of PV generation impact its

reliability. In fact, the solar irradiance that reaches the horizontal Earth surface is intermittent, and therefore, the output power of a PV is unpredictable [23]. Other ambient factors with derating effect on PV systems are temperature, dust and snow accumulation, shading and cloud cover, etc. [24], [25], [26]. The first part of this dissertation discusses the reliability of renewable generation systems, and specifically wind generation as the example. In addition, different analytical and simulation approaches are used to develop the models necessary for renewable generation reliability evaluation.

1.3 Reliability of the Future Power System

As previously mentioned, the future power system promises the integration of communication and control technologies as well as additional sensitive electronic devices in the network. Moreover, it accommodates new types of loads/generations, such as electric vehicles/distributed generation, etc. [5].

The reliability of an electric grid may be improved as a result of smart grid technologies, such as situational awareness, automated and fast control, and bidirectional communication. On the other hand, an efficient use of assets may push a power system to operating close to the edge, where it will be exposed to higher volatility and its reliability may adversely be affected [27]. Electricity outages are caused by failures in generation, transmission, or distribution systems. However, outages in the electrical distribution system are responsible for most of the hours that electricity is unavailable to customers [28]. So, it is critical to model and study the reliability of distribution systems including future electricity customers.

In fact, the future electricity customers have higher expectations from the power system than before. They demand for higher electric supply reliability, and may choose to actively participate in demand side management (DSM) programs and respond to the electricity rate signals, or even use their distributed energy resources (DER) in order to save on their electricity bills. In a future smart grid, incorporating automated control and communication Infrastructure, an effective customer-initiated DSM can alleviate the peak load and shift part of the demand to off-peak hours, and improve reliability of load supply [7].

The potential impacts of smart grid technologies on the reliability of the power system, for example by improving the outage management process and its control complexities, have been reported in [29]. Also, a reliability perspective of the smart grid has been explored in [27] where the implications of some key factors, such as renewable resources, load management strategies, and storage devices, have been discussed. Reliability studies including the stochastic nature of renewable resources, such as wind or solar energy, or uncertainties related to weather conditions have been reported in the literature [30], [31]. However, these studies do not model a smart grid framework incorporating DER and active customers with a variety of operational options. As such, the “smartness” of such a system is limited due to the lack of options in customer decision making.

The authors in [32] have modeled a distribution system that includes DSM schemes and has shown that a proper management can improve the reliability of the distribution system. However, the DSM schemes defined are for a specific case study,

where the dynamicity and intermittency of the smart grid due to customers' decisions, renewable generation, and storage systems has not been considered. Reliability of a power distribution system, from the system's perspective, has been evaluated in [33]. This model includes a renewable generation and communication system but does not take into account the impacts of DSM and the contribution of customers in reliability evaluation. Other researchers have presented a reliability evaluation approach for power systems using a multiagent system (MAS) [34]. However, in their approach, the agents do not completely model the smart grid entities.

The reliability is also critical in other aspects of a smart grid, such as communication reliability and cyber security. Cyber security is the approach taken towards securing the information that travels through the computer networks and Internet based communications networks. The use of these networks not only makes power systems components interoperable which is central for a smart grid transformation, but also opens the door for malware, viruses, and generally Internet based attacks. That is why Federal Energy Regulatory Commission (FERC) accepted the initial set of Critical Infrastructure Protection (CIP) Reliability Standards developed by the North American Electric Reliability Corporation (NERC) in 2008 [35].

A power system reliable communication and cyber infrastructure should be able to transfer the correct information to the right individuals within a certain allowable time. For example, Advanced Metering Infrastructure (AMI) is an indispensable part of the smart grid and includes smart meters, communication among appliances, meters and the utility, data management, etc. Basically, some of the security challenges for an AMI are

meter authentication in the network, maintaining confidentiality for privacy protection, and providing integrity for future system upgrades [36].

The reliability of the smart grid enabler components such as smart meters, their communication and control have been discussed in the literature [37], [38]. The reliability and risk assessment of the communication and cyber systems are out of the scope of this dissertation; but due to their potential impact on the smart grid reliability, they are essentially considered to be included in the future work.

It is important to note that the advent of smart grid impacts both the utility and customer side of a power distribution system. As the utilities adopt new technologies to establish automated and more efficient operation, the customers also start to take advantage of this new infrastructure, and that will sooner or later change the notion about the customer being electricity consumer only.

Therefore, an effective reliability assessment first requires an inclusive model of the emerging smart grid, accommodating the active customers and their interaction, DER, DSM, etc.; and then, it needs a modified reliability study approach to be used by electric utilities and customers for efficient planning and operation purposes. The uncertainties due to renewable resources, customers' decision making, and their interactions make the modeling and reliability evaluation of the future power distribution systems critical and challenging. None of the aforementioned research studies have developed an inclusive model for reliability analysis that takes the impact of future active customers into account.

Modeling and reliability evaluation of renewable generation systems (e.g. wind turbines) and future power distribution systems including a variety of customers are the

main focus of this dissertation. Here, based on the characteristics of the problem, distributed modeling approaches and simulation methods are essentially used for reliability assessment of the future power systems.

1.4 Publications

The following publications have been worked on in the course of the Ph.D. studies. This dissertation is mainly based on the work in publications 1 to 9 of this list.

1. S. Kahrobaee, R. Rajabzadeh, L.-K. Soh, and S. Asgarpoor, "Reliability assessment of future power distribution systems," submitted to *International Journal of Electrical Power and Energy Systems*, under review.
2. S. Kahrobaee, R. Rajabzadeh, L.-K. Soh, and S. Asgarpoor, "Multiagent study of smart grid customers with neighborhood electricity trading," *Journal of Electric Power System Research*, vol. 111, pp. 123-132, Jun. 2014.
3. S. Kahrobaee, S. Asgarpoor, W. Qiao, "Optimum sizing of distributed generation and storage capacity in smart households," *IEEE Transactions on Smart Grids*, vol.4, no.4, pp. 1791-1801, Dec. 2013.
4. S. Kahrobaee, S. Asgarpoor, "A hybrid analytical-simulation approach for maintenance optimization of deteriorating equipment: Case study of wind turbines," *Journal of Electric Power System Research*, vol. 104, pp. 80-86, Nov. 2013.
5. S. Kahrobaee, S. Asgarpoor, "The effect of demand side management on reliability of automated distribution systems," *IEEE Conference on Technologies for Sustainability*, Sustech, Aug. 2013.

6. S. Kahrobaee, S.Asgarpoor, "Reliability-driven optimum standby electric storage allocation for power distribution systems," *IEEE Conference on Technologies for Sustainability*, SUSTech, Aug. 2013.
7. S. Kahrobaee, R. Rajabzadeh, L.-K. Soh, and S. Asgarpoor, "A Multigent Modeling and Investigation of Smart Homes with Power Generation, Storage, and Trading Features," *IEEE Transactions on Smart Grids*, vol. 4, no.2, pp. 659- 668, Jun. 2013.
8. S. Kahrobaee, S.Asgarpoor, "Risk-Based Failure Mode and Effect Analysis for Wind Turbines (RB-FMEA)", Proceedings of *North American Power Symposium (NAPS)*, Boston, Massachusetts, 2011.
9. S. Kahrobaee, S.Asgarpoor, "Short and long-term reliability assessment of wind farms," Proceedings of *North American Power Symposium (NAPS)*, Arlington, TX, 2010.
10. S. Kahrobaee, S.Asgarpoor, "Optimum Renewable Generation Capacities in a Microgrid Using Generation Adequacy Study" T&D Conference, 2014.
11. S. Kahrobaee, S.Asgarpoor, "Optimum Planning and Operation of Compressed Air Energy Storage with Wind Energy Integration," Proceedings of *North American Power Symposium (NAPS)*, 2013.
12. S. Kahrobaee, M. Can Vuran, "Vibration Energy Harvesting for Wireless Underground Sensor Networks," *IEEE International Conference on Communications*, ICC'13, Budapest, Jun. 2013.

13. Salman Kahrobaee, Marcelo C. Algrain, Sohrab Asgarpoor, “Investigation and Mitigation of Transformer Inrush Current during Black Start of an Independent Power Producer Plant,” vol.5, no.1, pp.1-7, *Journal of Energy and Power Engineering*, Jan. 2013.

1.5 Overview of the Dissertation

The rest of this dissertation is organized as follows:

- Chapter 2 provides a background on reliability concept in power systems from both customer and utility perspectives. This chapter presents some common power system reliability evaluation metrics and a number of analytical and simulation methods used for reliability assessment.
- Chapter 3 discusses the models and methods used for reliability evaluation of distributed energy resources (DER) through an example of wind turbines. This chapter provides an introduction to DERs, and then, describes the models developed based on each analysis technique for wind generation reliability assessment.
- Chapter 4 provides the models and approaches toward reliability evaluation of smart power distribution systems (SDS). This chapter begins with an overview of an SDS and describes three simulation models developed for reliability analysis. Next, the required studies and sensitivity analysis are explained considering different aspects of a smart grid, such as demand management, renewable generation and storage, customer interactions, etc.

- Chapter 5 provides the case studies, results and discussions based on the models explained in the previous chapters. In the first part, the results of reliability evaluation for a single wind turbine or a wind farm are presented. The second part of this chapter presents the results of SDS reliability assessment based on customer and utility side indices along with the discussions on sensitivity analysis.
- Finally, Chapter 6 concludes this dissertation and provides further suggestions and recommendation for the future studies.

CHAPTER 2

RELIABILITY OVERVIEW

2.1 Reliability Concept in Power System

2.2 Reliability Evaluation Methods

2.1 Reliability Concept in Power System

The Reliability of a component or a system is defined as the probability that they perform their assigned task for a given period of time under the operating conditions encountered [17]. In statistics, reliability is often denoted by the survival function calculated using the cumulative distribution function of the failure probabilities, $F(t)$.

$$R(t) = 1 - F(t) = 1 - \int_0^t f(s) ds \quad (2.1)$$

In Eq. 2.1, $F(t)$ represents the probability that a failure happens before time t ; $R(t)$ is the reliability function, and $f(t)$ represents the probability density function of failure occurrence.

Power equipment and power systems are vulnerable to failures occurred due to internal or external sources. The failure of a component, is the inability of a component to perform its intended function at a particular time under specified operating conditions [39]. A failure is specified by its failure rate and repair rate. Failure rate (λ) is reciprocal of the mean time to failure, and it is defined as the number of failures of a component in a given period of time divided by the total period of time that component was operating. Repair rate (μ), on the other hand, is the reciprocal of the mean time to repair, and it is defined as the number of repairs of a component in a given period of time divided by the total period of time that component was being repaired.

Failure rates of deteriorating equipment are typically explained by the “bathtub curve”. The bathtub curve describes product’s lifecycle and consists of three intervals. It starts with an infant mortality period that has a decreasing failure rate followed by a

normal life period, with a low and relatively constant failure rate, and it ends with a wear-out period that represents an increasing failure rate. Based on Eq.2.1, with a constant failure rate and in case the failure of equipment can be shown by exponential distribution, the equipment reliability until time t will be derived from Eq. 2.2.

$$R(t) = 1 - \int_0^t \lambda \cdot e^{-\lambda s} ds = e^{-\lambda t} \quad (2.2)$$

The reliability analysis is an essential study for the design, operation, maintenance, and planning of the power system [28]. For example, with a specific reliability requirement, an optimum maintenance strategy can be determined to minimize the operation cost. In fact, the maintenance influences the deterioration process, failure rate, and reliability of the components and the system, accordingly [40].

The concept of reliability in the power system may be interpreted using three different categories: 1) *adequacy*, as the capability of the system to meet its demand at all times considering scheduled and expected unscheduled outage of the elements; 2) *security*, as the ability of the system to withstand disturbances such as a short circuit; and 3) *quality*, regarding voltage condition, and harmonic characteristics, etc. [41].

It should be noted that the definition of reliability may vary from different perspectives. The two main perspectives for reliability consideration of a power system are *customer perspective* and *utility perspective* [42]. The customers care about quality of service and being able to use their appliances any time needed during a day. Therefore any interruption in service is undesirable from the customer's perspective. The utility's perspective of reliability considers both the service reliability at the load points and

reliability of the supply side which may include the reliability of generation, transmission and distribution assets, as well [28].

Fig. 2.1 shows provides a summary of the reliability concern from different perspectives [42].

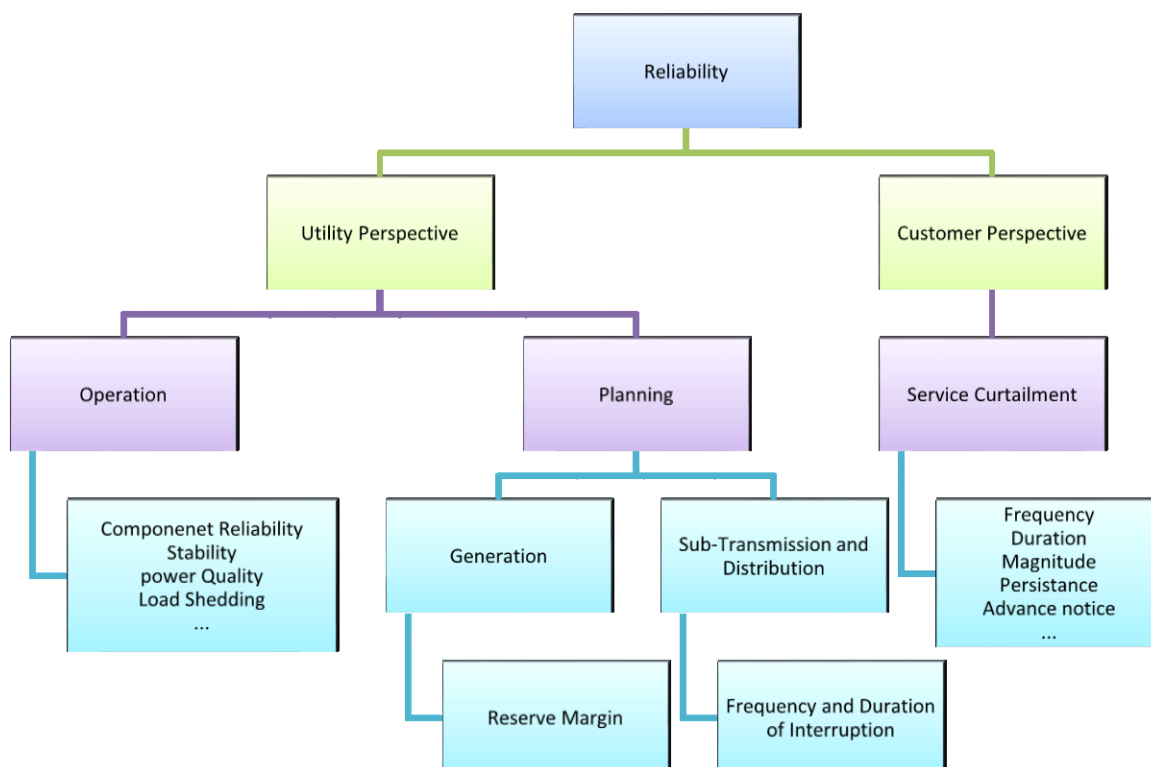


Figure 2.1 Reliability concept from different perspectives.

In order to study the reliability of a power system, three hierarchical levels have been defined [43]. The reliability of the power generation is studied through hierarchical level one (HL1). The reliability of a composite generation and transmission system is studied using HL2. Finally, the reliability of the whole system including generation, transmission, and distribution system is evaluated using HL3.

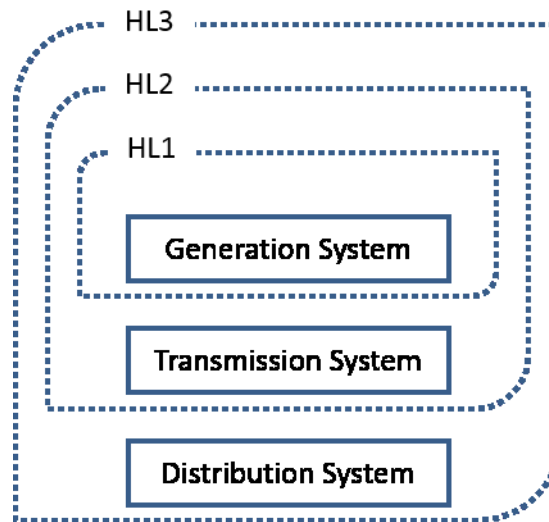


Figure 2.2 Hierarchical levels for power system reliability assessment

There are a number of indices for evaluation of the reliability throughout the power system. IEEE has developed a number of standards to include reliability related definitions and evaluation indices; IEEE Standard 762 is for generation reliability indices [44]; IEEE Standard 859 includes transmission facility reliability indices [45]; and IEEE Standard 1366 is for distribution reliability indices [46].

Typically, in reliability evaluation of a power distribution system dealing with the interruptions, three key factors should be considered: 1) frequency of the interruptions; 2) duration of the interruptions; and 3) severity or extent of the interruption. The first two factors are important from both customer and utility perspectives, and the third factor could represent the number of the customers affected or the priority of their loads [47]. In a smart grid structure, accommodating distributed generation and active customers, a combination of different indices should be employed to address the reliability of the system from both the customer and grid perspectives. Some of the commonly used system reliability indices according to the standards mentioned are:

- Expected Energy Not Supplied (EENS): The cumulative amount of energy that is not provided to the customers, and it is usually stated for duration of a year.

$$EENS = \sum_i \bar{L}_i \times r_i \quad (2.3)$$

where \bar{L}_i and r_i are the average load of customers and duration of interruption due to the outage i , respectively.

- System Average Interruption Frequency Index (SAIFI): total customers interrupted divided by total customer served, and it is usually stated for duration of a year.

$$SAIFI = \frac{\sum_i N_i}{N_T} \quad (2.4)$$

where N_i and N_T are the number of customers interrupted due to outage i and total number of customers, respectively.

- System Average Interruption Duration Index (SAIDI): total customer interruption durations divided by total customers served, and it is usually stated for duration of a year.

$$SAIDI = \frac{\sum_i r_i \cdot N_i}{N_T} \quad (2.5)$$

- Customer Average Interruption Duration Index (CAIDI): average interruption duration experienced by an interrupted customer.

$$CAIDI = \frac{SAIDI}{SAIFI} \quad (2.6)$$

- Average Service Availability Index (ASAI): average availability of service per customer served by the utility.

$$ASAI = \frac{N_T \cdot T - \sum_i r_i \cdot N_i}{N_T \cdot T} \quad (2.7)$$

where T is duration for reporting the index which is usually one year (8760 hours).

- Loss Of Load Expectation (LOLE): expected number of hours the load exceeds the generation due to generation deficiency, for the duration of interest.
- Loss of Energy Expectation (LOEE): expected energy lost due to generation deficiency, for the duration of interest.
- Expected Surplus Wind Energy (ESWE): average available wind energy that exceeds the load, and can therefore be stored or exported to the grid [48].
- Expected Interruption Cost (EIC): total cost of interruptions at all the load points, and it is reported in \$/year.

Similarly, Load Point Interruption Frequency (LPIF), Load Point Interruption Duration (LPID), Load Point Interruption Cost (LPIC), and Load Point Energy Not Supplied (LPENS) are defined to evaluate the reliability at specific load points of a power distribution system.

2.2 Reliability Evaluation Methods

Reliability evaluation methods can be divided into two categories: 1) analytical methods and 2) simulation methods. In addition, the reliability evaluation may be a qualitative study, in which the main factors that impact system reliability can be determined and prioritized, or a quantitative study, where the reliability is assessed through different parameters and indices defined and calculated for the system or equipment. A number of analytical and simulation methods are reviewed in this section.

2.2.1 Fault Tree Analysis (FTA)

Fault Tree Analysis is one of the most commonly used techniques for risk and reliability studies. Fault tree analysis is used as a tool to model the failure paths within a system which is important in reliable system design and development. As an analytical technique, fault tree analysis identifies events that can cause an undesired system failure. Therefore, by obtaining the probabilities of the causing events, one can end up calculating the overall probability of the main failure event [49].

Fault trees are built using gates and events. Most commonly, fault trees are composed of “AND” and “OR” gates, connecting the events toward the root failure. If either of a group of events causes the top failure to occur, then those events are connected using an “OR” gate. On the other hand, if all events need to occur to cause the top failure, they are connected by an “AND” gate. Each of the failure causes may also be further explored to determine the failure modes associated with them. However, the expansion of the tree is dependent on how much detailed data are available from operation history of the equipment [50].

2.2.2 Failure Mode, Effect, and Criticality Analysis (FMECA)

Failure Mode and Effect Analysis (FMEA) is considered as a process of ranking the most critical parts of a system; and it can be used for efficient resource allocation and maintenance scheduling based on higher priorities. FMEA is a proactive process to determine several key potential failures in the system through the comparison of some predefined factors, and as a result, it helps increase the reliability and availability of that

system. This process has been used on almost any equipment from cars to space shuttles [51].

In FMEA study, after determination of the failure modes, the main calculation procedure comprises of three steps:

1) The probabilities of the failure modes occurrences need to be determined.

These may be obtained from the previous data for the failed parts. These probabilities are then categorized and assigned a scaling number; with the lowest number for the least probable category.

2) The rate of severity of each failure mode is assigned and scaled due to the consequences of the failure and the amount of damage to the equipment.

3) Another scale number is assigned to the fault detection possibility; with the lowest number to the most likely detection of the failure.

The outcome of this study is the Risk Priority Number (RPN) which is calculated by multiplying all these three scale numbers. The RPNs are then ranked in order of importance [52].

Although FMEA has proven to be essential in various industries, there are some shortcomings with this method. Inherently, FMEA is a qualitative approach and the value of RPN is not conclusive unless it is used in comparison with other RPNs from other parts of a system, for prioritization purposes. This method also requires scaling of different affecting parameters and so far, there is no one-fits-all method for a proper scaling.

2.2.3 *Markov Processes*

A Markov process is a stochastic process in which given the present state of the system, the future behavior only depends on the present and not on the past. This is usually referred to as the Markov Property. A Markov Process is typically defined by a set of discrete states. At each state, there are a number of possible events which define the transitions between the current and the next state of the process. In a continuous time Markov process, it is assumed that the duration of time spent at each state is exponentially distributed and the transitions between the states are defined using a transition rate matrix [53].

Markov processes can be used for reliability assessment of power systems. In a component level, a simple state space representation includes two states: Up (working) and Down (not working). This basic model is called binary-state model, and may be extended to include certain state dependencies, for example among failures of different components or between a component state and the change in operation condition, by adding associated states to the model. Comprehensive models of the power system are capable to consider deterioration stages, inspection, and different types of maintenance and repairs for a more accurate representation of the components in an actual system [54].

Markov processes can be used in a format of Markov Decision processes (MDP) to determine optimum decisions at different states. An MDP is used to model an uncertain dynamic system in which a sequence of decisions needs to be made over time with uncertain outcomes. There is a reward associated with each state and action made at that state. Each action taken can either return a reward or incur a cost. Thus, in an MDP,

the goal is to find an optimal sequence of actions, called optimal policy, such that the expected reward over a given time interval becomes maximum [53]. For example, in a state space defined for the power system components, an optimum maintenance policy may be determined which minimizes the costs and meets a certain level of expected availability requirement.

2.2.4 Other Analytical Methods

There are a number of other analytical methods used for reliability evaluation of power systems, such as Minimum Cut-set method, and Network Reduction method [55]. These techniques involve reducing the number of components, by grouping series or parallel components together. The basic analytical equations include reduction of two components in series or reduction of two components in parallel into single equivalent components as shown by Fig. 2.3 [28]. In this figure, λ and μ represent failure rate and repair time, respectively.

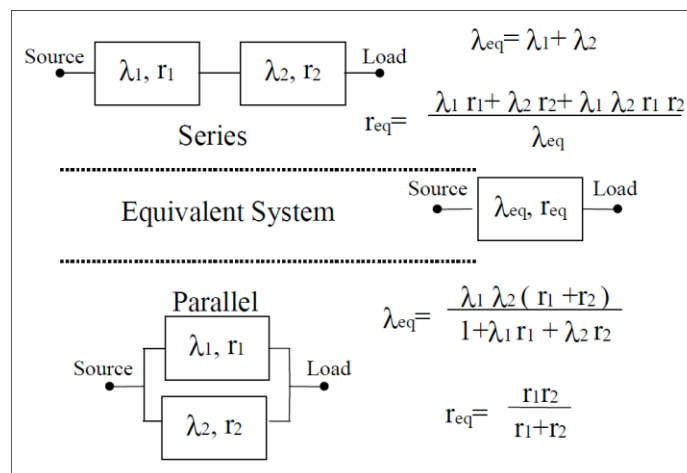


Figure 2.3 The equivalent network for series and parallel components

The drawback of an analytical method for reliability evaluation is that the indices are average values, and the failure and repair times are limited to be exponentially distributed.

2.2.5 Monte Carlo Simulation (MCS)

As an alternative to the analytic approaches, Monte-Carlo simulation may be used to model and evaluate the reliability of the power systems. The data required for this method include statistical component failure and repair information as well as system configuration. Randomly generated samples of failures and restoration times based on the probability distribution of the statistical data provided are used to calculate one set of numeric results for reliability indices. By repeating the process with new random values sampled from input probability distributions, new possible values for reliability indices are calculated. After large number of iterations, the expected reliability of the system is calculated, where the values calculated for each reliability index can be represented by a probability distribution for that index [47].

There are two different categories of MCS methods: 1) sequential; and 2) non-sequential. In a non-sequential MCS, the samples are taken without considering the time dependency of the states or sequence of the events in the system. Therefore, by using this method, a non-chronological state of the system is determined. On the other hand, a sequential MCS can address the sequential operating conditions of the system, and may be used to include time correlated events and states such as renewable generation, demand profile, customer decisions, etc., which is advantageous for power system

reliability assessment [56]. The sequential MCS has been used for modeling in different sections of this dissertation.

The MCS methods have also been divided based on the approach used for the sampling. Three common sampling approaches in MCS are: 1) state sampling approach; 2) system state transition sampling approach; and 3) state duration sampling approach. In the state sampling approach, which is non-sequential, the condition of each component is determined based on a uniformly distributed random variable between 0 and 1. If the random variable is larger than the failure probability, the component is in the Up state, and otherwise, it is in Down. The overall system state at each point in time is the combination of all component states. The disadvantage of state sampling method is that it does not consider the repair duration of the system components. In the state transition sampling approach, the transition probability from one state to another state is considered for sampling. Finally, the state duration sampling is based on the component Up and Down state duration distribution functions. This method is suitable to determine the duration of components states in a chronological manner and may be used for power system reliability assessment [57].

CHAPTER 3

RELIABILITY OF

DISTRIBUTED ENERGY RESOURCES

3.1 Introduction to Distributed Energy Resources (DER)

3.2 DER Reliability Assessment (e.g. wind turbines)

3.2.1 Fault Tree Analysis

3.2.2 Failure Mode, Effect, and Criticality Analysis

3.2.3 Markov Processes

3.2.4 Monte Carlo Simulation

3.2.5 Hybrid Analytical-Simulation Approach

3.1 Introduction to Distributed Energy Resources (DER)

Distributed energy resources (DER) will play a critical role in the reliability and efficiency of the emerging smart grid. In general, DER may consist of the following components: 1) distributed generation (DG), such as diesel engine, microturbine, photovoltaic (PV) system, wind power generation, etc. [58]; 2) energy storage such as batteries and capacitors; and 3) Demand Response (DR) by making informed load changes in response to electricity price over time [59].

Distributed generation may generally be categorized into conventional and renewable generation systems. Recently, increasing concerns about climate change, improved manufacturing technology, and cost reduction have been the major drivers toward integration of wind and PV power generation systems as distributed energy resources. Renewable DERs used in a distribution system are usually a combination of distributed intermittent generation, and a storage system [60]. In fact, distributed electricity generation and storage systems can contribute to peak load alleviation, investment deferral, voltage regulation, power loss reduction, etc. [61]. The infrastructure of the smart grid, incorporating real-time communication and control commodities, can well accommodate the efficient operation of these energy resources [62].

Different types of DER have a variety of impacts on the smart grid. Industrial, commercial, and residential customers can use DG to supply part of their demands and sell the excess electricity back to the grid. Small-scale generators usually generate DC output, and therefore, an inverter would be necessary to convert DC to AC before the grid connection. The capacities of these generators are usually less than 10kW. Capacities of

DG can be in a range of 10kW to 200kW for commercial and small industrial systems; and big industrial customers may use higher DG capacities, in megawatt range, with AC output [63].

Distributed storage systems can store electricity when there is excess electricity available at lower price and supply electricity at the time of deficit. Therefore, they act like both generation and load at different situations. Electricity storage systems are also used to smooth out the volatilities of renewable generation, and may be employed to shift the peak load or arbitrage electricity in a dynamic pricing scheme [64].

Demand response may also be considered as a DER. A DR scheme adopted by an electricity customer can simply be part of a demand side management (DSM) program that cuts out an air conditioner during peak load hours or it may involve customers who respond to dynamic electricity rates according to their load priority and resource availability [61]. DSM strategies have been used in the industry for many years [65]. The goal of the DSM is to provide efficient usage of the power system assets and reduce the electricity costs for the customers. In fact, a DSM alters the load curve of the customers through a variety of programs such as peak clipping, load shifting, valley filling, energy conservation, etc. [66]. Therefore, electric utilities are being advised to incorporate DSM in their resource planning by performing cost/benefit analysis [67].

The smart power distribution system will improve DER integration and DR by providing more efficient controllability and incentives based on dynamic electricity rates, in the near future [7]. Integration of the DER into the smart grid affects the performance metrics of the system, such as reliability.

3.2 DER Reliability Assessment (e.g. wind turbines)

A power distribution system includes a variety of components such as renewable generation and storage system, power lines, transformers, etc. In order to effectively evaluate the reliability of the overall distribution system, it is important to first study the reliability of each component of the system. Distribution energy resources are important components of the future distribution systems, and therefore, their reliability should be analyzed. For example, as the number of wind turbines is rising, new reliability challenges are introduced to the smart grid [68]. Wind turbine reliability studies are essentially critical in the design stage of the wind power generation systems, and they have been addressed in quite a few research studies [69] [48] [70].

On the other hand, the outcome of the reliability study for individual wind turbines is valuable in the operation stage, as well. It should be noted that the wind power generation depends on the wind speed which is a stochastic variable. In addition, exposure to outdoor weather condition and numerous rotating parts operating at high elevation make wind turbines more vulnerable and critical from the reliability perspective. The uncertainties related to wind generation can cause complications for the owners of the wind farms in order to estimate the day-ahead energy generation inquired by the market, where, off estimation, imposes penalties to them. Therefore, reliability evaluation and proper maintenance scheduling are indispensable to predict the expected energy not served, and to minimize the loss of the wind turbines failures and unavailability [71].

Based on the reliability study, the wind turbine owner may choose to adjust the manufacturer's primary maintenance recommendations in order to improve the turbine's

performance, provide more power to the market, and increase profits. These adjustments depend on the wind farm's specific operation conditions such as the location, site weather, power purchase agreement, and available facilities. In fact, major factors contributing to the total failure of the turbine have been studied through individual wind turbine reliability modeling [19].

Basically, wind energy systems can be categorized based on generator, gearbox, and converter types as shown in Table 3.1. The conventional type of wind turbine is called Single Cage Induction Generator (SCIG). This type of wind turbine is fixed speed and requires a gearbox to be connected to the grid. Using an induction generator, this wind turbine consumes reactive power to generate active power. Therefore, induction generators are equipped with an external capacitor bank. There is also another structure of SCIG which uses a full-scale power converter. This new configuration has advantages of more controllability, variable speed operation, and better performance of voltage control. However, the cost associated with power electronic devices is a drawback. The decreasing cost of power electronics will make this type be more desirable. Another popular type of wind turbine is Doubly Fed Induction Generator (DFIG). The configuration of this wind turbine corresponds to a wound rotor induction generator with a power converter. The power converter's rating is about 30% of the generators capacity, and so, it is economically favorable. Due to this fact, many manufacturers have used the doubly-fed concept in their products, and many researches have been conducted to find optimum control strategy for the converter. The main issue with this type of wind turbine is to protect the converter from damage during grid faults. Specially, this issue becomes

more important with high capacity generation which needs to have fault ride-through capability. Wound Rotor Induction Generator (WRIG) with limited variable speed capability is also known as Optislip wind generator. This type of generator uses an external resistor which is connected in series with the rotor windings. This amount of resistance in circuit is controlled by power electronics, and for higher speed control, higher ratings of resistor is required. For that reason, the range of speed control is limited to about 10% of the synchronous speed. There are some other types of wind turbines which use synchronous generators. In order to have higher reliability and less complexity, the excitation for the field is avoided by using Permanent Magnet Synchronous Generators (PMSG). Generally, PMSG structure may or may not have a gearbox, and they are connected to the grid through a full-scale converter. Using a gearbox would increase the speed of the generator shaft, and as a result, reduce the size of generator. The gearbox, on the other hand, raises many issues during its operation [72].

Table 3.1 Different types of wind generation systems

Type of generation system	Turbine concept	Gearbox	Converter
Single Cage Induction Generator (SCIG)	Fixed speed	Multiple stage	–
	Variable speed	Multiple stage	Full scale
Permanent Magnet Synchronous Generator (PMSG)	Variable speed	–	Full scale
	Variable speed	Single or Multiple stage	Full scale
Doubly Fed Induction Generator (DFIG)	Variable speed	Multiple stage	Partial scale
Electrically Excited Synchronous Generator (EESG)	Variable speed	–	Partial & Full scale
Wound Rotor Induction Generator (WRIG)	Limited variable speed	Multiple stage	Partial scale
Brushless Doubly Fed Induction Generator (BDFIG)	Variable speed	Multiple stage	Partial scale

From the reliability point of view, the gearbox is usually the main cause of failures in SCIG and all other wind turbines which need speed conversion in their drive train. Gearboxes are exposed to mechanical stresses caused by the wind fluctuations, and therefore, their performance worsens quickly. Oil leakage and broken teeth on the ring gear are among the most likely gearbox failure modes. In other types of wind turbines, electrical system, converters, and generator may also be the major causes of failure. Figure 3.1 provides annual failure rate and average downtime for different parts of wind turbine [73].

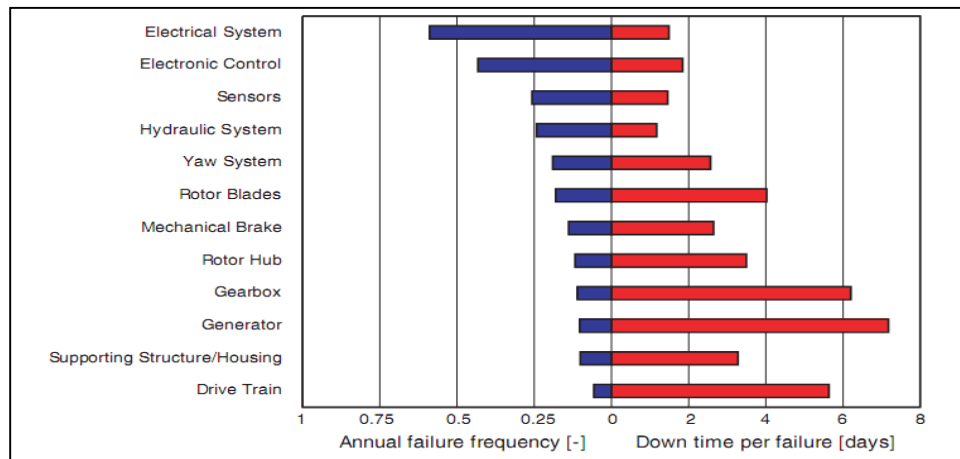


Figure 3.1 Failure rate and downtime for different parts of wind turbine

It is noticeable that the downtime for some parts of the wind turbine like the gearbox, generator, drive train, and blades, which are installed in high elevation, is higher than the downtime for the other parts because of accessing problems. The delay in accessing the crane, or purchasing equipment, for example, may also contribute to this time significantly.

As wind energy contributes more into the total electricity production in power system, the output power of wind farms should be able to better follow load demand

profile similar to a conventional generation system. Long/short term changes in load introduce another stochastic variable which should be considered in order to study the reliability of a stand-alone wind farm. Many studies have been conducted for reliability and availability assessment of wind turbines [69]. These studies have mainly discussed steady state estimation of system availability and reliability indices, and there has not been many research documents to describe wind farm's reliability in different time domains.

In this research, both analytical and simulation methods are used to model and analyze the reliability of individual wind turbines as well as a group of wind turbines as a wind farm.

3.2.1 Fault Tree Analysis

Reliability of a single wind turbine can be determined given the historical failure data of its parts using Fault Tree analysis. Figure 3.2 shows the proposed fault tree for the wind turbine including major failure causes. These failures are significant enough such that the failure of each component can stop operation of the entire wind turbine; and therefore, they are connected by "OR" gates in the diagram.

Each of the failure causes may also be further explored to find the failure modes associated with them. However, the expansion of the tree is dependent on how much detailed data are available from operation history of the wind turbines.

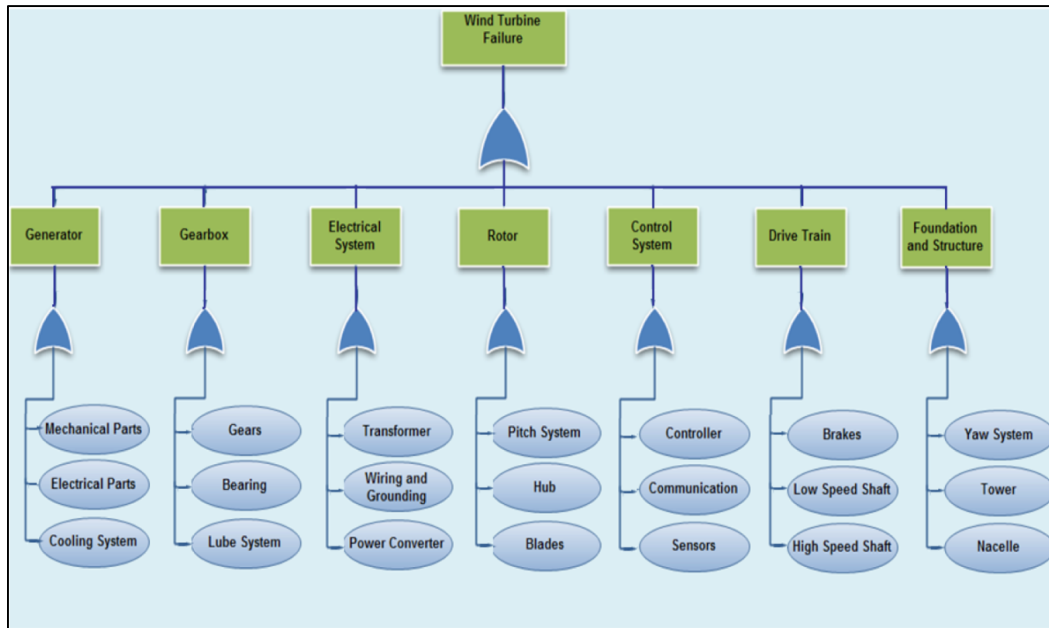


Figure 3.2 Fault Tree for a typical wind turbine

The essential input to the reliability model are the failure data coming from the operation of the wind turbines. These data may be categorized by the type of wind turbines which they belong to. Hence, the reliability of each turbine configuration can be studied separately, and compared to one another. Another approach is to divide the statistics based on the time of the year (e.g. seasonal) in order to incorporate the effect of weather changes in wind turbine reliability assessment.

Equation 3.1 calculates the reliability of the wind turbine, $R_{Turbine}$, as a function of time, t , and failure rates of each part of the wind turbine, λ_i assuming that the distribution of the time to failure follows exponential distribution.

$$R_{Turbine} = e^{-\sum_{i=1}^n \lambda_i t} \quad (3.1)$$

where, n is the number of parts of the wind turbine.

The availability of a single wind turbine is calculated from Eq. 3.2.

$$A_{Turbine} = \frac{\mu}{\mu + \lambda} \quad (3.2)$$

where, the total failure rate, λ , and repair rate, μ , of the wind turbine are obtained from Eq. 3.3, based on the failure and repair rates of the individual parts [50].

$$\lambda = \sum_{i=1}^n \lambda_i \quad , \quad \mu = \frac{1}{\sum_{i=1}^n \left(\frac{1}{\mu_i}\right)} \quad (3.3)$$

3.2.2 Failure Mode, Effect, and Criticality Analysis (FMECA)

The conventional FMECA study process of DER such as a wind turbine is shown in Figure 3.3 based on [52]. However, there are some shortcomings with using FMECA for wind turbines. First, researchers have to either define their own rating scales or adopt other developed tools which are not specifically designed for wind turbines, and, so, the result may not necessarily represent the true priorities of the wind generation system [74]. In addition, there are a variety of wind turbine types with different structures and it is not possible to assign the same set of scale numbers for all of them. For example, the damage to a synchronous generator in a direct drive wind turbine is generally more severe and more costly than an induction generator in a fixed speed wind turbine. Another issue with the current calculation method is that, the evaluated RPN doesn't inherently discriminate between a highly severe but low probable failure mode and a less severe with higher occurrence probability.

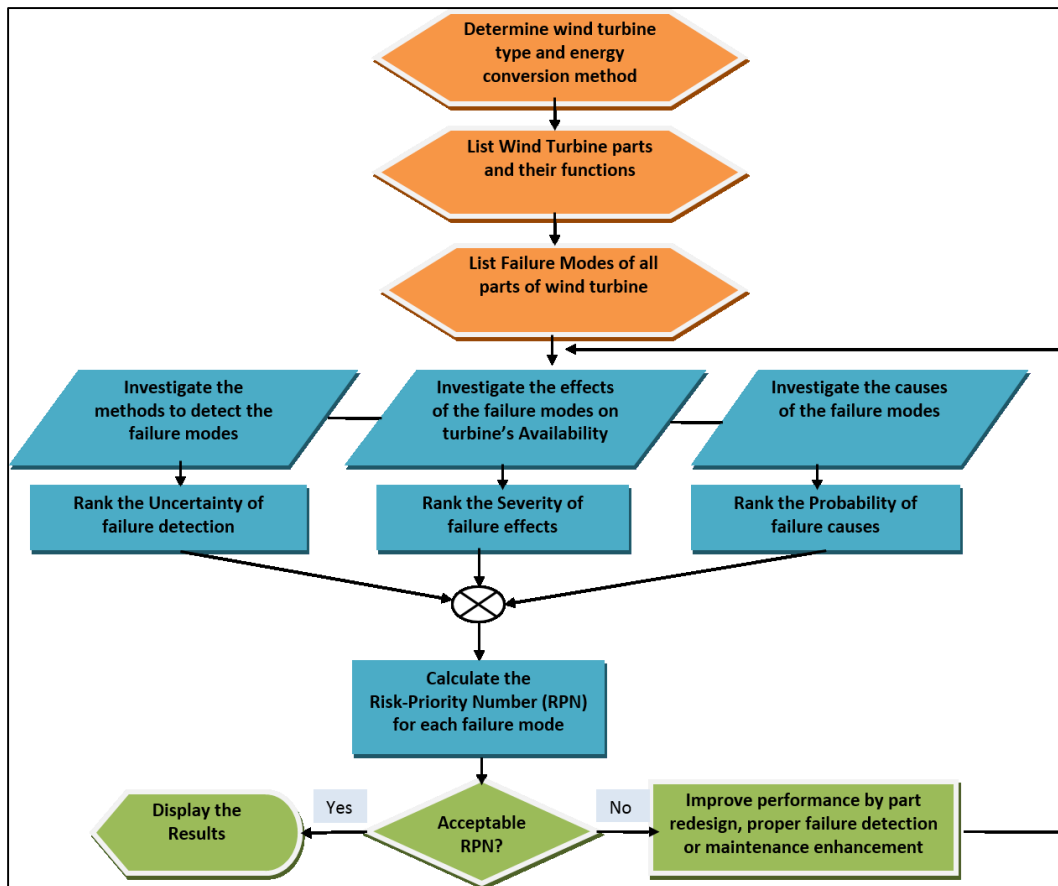


Figure 3.3 FMECA process for a typical wind turbine

In order to resolve these problems, we propose a modified process for FMECA analysis where the prioritization of the failure modes is based on numbers representing the cost consequences. In fact, the proposed method incorporates the cost associated with each failure mode, called Risk-Based FMEA (RB-FMEA). Limited use of this concept has been reported in the literature [75] [76]. We believe it is more realistic to consider cost which is the common language among different sectors of turbine design, operation and maintenance. In addition, RB-FMEA is a quantitative approach whose outcome is proportional to the equipment performance, and so can easily be compared with costs of different maintenance strategies or design improvements in order to make an optimum

decision. One of the advantages of this proposed strategy is its simplicity, where it is implemented using Microsoft Excel worksheets and can be easily edited or adapted for use by manufacturers of different types of equipment.

3.2.2.1 Proposed RB-FMEA Process [77]

Given the failure modes, the proposed RB-FMEA procedure is described by the following steps, where the calculations are presented subsequently.

- Given that the equipment has failed, determine the probability of occurrence of each failure mode, P_F , based on the historical data.
- Determine the probability of not detecting the failure, P_{ND} .
- Calculate the cost consequence of the failure, C_F .
- Calculate the risk of each failure mode, called Cost Priority Number (CPN), by multiplying the probabilities and the cost calculated in the previous steps.

$$CPN(i) = P_F(i) \times P_{ND}(i) \times C_F(i) \quad (3.4)$$

where, “ i ” is the index of i th failure mode. The calculated CPN is expressed in dollars and can easily be compared for different failure modes.

P_{ND} is calculated by dividing the number of actual failures, N_F , to the total Number of Failure Vulnerabilities, N_{FV} ,

$$P_{ND}(i) = \frac{N_F(i)}{N_{FV}(i)} \quad (3.5)$$

Number of Failure Vulnerabilities is defined as the sum of number of actual failures and the number of detected possible failures prior to their occurrences, for any

given period of time. These risks of failure may be detected during online monitoring, inspection, or maintenance.

The cost of failure incurred, C_F , depends on the severity of failure consequences. The consequence of a failure may impact the equipment itself or have other consequences, such as endangering the safety of the site crew, etc., which is specific to a given operation condition and may be included in C_F , as well.

While CPN represents a cost based risk factor, it can easily be incorporated in calculation of the total failure cost of the system for any specific duration of interest (D_{Int}). The total failure cost can be derived as:

$$TFC = \sum_{i=1}^m N_{FV}(i, D_{Int}) \times CPN(i) \quad (3.6)$$

where, m represents the total number of the failure modes, and $N_{FV}(i, D_{Int})$ denotes the number of failure vulnerabilities of failure mode i for the duration of interest.

3.2.2.2 *RB-FMEA for Wind Turbines*

The proposed RB-FMEA method can be applied to a wind turbine. Figure 3.4 demonstrates the flowchart for the study.

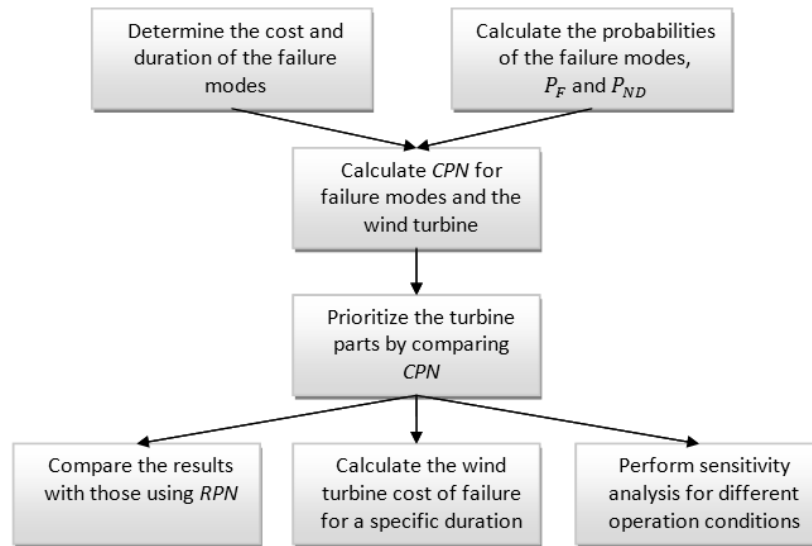


Figure 3.4 Study steps of RB-FMEA for a wind turbine

In case of the wind turbines, the cost consequence of a failure is comprised of four major segments:

$$C_F(i) = C_P(i) + C_S(i) + C_O(i) + C_L(i) \quad (3.7)$$

where, C_P , is the cost of parts which need to be replaced due to the failure; C_S , is the cost of service, and it includes all the costs associated with the required facilities and devices due to the failure, such as renting a crane, or transportation, etc.

C_O , represents the opportunity cost, which is the sum of revenues the wind farm owner would have received from selling power generation, in case the failure didn't occur. It can be expressed as:

$$C_O(i) = D_F(i) \times \overline{WP}_{out} \times \overline{EPR} \quad (3.8)$$

where, D_F corresponds to the duration of failure, and \overline{WP}_{out} and \overline{EPR} are the average output wind power of turbine, and average energy purchase rate, within this duration, respectively.

Finally, C_L in equation (3.7) represents the total cost of extra labor required for the repair, and can be calculated as:

$$C_L(i) = D_F(i) \times N_C \times MHR \quad (3.9)$$

In the above equation, N_C and MHR are number of repair crew, and man-hour rate of the repair crew in dollars per hour, respectively. There has been a variety of wind power generators developed in recent decades. For the RB-FMEA study, various wind turbine structures and their sub-assemblies need to be identified. The failure of the wind generation system is defined through three levels as shown in Figure 3.5. The wind turbine stands in the highest level (level I); where, wind turbine sub-assemblies and parts are divisions of middle (level II) and low (level III) levels respectively.

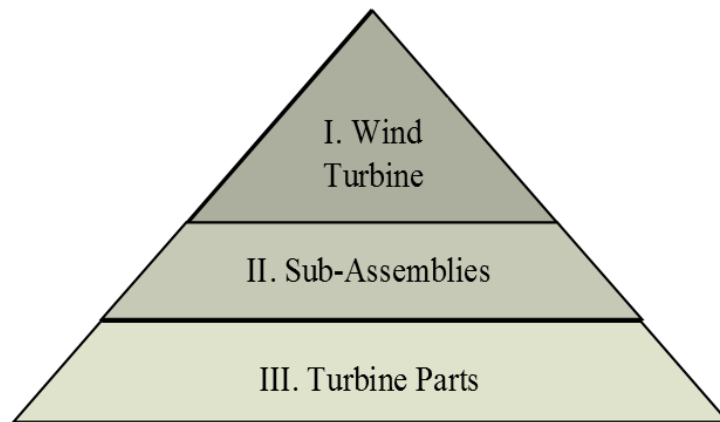


Figure 3.5 Wind turbine hierarchy for RB-FMECA

Wind energy systems can basically be categorized by their types of generator, gearbox, and converter. After recognizing the wind turbine types in level I, a general set of wind turbine sub-assemblies and parts are defined for levels II and III of Figure 3.5, as presented in Table 3.2.

Table 3.2 General set of Wind turbine sub-assemblies and main parts

Sub-assemblies	Main Parts
Structure	Nacelle, Tower, Foundation
Rotor	Blades, Hub, Air brake
Mechanical Brake	Brake disk, Spring, Motor
Main shaft	Shaft, Bearings, Couplings
Gearbox	Toothed gear wheels, Pump, Oil heater/cooler, Hoses
Generator	Shaft, Bearings, Rotor, Stator, Coil
Yaw system	Yaw drive, Yaw motor
Converter	Power electronic switch, cable, DC bus
Hydraulics	Pistons, Cylinders, Hoses
Electrical System	Soft starter, Capacitor bank, Transformer, Cable, Switchgear
Pitch System	Pitch motor, Gears
Control system	Sensors, Anemometer, communication parts, processor, Relays

There are other wind turbine parts that could be included subject to the details required. However, for this study, the focus is on the major parts with higher failure probabilities and critical consequences.

The failure occurs when a device no longer operates the way intended. There are numerous failure modes that can be defined for a complicated assembly such as wind turbines. These failure modes can cause partial or complete loss of power generation. Mainly, the key failure modes, which cause complete loss of power generation, are malfunction and major damage of the main parts of the turbine stated in Table 3.2. Other failure modes such as surface damage and cracks, oil leakage, loose connection, etc. may be considered as less significant. However, if they are not taken care of, minor failure modes can initiate major failures as well.

In fact, each one of the failure modes has a root cause, and the probability of that failure mode is directly related to the probability of its root cause. Table 3.3 provides different categories for these causes. Human error in this table, refers to the errors occurred during operation or maintenance.

Table 3.3 Root causes of the wind turbine failure modes

Weather	Mechanical	Electrical	Wear
High wind Icing Lightening	Manufacturing and material defect Human error External damage	Grid fault Overload Human error Software failure	Aging Corrosion

Failure probability of each failure mode is calculated from the contribution of that failure mode in the interruption of the wind turbine operation. The limiting factor in RB-FMEA study of wind turbines is that the detailed failure data are not available for all of the failure modes. Today, the number of reports providing statistics on failure probabilities is increasing. Some of these statistics have been categorized based on the capacity of the wind turbines, while some others have been divided according to the type of the wind generation system [78] [79].

There are different approaches to detect the probable failure modes as categorized in Table 3.4. The common approaches are through inspection or while the turbine is being maintained. However, the fastest and the most reliable method is condition monitoring which can increase the availability of wind turbine considerably by using online systems. By having a condition monitoring system, the probability of not detecting the failure decreases to the failure probability of the human error or the monitoring

system itself. The cost representing failure criticality should include repair or new part expenses, duration of the repair, etc., which are specific for each wind turbine type and provided by the wind farm owner for the study.

Table 3.4 Major detection methods of the wind turbine failure modes

Inspection	Condition Monitoring	Maintenance
Visual Auditive	Vibration analysis Oil analysis Infrared thermography Ultrasonic	Time-Based Condition-Based

3.2.3 Markov Processes

For a complete reliability study of DER, one should consider the impact of the DER on the grid as well as modeling the loads. In a case of wind turbine reliability, Markov Processes allow for modeling the time domain operation of a group of wind turbines (as a wind farm) considering failure and repair of wind turbines, wind speed changes, and the load profile. Calculation of time-based reliability of a wind farm is beneficial for site selection and long-term electricity production estimation as well as short-term operations, especially in deregulated energy market where the owner of a wind farm needs to evaluate cost-benefit of alternative decisions at different times while providing an acceptable level of reliability.

Typically, in order to evaluate the reliability of wind farms, a two-state Markov model of “working” or “failure”, is used to present equipment such as wind turbine. Using this model, the number of states for a wind farm with N number of wind turbines will be 2^N . Since there are tens and sometimes hundreds of wind turbines installed in today’s wind farms, this modeling approach increases the number of states dramatically.

Here, a Markovian model has been used to study wind farm availability and reliability due to wind variability and load changes for short-term and long-term periods. The model is developed based on the fact that wind turbines in a wind farm are usually from the same model and manufacturer. The wind farm is modeled using Markov Processes with $(N+1)$ number of states where each state represents the number of working wind turbines at a time. Kendall-Lee notation of this birth and death process is $M/M/S/GD/N/N$ where the two “M”s stand for Markovian assumptions for failure and repair times; “S” denotes the number of parallel repair crew; failed turbines waiting times are based on general queue discipline “GD”; the first “N” shows the system capacity assuming that repair process has enough capacity for all wind turbines if they fail, and the second “N” is the number of similar wind turbines installed in the wind farm. Figure 3.6 shows the diagram of this modeling, where λ and μ are failure and repair rates respectively. To explain the repair transition rates, assume that there was r number of failed wind turbines being repaired simultaneously. In that case, the repair rate would be $r \times \mu$ according to Markovian property. Because in our model the number of repair crew is limited to S , at each time the coefficient of μ will be the minimum of S and number of failed wind turbines [70].

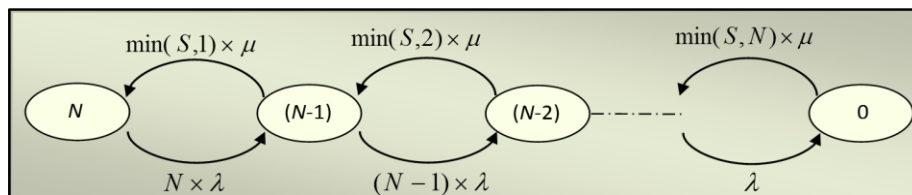


Figure 3.6 Rate diagram for the wind farm Markov model

This model assumes wind turbines of the same make and model are identical. In a case that a wind farm consists of turbines from more than one manufacturer, each group of similar turbines must be modelled separately. Although some studies show a correlation between wind turbine failures and weather condition (humidity, temperature, and wind speed) at the installation site, it is difficult to determine its effect explicitly specially in a short term because failures may often occur sometime after their causing event [18]. Here, wind turbine failures and wind speed changes are assumed to be independent for simplicity so that we can model them separately. However, the effect of weather can still be taken into account by defining non-stationary failure rates for different periods, say each season.

Wind speed variability, on the other hand, can also be represented by various wind states at different points in time. To do so, wind speed changes may be binned based on the corresponding output power changes of the installed wind turbine. For example, a typical power curve of a 1.5MW wind turbine is shown in Figure 3.7, where the cut-in and cut-out wind speeds are 4m/s and 25m/s respectively. Beyond those points, the output power of the wind turbine will be zero. There is also a rated wind speed (12m/s in Fig.3.7) for which the turbine produces its rated output power, and this rated power remains approximately constant within this rated and cut-out wind speed due to turbine's power control system. Wind changes between cut-in and rated wind speeds lead to different wind power generation and can be binned with a specific interval.

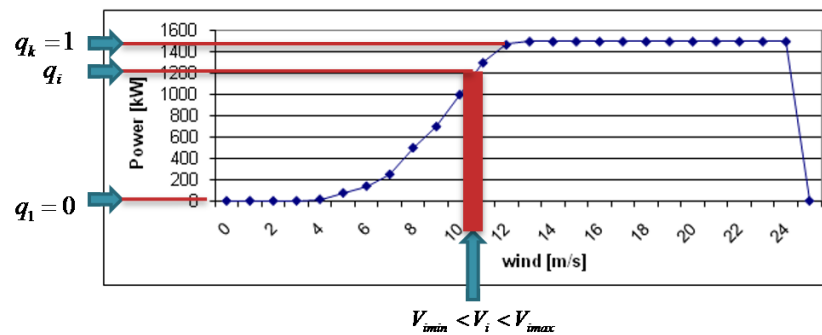


Figure 3.7 Power curve of a 1500kW wind turbine

The probabilistic changes of wind speed may be translated into relevant output power of the specific turbine installed at that location, and represented by output power states. Each output power state, q_i , corresponds to a fraction of turbine's rated output power; in other words, the output power of wind turbine is q_i times its rated power due to the wind speed. K is the total number of states; therefore:

$$q_1 = 0, q_K = 1 \text{ and } 0 < q_i < 1 \quad (3.10)$$

Here, rather than looking for transition rates between the states, the frequency of occurrence of different wind speeds (or equivalently histogram of corresponding power production) is considered for reliability studies since this is the format in which the data are available from measurements or weather forecast models.

A simple power system structure used for reliability study is depicted in Fig.3.8.

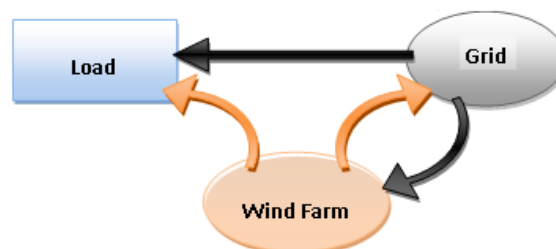


Figure 3.8 Power system model for reliability study of the wind farm

The system consists of a regional load supplied by the power grid, as a slack bus, and an installed wind farm. The arrows show the possible directions of power flow. Depending on the amount of power production and load demand, the wind farm may send its excess production to the grid or receive some power from the grid, when there is not enough wind, to supply the local loads. In this structure, the equivalent total load changes with time.

In order to determine the reliability of wind farms in supplying the load, its time-based behavior must be considered. For the short-term reliability studies, time series model of the load (e.g. hourly load changes) may be used derived from the load forecasting methods [80] [81]. For the reliability assessment in long-term, the probability distribution of the peak load can be considered to model the load [82].

The reliability indices are used to determine how reliably the wind turbines can contribute to supply a time-varying demand, for a certain period of time. The duration of interest may vary from hourly to yearly basis where turbines' failure and repair rates may change, accordingly. Fig.3.9 shows the steps toward the calculation of reliability and availability indices.

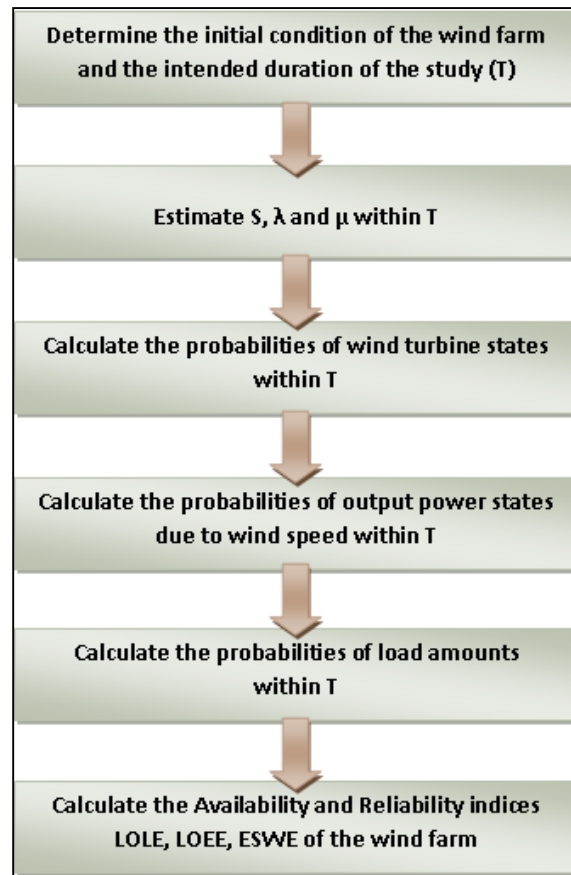


Figure 3.9 Procedure of wind farm reliability calculation using Markov Processes

According to the formulation of continuous-time Markov processes, state probabilities of wind farm model in Fig.3.6 can be expressed by an $(N + 1)$ element row vector, \mathbf{P} , which should satisfy the following differential equation [83]:

$$\frac{d\mathbf{P}}{dt} = \mathbf{P} \times \mathbf{A} \quad (3.11)$$

where, \mathbf{A} is the matrix of transition intensities. The elements of this square matrix are probability per time unit that the system makes a transition from one state to another. The values of each row sum up to zero in order to conserve the rule that the probability mass flow out of each state should go to other states. Elements of matrix \mathbf{A} can be set up based

on failure rate and repair rate of the single wind turbine. In the case of the wind farm model, matrix \mathbf{A} is arranged as shown below.

$$\mathbf{A} = \begin{array}{c} \boxed{0} \\ \vdots \\ \boxed{i-1} \\ \boxed{i} \\ \boxed{i+1} \\ \vdots \\ \boxed{N-1} \\ \boxed{N} \end{array} \begin{array}{c} \boxed{0} \quad \dots \quad \boxed{i-1} \quad \boxed{i} \quad \boxed{i+1} \quad \dots \quad \boxed{N-1} \quad \boxed{N} \\ \left[\begin{array}{cccccccc} -\mu & \dots & 0 & 0 & 0 & \dots & 0 & 0 \\ \vdots & \vdots & \vdots & \vdots & \vdots & & \vdots & \vdots \\ 0 & \dots & -((i-1)\lambda + \mu) & \mu & 0 & \dots & 0 & 0 \\ 0 & \dots & i\lambda & -(i\lambda + \mu) & \mu & \dots & 0 & 0 \\ 0 & \dots & 0 & (i+1)\lambda & -((i+1)\lambda + \mu) & \dots & 0 & 0 \\ \vdots & \vdots & \vdots & \vdots & \vdots & & \vdots & \vdots \\ 0 & \dots & 0 & 0 & 0 & \dots & -((N-1)\lambda + \mu) & \mu \\ 0 & \dots & 0 & 0 & 0 & \dots & N\lambda & -N\lambda \end{array} \right] \end{array}$$

Solving the Eq.3.11 mathematically determines the probabilities for simultaneous operation of any number of wind turbines with time. The solution as a function of time is given by:

$$\mathbf{P}(t) = \mathbf{P}(0) \times \exp(\mathbf{A}t) \quad (3.12)$$

where $\mathbf{P}(0)$ is the initial condition of working wind turbines.

3.2.3.1 Short-term study

In short term reliability studies, the initial condition of the wind turbines impact the results. The wind turbine state probabilities can be calculated at each time step (e.g. one hour) for the short-term duration of interest. If the elements of $\mathbf{P}(t)$ are denoted by $P(j, t)$, Eq. 3.13 can be used to calculate the total availability of the wind farm.

$$A(t) = \frac{\sum_{j=0}^{j=N} (P(j, t) \times j)}{N} \quad (3.13)$$

where, $A(t)$ is the availability of wind farm at time t , $P(j, t)$ is the probability of j turbines working simultaneously at time t .

At each time instant, total output power of the wind farm results from the output power due to wind speed at that time multiplied by the availability of the wind farm. During the short-term study, it is possible that for some hours, the production of the wind farm exceeds the load demand, and so, the excessive power can be transferred to the grid; other times, grid needs to compensate for the lack of wind farm power production. The Loss of Load at each hour t_n can be defined as:

$$LOL(t_n) = \begin{cases} 1 & (A(t_n) \times PWR_{WT}(t_n) \times N) < PWR_{load}(t_n) \\ 0 & \text{Otherwise} \end{cases} \quad (3.14)$$

where, $PWR_{WT}(t_n)$ and $PWR_{load}(t_n)$ are power production of a wind turbine and power demanded by the load at hour t_n , respectively. n is an integer denoting the time step.

Consequently, Loss of Load Expectation from the wind farm's point of view for a period of T hours can be derived using Eq. 3.15.

$$LOLE(T) = \sum_{n=1}^T LOL(t_n) \quad (3.15)$$

3.2.3.2 Long-term study

If the intended study time, T , becomes long enough, the effect of wind farm's initial condition will be negligible and the results will converge to the steady state probabilities. By definition, traffic intensity is the ratio of failure rate to the repair rate:

$$\rho = \frac{\lambda}{\mu} \quad (3.16)$$

Steady state probability of having j out of N number of turbines working together, π_j , is calculated using Eq. 3.17. [84]

$$\pi_j = \begin{cases} \binom{N}{N-j} \rho^{(N-j)} \pi_N & j = N - S, N - (S - 1), \dots, N - 1, N \\ \frac{\binom{N}{N-j} \rho^{(N-j)} j! \pi_N}{S! S^{(N-j-S)}} & j = 0, 1, \dots, N - (S + 1) \end{cases} \quad (3.17)$$

where π_N is calculated using the fact that:

$$\sum_{j=0}^N \pi_j = 1 \quad (3.18)$$

Equation 3.19 calculates the average availability of the wind farm in the long-term.

$$A = \frac{\sum_{j=0}^{j=N} (\pi_j \times j)}{N} \quad (3.19)$$

Considering wind farm's availability and turbines output power due to wind speed distribution, power production of the wind farm for each state q_i is:

$$PWR_{WF,q_i} = q_i \times PWR_r \times A \times N \quad (3.20)$$

where PWR_r is the rated power of a wind turbine. Estimated energy production of wind farm for duration of T can be derived using Eq. 3.21.

$$E_{WF} = \sum_{i=1}^K (P_{q_i} \times PWR_{WF,q_i}) \times T \quad (3.21)$$

where P_{q_i} is the probability of having output power state q_i ; and K is the total number of output power states. Using the total probability theorem, Loss of Load Expectation of the wind farm for long-term operation duration of T is calculated.

$$LOLE = \sum_{i=1}^K P(PWR_{load} > PWR_{WF,q_i}) \times P_{q_i} \times T \quad (3.22)$$

3.2.4 Monte Carlo simulation

In addition to the analytical techniques, the simulation methods may also be used to estimate the output power and evaluate the reliability of a renewable generation system. The modeling for Monte Carlo simulation (MCS) is done using the Arena software [85]. This software is modular and features a flowchart-style modeling methodology enabling MCS studies and performance evaluation. Figure 3.10 shows the schematic of a single wind turbine model used for output power estimation based on the wind speed probability distribution.

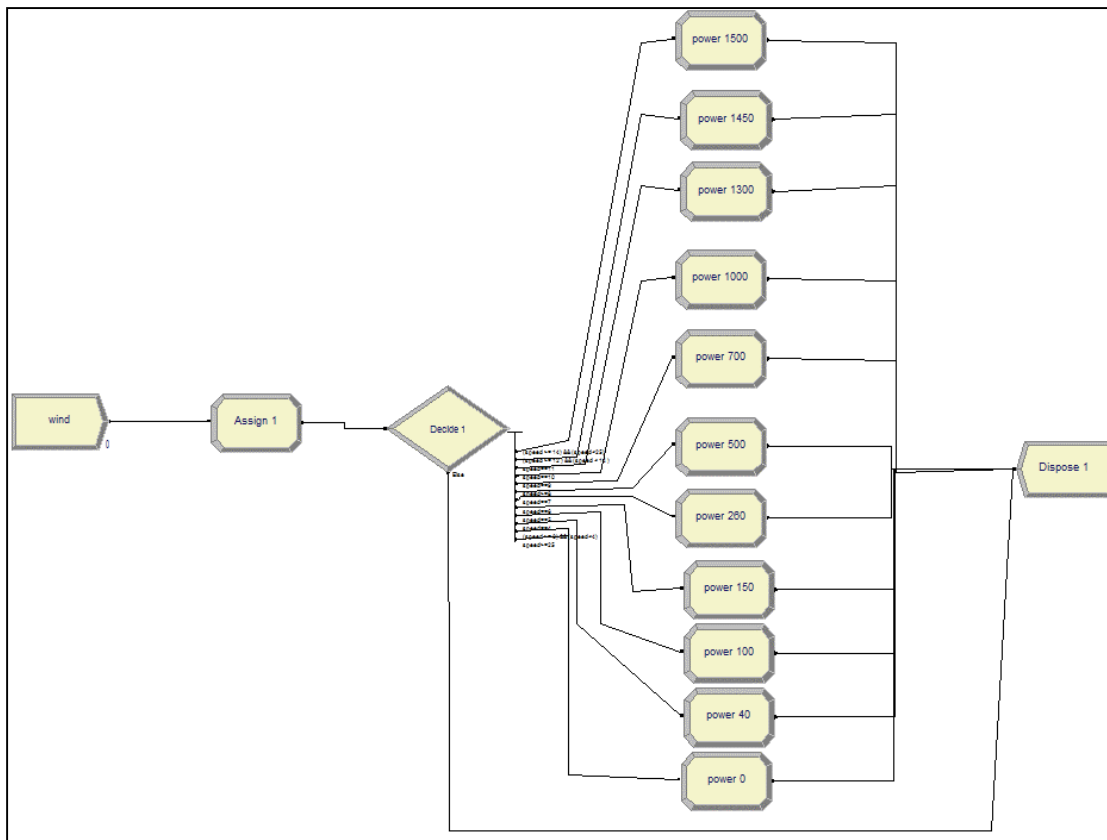


Figure 3.10 Wind turbine model for output power estimation in Arena software

The advantage of this approach is that any wind speed profile and type of wind turbine with its power curve can be modelled in the software using block diagrams. In fact, at any point in time, a wind speed is generated based on its distribution and moved to the decision block. The decision block performs as a look-up table built according to the specific power curve of the wind turbine in order to determine how much power will be generated based on the input wind speed. The simulation is run for thousands of iterations and the average expected power generated by the wind turbine is calculated along with its confidence interval. The expected average wind energy is calculated by multiplying the average expected generated power by the number of turbines and the duration of interest.

In addition, the model shown by Figure 3.11 is used to simulate the failure and repair process of a wind turbine. The time between failures is based on exponential distribution, and the mean time to repair may be assumed to follow the Log-normal distribution [86]. The result of this simulation is the outage duration of each major subassembly of the wind turbine from which the availability of the wind turbine can be calculated. By adding all the individual outage durations, the total unavailability duration of a single wind turbine is determined. Then, the average availability is the total available hours over the total study hours.

Similarly, the availability of a fleet of wind turbines in a wind farm is determined using MCS. The main difference between this model and the one for a single wind turbine is that in a wind farm, the number of wind turbines, and consequently, the number of vulnerable parts are higher. Therefore, occasionally, there may be some parts which need to wait in a queue to be repaired in case of simultaneous incidents. This will definitely add to the total outage time of that part and decrease the overall availability of the wind farm.

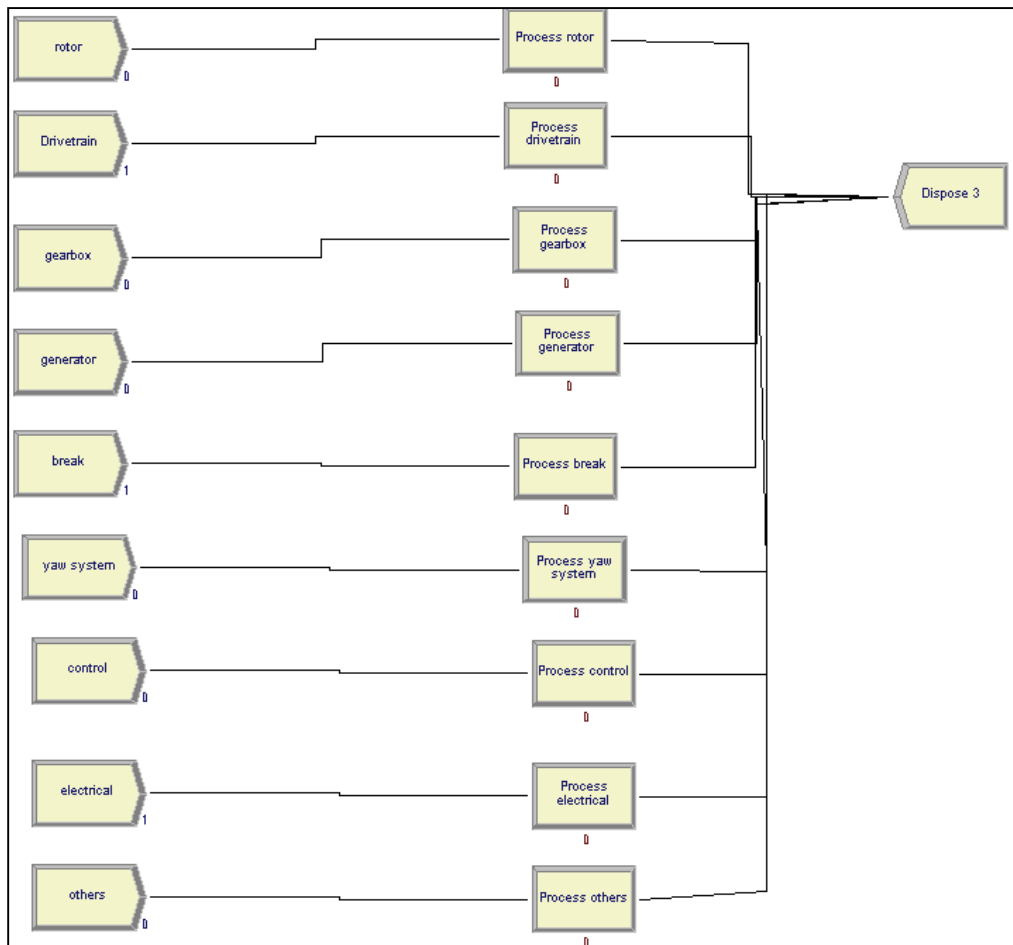


Figure 3.11 Failure and repair model of main subassemblies of a wind turbine in Arena

3.2.5 Hybrid analytical-simulation approach

Another important factor to be considered for reliability assessment of equipment, such as a wind turbine, is maintenance. Usually, during a maintenance, the equipment should be taken out of service for technical and safety reasons. Therefore, maintenance impacts the availability and reliability of the equipment, and it is critical to be modeled and optimized such that a certain required level of system reliability can be met.

Maintenance is a critical issue particularly for systems such as wind turbines which are typically installed in remote areas and are not easily accessible or may require

special maintenance equipment, such as a crane. In addition, maintenance may be influenced by crew constraints. For example, in the case of simultaneous failures or multiple warnings from condition monitoring systems on a wind farm, a limited number of maintenance crew may cause additional maintenance delays. The hybrid analytical-simulation approach proposed intends to provide a model for the operation and maintenance (O&M) of a deteriorating system, such as a wind turbine, determine the optimum maintenance, and address the effect of maintenance constraints on the availability and total gain (average revenue per unit time) of the system.

There have been numerous research studies in maintenance and its optimization. Due to the probabilistic nature of deterioration and failure of equipment, stochastic models have proven to be more suitable for maintenance studies.

Among the analytical techniques, Markov models have been widely adopted in the literature [87]-[68]. Markov Decision Processes (MDP), and semi-Markov Decision Processes (SMDP) have been used for maintenance optimization in various sections of a power system, such as traditional power plants [87], [88], substation equipment [89], and renewable energy sources [90], [91]. Time-based Markov models [92] are limited in the sense that they only consider time as a deterioration factor. To solve this problem, “inspection” has been added to the model to incorporate CBM as well [93]. However, current Markov models are still limited in modeling complex situations with deterioration, inspection, and maintenance [94], [95]. The model becomes even more complex by including the realistic aforementioned restricting factors affecting maintenance and repair.

Simulation models based on Monte Carlo simulation (MCS) have also been employed for maintenance studies. MCS may be performed to study a power system [96], [97] or its individual pieces of equipment [98], [99]. The main goal of these studies is generally to determine the optimum maintenance policy considering cost and overall reliability. MCS is favorable because it can also be applied to system states with non-exponential distribution times without an extra computational burden [100]. However, due to the need for a large sample size, utilizing MCS for maintenance optimization could be computationally intensive.

None of the previous research has incorporated both maintenance optimization and the consequences of restricting conditions, such as extended duration of maintenance/repair, lead time, and opportunity costs, on the availability and profit of the system. Here, we develop a hybrid of analytical and simulation methods incorporating SMDP and a replicated sequential-based MCS model for wind turbines in order to determine the optimum maintenance strategy and, at the same time, the effect of maintenance constraints on the availability and gain of the system. By choosing a hybrid method, we benefit from the combined aforementioned advantages of both types of modeling.

In the first stage, it is computationally more efficient to use an analytical method, similar to the SMDP introduced in [93], to obtain the optimum maintenance of equipment, such as a wind turbine, under different decision policies. Then, the MCS-based model is developed emulating the SMDP and validated through comparison of the results. In the second stage, the MCS-based model developed is employed to analyze the effect of

maintenance and repair resource constraints on the availability and cost of the wind turbines.

The process for the proposed analytical and simulation-based modeling can be summarized as follows:

- A. Build a SMDP model for operation and maintenance of a wind turbine, considering equipment deterioration, failure, inspection, and maintenance rates.
- B. Define the types of maintenance and decision options at different deterioration stages. Different combinations of possible maintenance decisions determine a set of applicable maintenance scenarios.
- C. Determine the optimum maintenance policy based on SMDP under various decision frequencies. Decision frequency is the rate at which the maintenance is feasible considering the actual operational constraints. Therefore, in this step, an optimum maintenance policy is determined for each decision frequency.
- D. Develop an MCS-based model according to the state diagram of Step A and determine the optimum maintenance policy. In this step, MCSs are run iteratively for each possible maintenance policy; and the expected gain for each scenario is determined. The optimum policy is the one with the highest expected gain.
- E. Validate the MCS-based model by comparing the results from Steps C and D.

- F. Study the effect of maintenance constraints, such as maintenance lead time and repair crew readiness, on availability and cost of a single wind turbine and a group of wind turbines on a wind farm with the MCS model.

3.2.5.1 Analytical approach

The state transition diagram of the analytical semi-Markov processes model is shown in Fig. 3.12 [93]. The model is comprised of three operating states, D_i ; $i = \{1, 2, 3\}$ representing three deterioration stages where D_1 implies “like new” condition and the condition of equipment deteriorates by moving toward D_3 . Eventually, the deterioration leads to a failure state, F_1 , where it would require substantial repair in order to bring the equipment back to its initial working state. There is also another type of failure due to random events denoted by F_0 . In this model, λ and μ represent transition rates between adjacent states, where λ_i is a random failure rate originating from D_i ; and μ_j ($j = \{0, 1\}$) is the repair rate after failure F_j . M_i and m_i denote major and minor maintenance at the deterioration stage, i , respectively. Following a maintenance activity, equipment should be in a better condition; however, there is a possibility that its condition worsens due to defects in replacement parts or human error. Therefore, the next state after visiting an M_i or m_i state can be either one of the D_i states or an F_1 state; and their transition rates are denoted by $\lambda_{M_i-D_i}$, $\lambda_{m_i-D_i}$, $\lambda_{M_i-F_1}$, and $\lambda_{m_i-F_1}$. The rates of leaving the major and minor maintenance states, μ_M and μ_m , are the same at each deterioration stage and can be defined using Eq. 3.23 and Eq. 3.24, respectively. These rates are inversely related to the duration of the maintenance.

$$\mu_M = \left(\sum_{k=1}^3 \lambda_{M_i-D_k} \right) + \lambda_{M_i-F_1} , \quad i = \{1, 2, 3\} \quad (3.23)$$

$$\mu_m = \left(\sum_{k=1}^3 \lambda_{m_i-D_k} \right) + \lambda_{m_i-F_1} , \quad i = \{1, 2, 3\} \quad (3.24)$$

In formulating SMDP, for each level of deterioration, a decision can be made from the three possible options: d_1 (do nothing), d_2 (do major maintenance), or d_3 (do minor maintenance). The “Inspection” state in an SMDP model is where the decisions are made; and, therefore, they are represented by “Decision” states in our model. The availability of the wind turbine in this model is defined as the fraction of the total time in which the turbine is in either of the operating states, D_i .

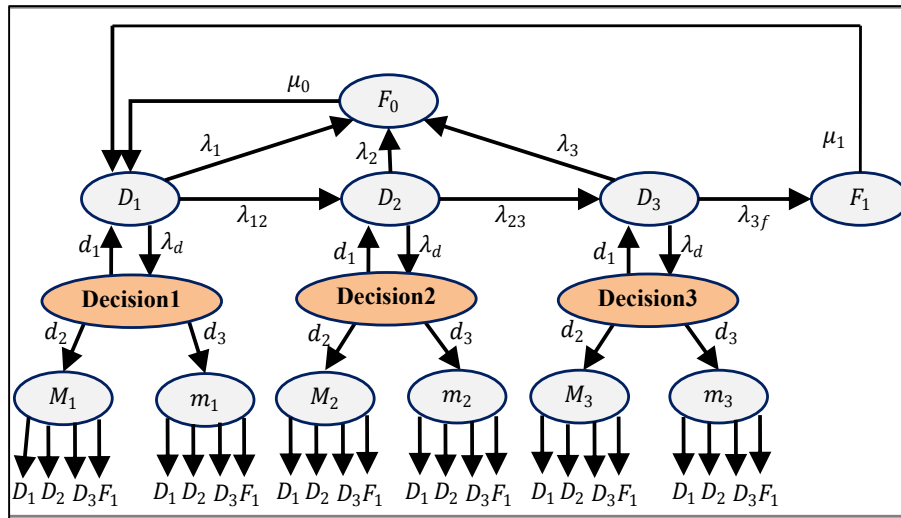


Figure 3.12 State transition diagram for SMDP study of deteriorating equipment

Generally, there are three methods to solve this problem: Linear Programming, Value Iteration, and Policy Iteration. Linear Programming usually requires higher number of iteration to reach an optimal policy; and Value Iteration method is suitable for discrete-time Markov decision processes [54], whereas in this dissertation, the Markov process is

continuous. Therefore, the policy iteration approach is used to solve this SMDP scheme [101]. In this method the preliminary step is to select of an initial policy; then, there is an iterative process with two main steps to evaluate and improve the policies until an optimum policy is determined.

In the evaluation step, a policy is assessed by solving a set of Eq. 3.25 which calculates the gain, g , and the relative values of this policy.

$$v_i + g = q_i t_i + \sum_{j=1}^N \Gamma_{ij} v_j \quad i = 1, 2, \dots, N \quad (3.25)$$

where v_i , q_i , and t_i are the relative value, the earning rate, and the sojourn time of state i , respectively. Γ_{ij} represents the transition probability from state i to j , and N is the total number of states.

In the policy improvement step, the relative values derived by solving Eq. 3.25 are utilized. For each state i , a search is performed for an alternative, a , that maximizes the test quantity, G_i^a , expressed by Eq. 3.26.

$$G_i^a = q_i^a + \left(\frac{1}{t_i^a} \right) \left[\sum_{j=1}^N \Gamma_{ij}^a v_j - v_i \right] \quad (3.26)$$

This alternative is set as the new decision in state i , and the process is repeated for all states to determine the new policy.

It should be noted that the process explained above solves SMDP for a specific decision frequency, λ_d . However, the optimum maintenance policy may vary based on the feasibility of the intended maintenance frequency. To address this aspect, SMDP should be solved for different decision frequencies.

3.2.5.2 *Simulation approach*

A MCS model is developed based on the same set of states described for SMDP using Rockwell Arena software. The model developed is illustrated in Fig. 3.13 where the wind turbine enters the simulation environment and travels within the state space for a designated lifetime. Then the simulation is repeated with the required number of replications to determine confidence intervals.

The majority of the states in the SMDP configuration are modeled by three components representing sojourn time, expected reward, and transition probabilities, in the Arena model. First, the block representing the sojourn time imposes a delay with a desired probability distribution. Next, the expected reward associated with that state is allocated. Finally, a decision block is used to assign transition probabilities between the states. The failure states, F_0 and F_1 , do not require the third component mentioned above because the next state after a failure is always D_1 . In each iteration of the MCS, the equipment starts at D_1 and travels through the states based on the probabilities defined. At the end of the simulation, Arena calculates the expected output parameters, such as the average gain and the availability of the system.

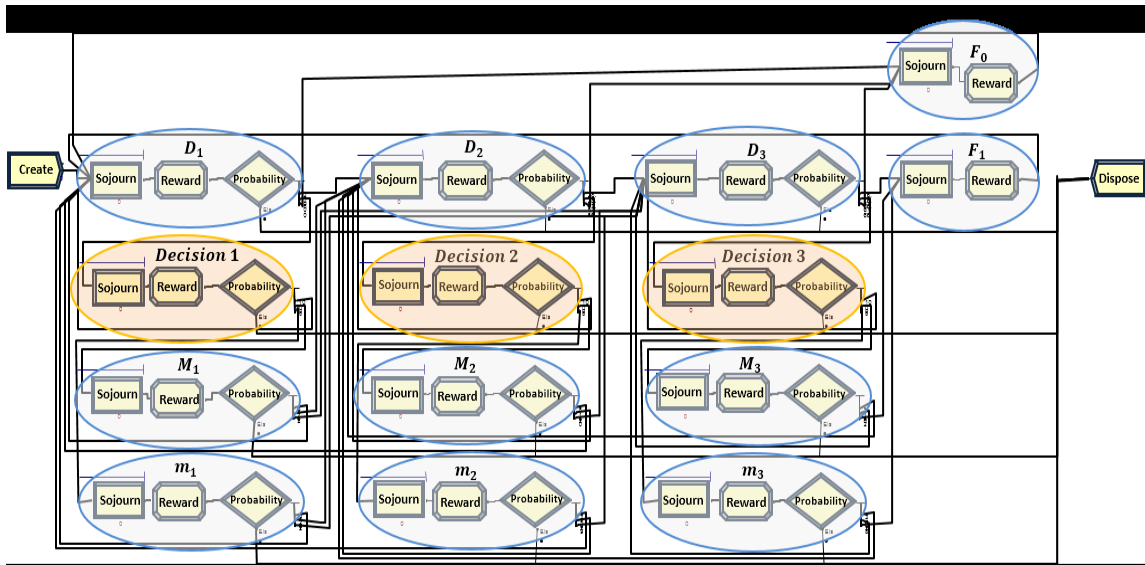


Figure 3.13 State transition diagram for MCS-based modeling of deteriorating equipment

In addition, using this model, a cost analysis is performed and the opportunity cost of the wind turbine in different conditions can be compared. Here, the opportunity cost is defined as the amount of expected profit that would have been realized had the wind turbine not operated below a reference availability.

The opportunity cost of wind turbine k for duration of T can be calculated from Eq. 3.27.

$$OC_k = \Delta A_k \cdot T \cdot P_{out_k} \cdot CF_k \cdot \overline{PR} \quad (3.27)$$

where OC_k and ΔA_k are the opportunity cost and relative availability compared to the reference case, respectively; P_{out_k} is the rated output power of the turbine; CF_k represents the capacity factor of the wind turbine determined based on the wind resource of the area; and \overline{PR} is the expected rate of profit from selling the electricity generated.

CHAPTER 4

RELIABILITY OF

SMART POWER DISTRIBUTION SYSTEM

4.1 Introduction to Smart Power Distribution Systems

4.2 Modeling of Smart Distribution Systems (SDS)

4.3 SDS Reliability with Demand Side Management

4.4 SDS Reliability with Energy Storage System

4.5 Optimum DER Capacity for Reliable SDS

4.6 SDS Reliability with Active Customer Interactions

4.7 Summary of the Models and Proposed Studies

4.1 Introduction to Smart Power Distribution Systems

A power system, as a critical energy-providing structure, must continuously adopt new technologies in order to improve its efficiency in terms of reliable operation and cost. Smart grid is a general term recently used to label the emerging power grid resulting from current technological adoptions in power systems [6]. This new type of grid incorporates recent improvements in different areas of engineering and science and, for the most part, in communication and networking in order to operate more efficiently [5]. As more real-time data become available through the sensory devices, the power system becomes more alert and responsive to the potential contingencies and the reliability of the system may be improved.

A smart grid in a power distribution system may be called a “smart power distribution system” which accommodates new types of loads/generations, such as electric vehicles/distributed renewable generation (wind, PV), etc. In a conventional power distribution system, most of the demand side management programs consider the load control problem from the grid’s perspective. In a smart distribution system, however, the bidirectional data flow and interoperability between the end-user equipment and the grid have created an opportunity to optimize an individual customer’s power consumption, and, at the same time, enhance the overall system-wide operation of the grid through peak load alleviation. In other words, the customers’ objective to minimize their electricity bills is in agreement with the grid’s intention to flatten the total demand curve.

Implementation of distributed generation and battery storage systems enable electricity customers and small businesses to make profit by selling excess generated power back to the grid. In the paradigm of the smart distribution system, individual customers can be active power grid participants by continuously making rational decisions to buy, sell, or store electricity based on their present and expected future amount of load, generation, and storage, considering their benefits from each decision.

Electrical engineers are required to model and study the future power distribution system including its new types of customer loads as well as the behavior of the customers, in order to operate and plan for the system reliably and efficiently. In a smart power distribution system, due to the large number of potentially active consumers diversely distributed in the system, it is difficult to grasp the overall aggregated behavior of the consumers. Therefore, in recent years, more research efforts have focused on distributed approaches for demand-side modeling and control [102], [103].

4.2 Modeling of Smart Distribution Systems (SDS)

With the advent of the smart grid and smart power distribution systems, many recent studies have focused on simulating these systems and interactions between the customers and the grid with different perspectives, such as cost reduction [104], efficient load management, etc. [105], [106]. It is challenging to include unpredictability and dynamism introduced to the future power system as a result of supplying a large number of prosumers with varying demands and renewable generation volatilities, each with their own aims and priorities, operating within an uncertain environment affected by the power system contingencies and the outcomes of actions taken by individual customers [107].

Due to these complexities, there may be many details and approaches to model a smart grid. In this dissertation, we propose three models of smart distribution system that can be used for power system studies, such as reliability assessment. These models are developed using different simulation programs and with different perspectives. Hereafter, we call these models SDS (smart distribution system) model-I, model-II, and model-III. The software used for these three models are Repast symphony, MATLAB, and DIgSILENT Power Factory, respectively.

4.2.1 SDS model-I

SDS model-I is based on distributed modeling of power system customers within the power system. As far as distributed grid modeling, techniques based on multiagent systems (MAS) have been adopted due to their versatility, scalability, and ability to model stochastic and dynamic interactions among customers (as agents) and between a customer and the grid. Indeed, there have been several MAS-based applications in the power system literature, such as electricity market [108], [109], voltage control [110], load restoration [111], load shedding [112], and the smart grid area [113], [114].

None of the power system models have fully utilized the smart distribution system features described in Section 4.1. The research is either descriptive without any experiments [115], or the capabilities of the smart customers are simplified and restricted to such an extent that the problem may even become solvable without an MAS design [113]. The inability of the customers to generate power is an example of those restrictions [116]. An efficient load management system, with green energy and conventional power suppliers, is proposed in [114], aiming to reduce electricity cost and carbon emissions.

Nevertheless, the ability of customers to generate electricity, adjust their load based on the price signal, and sell electricity back to the grid has not been included in this paper.

Here, we propose and discuss customers that not only consume electricity but are also capable of generating and storing it using their own power generation and electricity storage system. Taking it one step further, we consider these customers to be flexible and make autonomous decisions to manage their load, generation, and electricity storage. Moreover, they can interact with the grid to trade electricity in a way that benefits them the most.

This system has been implemented using Repast Symphony software [117], based on the Java programming language. Repast Symphony is the latest version of Repast (REcursive Porous Agent Simulation Toolkit), a powerful tool designed to provide a visual platform for an agent model and spatial structure design, agent behavior specification, model execution, and results examination [118].

Our approach is to model the customers as agents in a smart grid environment. Each individual agent tries to minimize its cost of electricity by making decisions from the following options: buy electricity from the grid, charge or discharge batteries, sell electricity to the grid, and, sometimes, ignore low priority loads. Decisions made by the customers affect the electricity market and vice versa. Therefore, sound decisions are critical to lead the entire system toward efficient and reliable operation. Fig. 4.1 shows different entities of the model as well as possible directions of electricity flow, illustrated by the arrows.

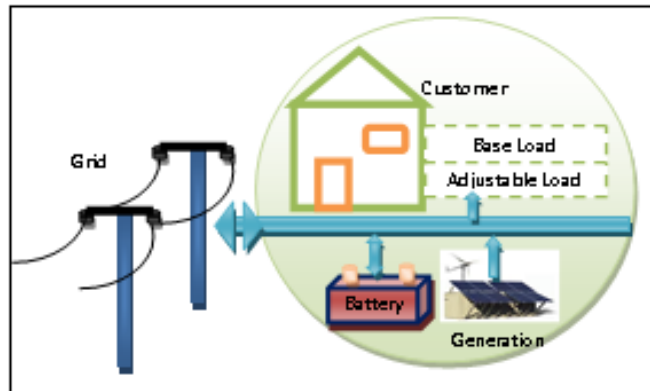


Figure 4.1 Different entities of SDS model-I

4.2.1.1 Electrical grid and electricity rate

The electric grid in SDS model-I is modeled as a simple agent that is responsible to balance the generation and the load at each time step, i.e., it buys the surplus generation of the customers or sells to them the amount of electricity demanded. The amount of sold-back power by each customer, however, may be limited according to a contract, due to the grid operation load flow constraints and/or stability considerations. The power sell-back limit is considered in this dissertation but the stability analysis is out of the scope of this study.

The rate at which the electricity can be purchased from the grid is electricity purchase rate (EPR) calculated as a function of the customers' electricity demand from the grid. There are two rates associated with each hour: the rate announced before the submission of the household's electricity demand (e.g. day-ahead), $EPR(t^-)$, and the real-time rate after the demand requests have been received by the utility, $EPR(t)$.

Due to the correlation between the prices of electricity per hour in nearby consecutive days [103], the early announced electricity rate is modeled based on the weighted sum of past days' electricity rates at the same hour, as expressed by Eq. 4.1.

$$EPR(t^-) = \sum_{d=1}^m k_d \cdot EPR(t - 24 \cdot d) ; \sum_{d=1}^m k_d = 1 \quad (4.1)$$

where k_d is the weighting factor to model the correlation between the price on the current day and that on d days ago; and m is the number of days to be included from the past.

$EPR(t)$ represents the modeled electricity market by fitting a typical set of points (electricity price, load demand) [119] into a monotonically increasing function and normalizing it for each household, as expressed by Eq. 4.2.

$$EPR(t) = \alpha_1 \cdot e^{\alpha_2 \cdot \bar{l}(t)} + \alpha_3 \cdot e^{\alpha_4 \cdot \bar{l}(t)} \quad (4.2)$$

where α_1 to α_4 are coefficients of the fitted function and $\bar{l}(t)$ represents the actual load demand of the average customer for hour t in kWh.

Customers with generation-battery systems may sell their excess electricity to the grid at EPR or at a different rate named electricity selling rate (ESR), which could be lower than the EPR.

4.2.1.2 Customers

Customers are the agents of the MAS model. Each customer agent may have the properties, such as the demand (installed load; actual hourly load), load priority, renewable generation (capacity; actual hourly generation), and electricity storage (capacity; available storage). The model allows inter-customer communication and power transaction, and it includes various load sectors (e.g., residential, commercial, industrial) and renewable generation technologies (e.g., wind, PV).

Each customer sector has its own average load profile for a 24-hour period. In our model, the average demand of a load category at each hour of the day is used to calculate

the expected load of the corresponding customers during that hour based on a normal distribution. The demand of the customers may be met by their own resources or by the power purchased.

The features of a customer in a SDS model-I are shown in Fig. 4.2. An active customer may utilize these resources to reliably meet its electric demand.

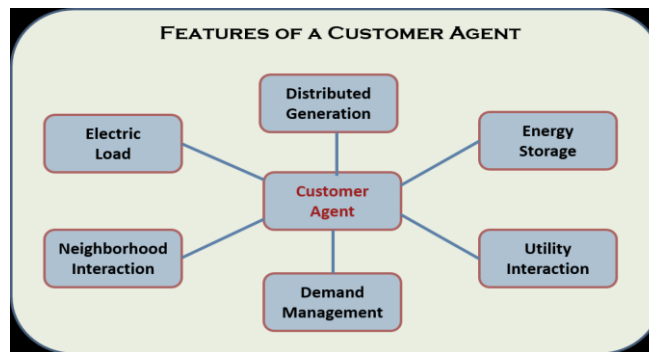


Figure 4.2 The features of an active customer agent in SDS model-I.

The neighborhood of a customer includes all the geographically close customers with whom direct electric connection and data communication are permissible. Within a neighborhood, the customers are able to establish peer-to-peer communication and trade electricity. Each customer may belong to several neighborhood communication networks at the same time. The communication infrastructure allows the customer agents to demand electricity from their neighbors upon an interruption in the electric network and determine when their load exceeds the summation of their local generation and stored power. The details of the neighborhood configuration in our model have been provided in [120].

4.2.1.3 Renewable generation and storage system

The hourly output power of two renewable generation systems (wind and PV) are modeled using probability distributions. Hourly wind speed can be adequately represented by the Weibull distribution [121]. A simple power curve formula is then used to calculate the hourly wind power generation (in MW) as described by Eq. 4.3 [122].

$$g_w(t_j) = \begin{cases} Cap_W \left(\frac{V_W(t_j) - V_{ci}}{V_r - V_{ci}} \right) & V_{ci} \leq V_W(t_j) \leq V_r \\ Cap_W & V_r \leq V_W(t_j) \leq V_{co} \\ 0 & otherwise \end{cases} \quad (4.3)$$

The output power of a PV system depends on a variety of parameters, including environmental factors (e.g., temperature, cloud cover, dust, etc. [23]) and solar panel related (e.g., technology, type of installation, etc. [123]). We use the daily mean hourly solar irradiance data and assume the irradiance for different hours follow normal distributions. Next, the PV generation in MW is calculated using Eq. 4.4 [124].

$$g_{PV}(t_j) = \begin{cases} Cap_{PV} \left(\frac{IR(t_j)^2}{IR_{std} \times IR_C} \right) & IR(t_j) \leq IR_C \\ Cap_{PV} \left(\frac{IR(t_j)}{IR_{std}} \right) & IR_C \leq IR(t_j) \leq IR_{std} \\ Cap_{PV} & IR(t_j) \geq IR_{std} \end{cases} \quad (4.4)$$

In Eq. 4.3 and 4.4, Cap_W and Cap_{PV} are wind turbine and PV rated capacities. $V_W(t_j)$ and $IR(t_j)$ represent wind speed and solar radiation at time t_j in m/s and W/m^2 respectively. V_{ci} , V_{co} , and V_r denote cut-in, cut-out, and rated wind speed, respectively; finally, IR_C and IR_{std} are irradiance at specific point of power change and standard environment set, typically $150 W/m^2$ and $1000 W/m^2$ respectively [124].

The electricity storage system is modeled by its capacity, possible charging rate and depth of discharge.

4.2.1.4 Demand side management (DSM)

Peak demands in the existing power systems are caused by large load variations for industrial, commercial, and residential customers during different hours of a day. Residential customers, for example, are usually at work during the day; and as they return home and start using appliances and lights in the evening, the electricity demand escalates. Likewise, the peak load hours of industrial and commercial customers depend on the particular business and workload. A power system infrastructure should be designed to be capable of handling this peak load which lasts only a few hours. This results in a lot of overinvestment and inefficient asset utilization. Furthermore, power generation at high demand hours is more costly than at base load hours. Therefore, from the grid's perspective, it is desirable that the overall load profile come as close to a flat line as possible. By the same token, since electricity rates at peak demand hours are higher for consumers in a dynamic pricing scheme, customer agents prefer to better distribute or flatten their electricity usage throughout the day, as well. In the smart distribution systems, customers owning a generation/storage system have an opportunity to reduce their peak demand by compensating for part of their load with generated power. Considering that the availability of renewable generation does not necessarily coincide with the peak load, customers need to store the electricity generated or shift their loads in time.

There are two demand side management programs proposed for SDS Model-I; *Utility-based method*, and *Average Deficit method*.

In the *Utility-based method*, customer agents autonomously make decisions by comparing the utilities of their available options. There are three utilities used by the agents to assign priorities to decision options of a customer. In each time step, agents use their load data and determine the priority of that load by assigning a *Load Utility*. The agents also receive the current wind speed and the electricity price for that time duration (e.g. one hour). Customers have their predicted future load, generation, and the electricity price. Using these parameters, the agent computes its utility of storing the electricity, *Store Utility*, or selling the available generation to the grid, *Selling Utility*. Based on a comparison of these utilities, which are normalized between 0 and 1, the agents make their decision for the current hour.

In a case where a restriction occurs, the DSM prevents the execution of the decision with the winning utility, and the next highest priority decision will be selected to avoid any constraint violations in the system. Examples of these restrictions can be the maximum power purchased by the grid and the maximum available charging capacity of the battery.

Generally, with the *Utility-based method*, the customer agents try to avoid buying electricity when the prices are high in order to save on their electricity bills. Each hour, the agent will encounter one of the following situations: a generation surplus or a generation deficit. A generation surplus occurs whenever the amount of electricity generated is higher than the amount of the load demand, and a generation deficit occurs

when the load demand is greater than the amount of electricity generated. When a customer agent is in generation surplus mode, it looks for the most profitable decision between three possible options: supplying the load, charging a battery, and selling to the grid. It chooses the option with the highest utility. On the other hand, if the customer agent is in the generation deficit mode, it aims to manage the situation at the lowest possible cost, which means the agent searches for the decision with the lowest associated utility to take care of the electricity deficit. If it turns out that the lowest utility belongs to its own load, i.e., load utility is the minimum, the agent will reduce the load for that hour because the utility implies that the load is not having a high enough priority. Load reduction may be managed by adjusting the thermostats, and/or turning off the lights and low priority appliances. According to the design of the *Utility-based method* the demands are not shifted in time. The details of the three utilities are provided as follows:

- *Load Utility (LoU)*

Load Utility is a random number between 0 and 1, and models the priority of the load to be satisfied at a specific hour relative to other decision utilities. If the demand has a higher priority for a customer at a specific hour, the *Load Utility* for that customer will be set closer to 1 at that hour. In fact, load priority evaluates customer agent's behavior and preferences. The actual value of this utility depends on many other factors which are not in the context of this study.

- *Selling Utility (SeU)*

Selling Utility represents a customer agent's incentive to sell its excess electricity to the grid. SeU is defined such that as it decreases, there will be more motivation to buy

from the grid instead of selling to it. Eq. 4.5 is empirically derived for each customer i based on the fact that customer benefits more from selling back to the grid whenever it has additional generation and the electricity rate is higher.

$$SeU_i(t) = \begin{cases} \sqrt{\frac{ESR(t^-)}{\max_{t \leq t' < t+\tau} (ESR^P(t'))} \cdot \frac{(g_i(t) - l_i(t^-)) \cdot ESR(t^-)}{\max_{t \leq t' < t+\tau} ((g_i^P(t') - l_i^P(t')) ESR^P(t'))}} & \text{if } g_i(t) > l_i(t^-) \\ \frac{EPR(t^-)}{\max_{t \leq t' < t+\tau} (EPR^P(t'))} & \text{if } g_i(t) < l_i(t^-) \end{cases} \quad (4.5)$$

where $g_i(t)$ and $l_i(t^-)$ are the amount of wind generation and the initial load of household i . Index P identifies the predicted variable, and τ is the desired foreseen duration for utility calculation. EPR and ESR have been previously defined in this chapter. If the generation of a customer for the current hour is higher than the load ($g_i(t) > l_i(t^-)$), there will be a high incentive to sell that power to the grid because either that customer has a large generation or the current ESR is higher than its future's predictions. A geometric mean is used to include both parameters and keep the utility within the defined limits. On the other hand, if the generation is less than the load ($g_i(t) < l_i(t^-)$), the customer agent should buy from the grid when the cost of supplying the remaining demand is low enough compared with the future predicted costs.

To compute SeU, customer agents obtain the current hour selling price, $ESR(t^-)$, from the grid and use a normal distribution to predict the required variables for the duration of τ . Higher values of SeU(t) imply that, by selling to the grid at the current hour t , customers get more benefit than if they wait to sell at future hours.

- *Store Utility (StU)*

Store Utility represents a customer agent's incentive to store electricity. With a similar approach to what was described for the *Selling Utility*, StU is defined by Eq. 4.6 which can be perceived as an analogous to Eq. 4.5 except that all of the parameters used here are estimated future values.

$$StU_i(t) = \begin{cases} \frac{\text{Average}_{t < t' < t + \tau} (ESR^P(t'))}{\max_{t < t' < t + \tau} (ESR^P(t'))} \\ \text{for all } g_i^P(t') > l_i^P(t'), t < t' < t + \tau \\ \sqrt{\frac{\text{Average}_{t < t' < t + \tau} (EPR^P(t')) \cdot \text{Average}_{t < t' < t + \tau} \left((l_i^P(t') - g_i^P(t')) \cdot EPR^P(t') \right)}{\max_{t < t' < t + \tau} (EPR^P(t')) \cdot \max_{t < t' < t + \tau} \left((l_i^P(t') - g_i^P(t')) \cdot EPR^P(t') \right)}} \\ \text{for all } g_i^P(t') < l_i^P(t'), t < t' < t + \tau \end{cases} \quad (4.6)$$

where averaging is utilized to capture the overall trend of the predicted decision variables in the future. Generally, customer agents may want to store electricity in order to sell it to the grid if they expect to generate enough electricity in the future ($g_i^P(t') > l_i^P(t')$) at a high price. If the expected generation is less than the expected load ($g_i^P(t') < l_i^P(t')$), agents will be willing to store electricity if they predict having a large power deficit or high electricity rate in the future.

Fig. 4.3 shows the decision making diagram of the Utility-based method.

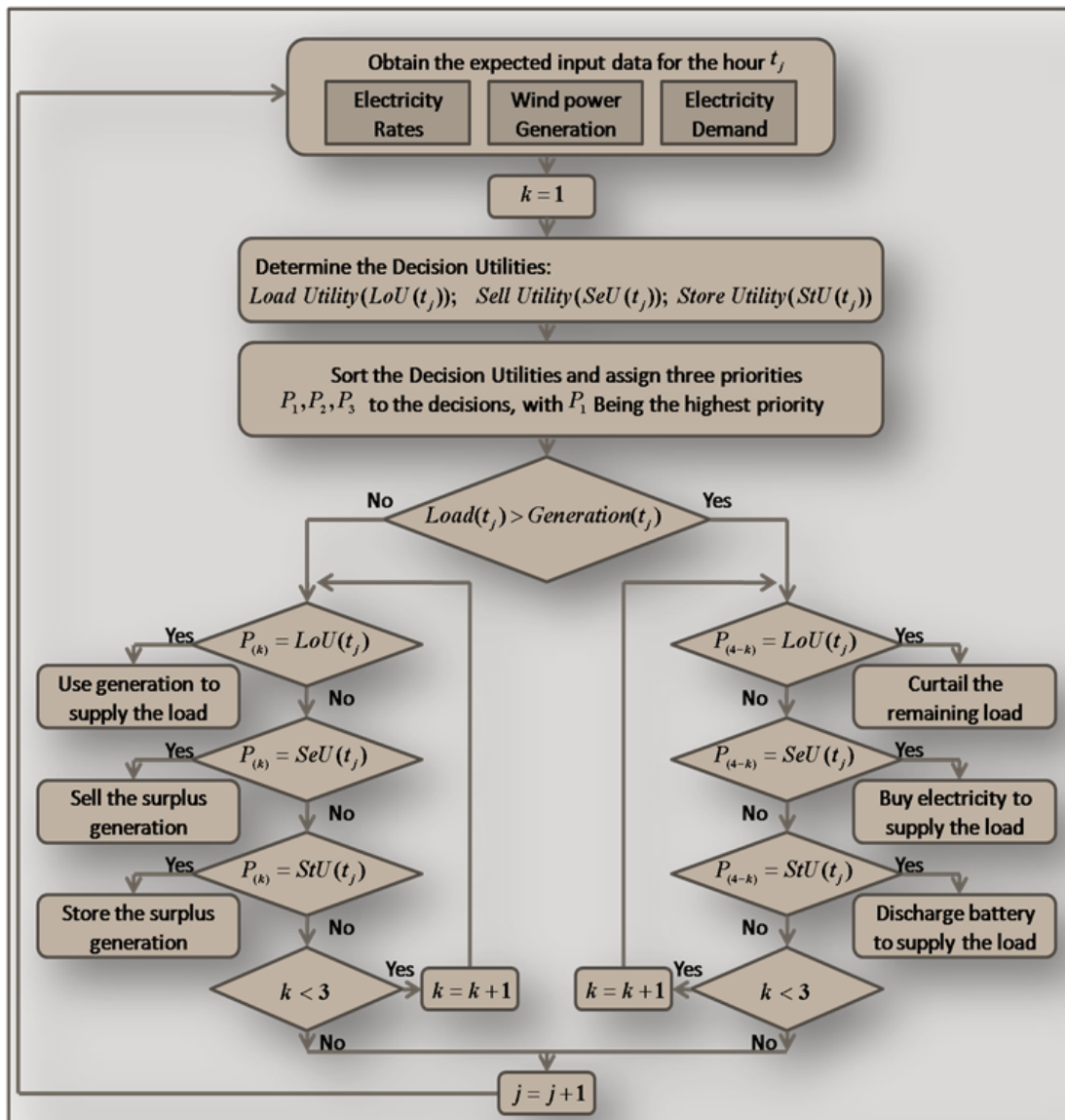


Figure 4.3 Illustration of the *Utility based method* for DSM

Study results have shown that using *Utility-based method* for DSM modifies the electricity prices to be modified, and customer agents can successfully reduce their electricity costs by managing their load, generation, and storage [125]. In addition, the emergent behavior of the system is moving toward a flatter load curve and alleviation of peak demand which is desirable from the grid's perspective. Considering the cost of electricity generation and storage, we can also determine the inflection point where

conventional customers would benefit from purchasing their own local wind generation-storage system [125].

The *Average Deficit method* is based on customers shifting their load and using DER to alleviate their peak demand. In fact, the electricity rate exponentially increases with higher demand values. Therefore, a flatter electricity demand leads to less electricity cost for customers. The electricity deficit at hour j is defined by load minus generation for that hour for each customer.

$$def(t_j) = l(t_j) - g(t_j) \quad (4.7)$$

Thus, a negative deficit becomes feasible when there is excess generation available. Eq. 4.8 calculates the mean deficit over the duration of past t_0 hours.

$$\overline{def(t_j)} = \sum_{t=t_j-t_0}^{t_j} \frac{def(t)}{t_0} \quad (4.8)$$

To demonstrate the proposed method, assume that $def(t)$ of a customer is as shown in Fig. 4.4. There are two conditions based on whether the amount of deficit at the current hour is below or over the average deficit line.

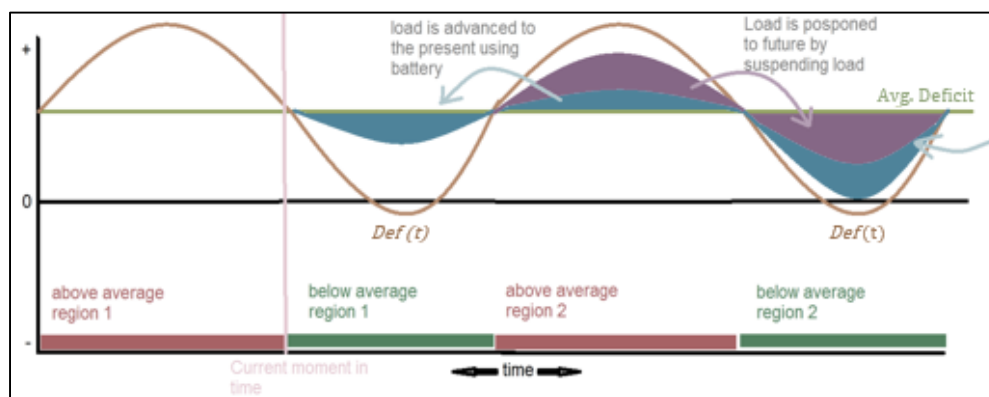


Figure 4.4 Illustration of the *Average Deficit method* for DSM

At the beginning of a below average region, the customer agent starts to increase the demand by charging the battery with a percentage of the future expected above-average deficit. As the agent enters the above average region, it can gradually discharge the battery to reduce the demand toward the average deficit. In order to smoothly distribute the tasks of charge/discharge of the battery and/or the supply of the shifted demand over the above mean and below mean regions, two corresponding ratios $OMR(t_j)$ and $UMR(t_j)$ are defined, respectively.

$$OMR(t_j) = \frac{def(t_j) - \overline{def(t_j)}}{\sum_{t=t_j}^{t_e} (def(t) - \overline{def(t)})}; def(t_j) > \overline{def(t_j)} \quad (4.9)$$

$$UMR(t_j) = \frac{\overline{def(t_j)} - def(t_j)}{\sum_{t=t_j}^{t_e} (\overline{def(t)} - def(t))}; def(t_j) < \overline{def(t_j)} \quad (4.10)$$

where,

$$t_e = E(\min(t)): [t > t_j \ \& \ def(t_j) = \overline{def(t_j)}] \quad (4.11)$$

In the next step, if any unsupplied load is still remaining, the agent tries to postpone the shiftable part of that load ($l_{sh}(t_j) < l_{sh,max}(t_j)$) to the future. Finally, for the residual demand, the agent has to buy the power from the neighbors or the grid. The customers always redirect any requests to their neighbors before asking from the grid. Fig. 4.5 provides the flowchart of this method in more details.

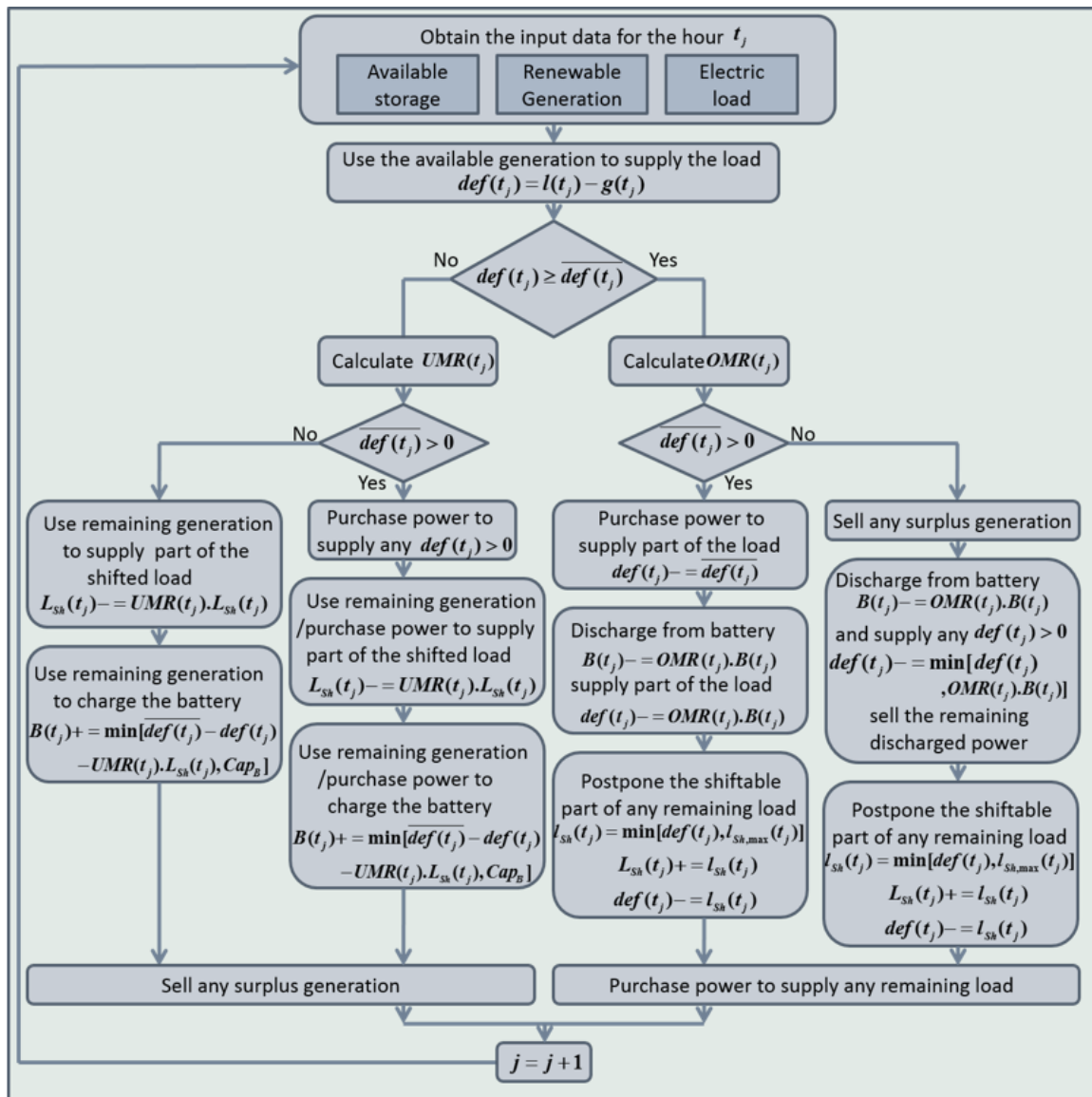


Figure 4.5 Flowchart of the proposed *Average Deficit method* for DSM

4.2.2 SDS model-II

The SDS model-II is aimed to be used for design and planning applications. Therefore, different components of this model is developed based on long-term stochastic behaviour of energy resources, load profile, and electricity rates. This model is developed using MATLAB software.

As mentioned before, the structure of a customer in a smart distribution system is comprised of loads, renewable generation and storage system, all of which are controlled by a DSM. A schematic similar to Fig. 4.1 may be used to show the power flow between different entities of SDS model-II. The power flow is bidirectional, which means electricity may be bought from or sold to the grid at any time. The models for different entities of the SDS model-II are explained in the following sub-sections.

4.2.2.1 Electrical grid and electricity rate

The power grid represents a utility that provides electricity to the customers and charges them based on a real-time pricing scheme. The electricity market prices, which are different at each hour of the day, are provided to the end customers [7] and denoted by EPR in this study. It has been indicated that real-time pricing signals will provide more operational information, enabling power system load flattening and peak demand reduction compared to other dynamic pricing methods [126]. The customers may have a power contract or net metering agreement with the utility (grid) that defines the rules and rates of buying and selling power [127]. These rules and grid connection requirements vary among different utilities and can address power quality and safety concerns as well [128]. It is assumed that the utility buys the excess electricity generated by its customers at ESR and provides them with electricity at EPR whenever they need it. However, the amount of sell-back electricity to the grid is limited. ESR is lower than EPR, and it is assumed to follow EPR by a constant difference of ΔR . The power flow constraint requires for any time, t_j , that:

$$\delta(t_j) = E_{Buy}(t_j) - E_{Sell}(t_j) - E_B(t_j) \quad (4.12)$$

$$E_{sell}(t_j) < E_{sell,max}$$

In this equation, $\delta(t_j)$ is the electricity demand of the customer defined as the total load minus generation at t_j . E_B is the energy charged in the battery. Therefore, negative values of E_B represent battery discharge.

The EPR data may be derived from the time series of the historical data from the utility. Then, the EPR for each hour, t_j , is separately analyzed and fitted to a probability distribution. As an example, analyzing the electricity rates from Ameren utility [129] indicates that these hourly electricity rates can best fit into either a normal or lognormal probability distribution described by Eq. 4.13, with the mean values shown in Fig. 4.6.

$$\begin{cases} EPR(t_j) \sim N(\mu_{r_j}, \sigma_{r_j}) & \forall j \in \{1, 2, \dots, 6\} \cup \{22, 23, 24\} \\ EPR(t_j) \sim \ln N(\mu'_{r_j}, \sigma'_{r_j}) & \forall j \in \{7, 8, \dots, 21\} \end{cases} \quad (4.13)$$

$\mu_{r_j} \in [0.8, 1.77]$, $\sigma_{r_j} \in [0.05, 0.15]$ and $\mu'_{r_j} \in [0.8, 1.77]$, $\sigma'_{r_j} \in [0.05, 0.15]$

where, μ_{r_j} and σ_{r_j} are the mean and standard deviation of the normal distribution; μ'_{r_j} and σ'_{r_j} are the location and scale parameters of the fitted lognormal distribution, for electricity rate, respectively.

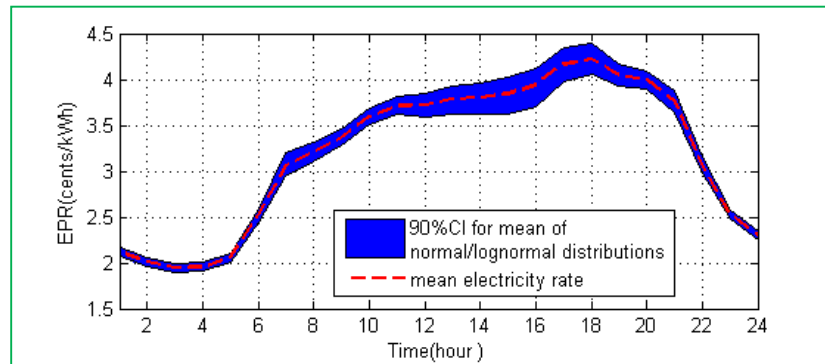


Figure 4.6 Mean EPR and 90% confidence interval for the fitted probability distributions

4.2.2.2 Customers

Customers in SDS model-II are represented by their loads which are classified into three categories: L_1 , L_2 , and L_3 . The first two categories basically define the customer's regular electricity consumption. The base load, L_1 , for a residential customer, consists of end-use devices whose power usage is predetermined and nonreschedulable, such as refrigerators and most lighting. The loads in the second category, L_2 , are shiftable in time and prone to delay. Washers, dryers, and dishwashers are often among the residential loads which can be delayed; but the task should be accomplished by a certain deadline. Air conditioners and water heaters may be assigned to either one of the first two categories according to customer preferences and level of comfort desired. The third category, L_3 , consists of unscheduled loads which may be plugged in without any predetermined plan. Hair dryers and electric drills may be included in the last category if it is impossible for the end users to schedule their use.

For example, using the average residential electricity consumption of a typical U.S. home [130], the base load may be modelled. In fact, the loads and the category they belong to are highly dependent on the electricity consumption behaviour of the households. The main appliances in the L_1 group consist of refrigerators, freezers, air conditioners, water heaters, lighting, microwave ovens, etc. [131]. For the long-term study, this load is assumed to follow the normal distribution for each hour. The mean base load this residential customer and the 90% confidence interval for the mean of hourly fitted distributions are shown in Fig. 4.7. The mean and standard deviation of the distribution are described by Eq. 4.14.

$$L_1(t_j) \sim N(\mu_{l_j}, \sigma_{l_j}) \quad \forall j \in \{1, 2, \dots, 24\} \quad (4.14)$$

$$\mu_{l_j} \in [0.8, 1.77], \quad \sigma_{l_j} \in [0.05, 0.15]$$

where, μ_{l_j} and σ_{l_j} are the mean and standard deviation of the normal distribution for the load, respectively.

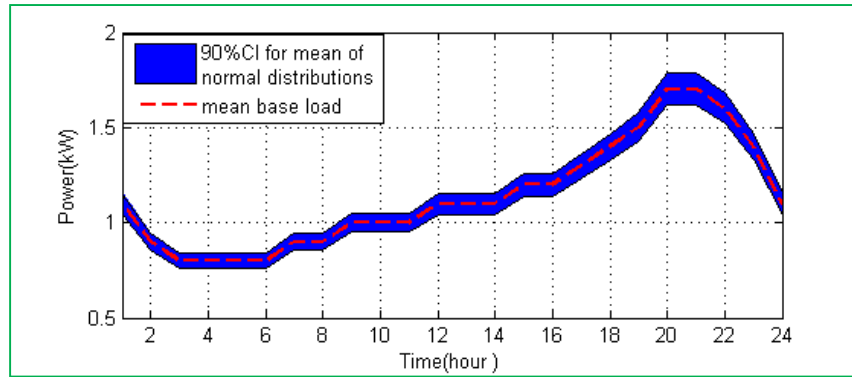


Figure 4.7 Mean base load and 90% confidence interval for the fitted normal distributions

4.2.2.3 Renewable generation and storage system

A wind turbine, as a renewable generation system, is used to explain the modeling. The power curve of the wind turbine can be modeled similar to what was explained in SDS model-I. The wind speed data for long-term studies are derived from the time series of the historical data from weather stations, and be fitted into the proper probability distributions. As an example, the long-term data from Kimball, Nebraska have been binned with the wind speed intervals of 0.5 m/s, and, for each hour, wind speeds can be best fitted into a Weibull distribution as denoted by Eq. 4.15. Therefore, 24 pairs of shape (λ_w), and scale parameters (K_w) can be generated for these fitted Weibull distributions. The mean wind speeds of the data for this example are shown in Fig. 4.8.

$$V_w(t_j) \sim \mathbf{WEIB}(\lambda_{w_j}, K_{w_j}) \quad \forall j \in \{1, 2, \dots, 24\} \quad (4.15)$$

$$\lambda_{W_j} \in [4.22, 7.61], K_{W_j} \in [1.65, 2.35]$$

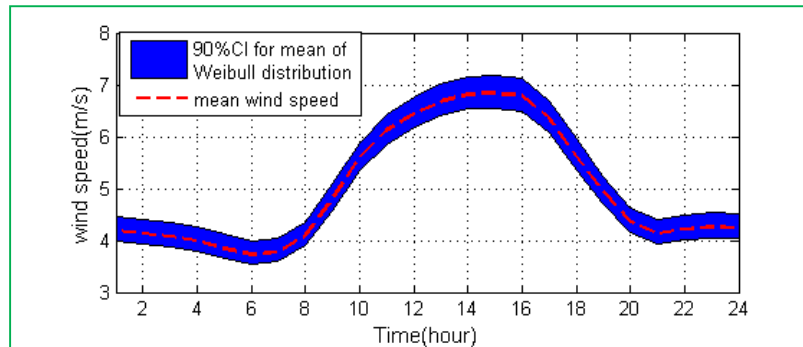


Figure 4.8 Mean wind speed and 90% confidence interval for the fitted Weibull distributions

The cost of generation, C_G , may be considered as an average cost known as the levelized cost of generation. This cost is calculated by dividing the costs of generation, including those for installation, operation, and maintenance, over the lifetime of the renewable generation system and is expressed as cents per kWh of power generation.

Next, an electricity storage system is critical for electricity management of the customers. There are two types of tasks defined for the storage system in SDS model-II.

Task 1: The primary task of this system is to store the surplus energy produced by renewable generation, which can be used to supply future demand.

Task 2: The secondary task assigned to the storage is to provide an opportunity to make a profit from electricity trade with the grid. The rationality of this task is that the customer buys and stores electricity at a low electricity rate and sells it back to the grid at a desired high electricity rate.

A variety of batteries with different cell technologies and prices are available on the market for use in electricity storage systems [132]. Two major factors affecting the cost of a battery are its technology and capacity. Meanwhile, there are a number of

parameters that affect the operation or lifetime of a battery. R_c , and DOD of the battery, are among the parameters considered in the model. R_c and DOD represent the allowable amount of battery charge /discharge per unit of time and the percentage of energy from the total capacity which can be withdrawn without damaging the battery, respectively.

During the operation, the DSM system should comply with the operational limits of the battery, defined by Eq.4.16.

$$\begin{cases} E_B(t_j) < R_c \times \Delta t \\ -E_B(t_j) < DOD \times Cap_B \\ B(t_j) < Cap_B \end{cases} \quad (4.16)$$

where, Δt , Cap_B , and $B(t_j)$ are simulation time step, battery capacity, and available battery charge at the end of time step j .

The total expected cost of a battery may also be considered as a levelized cost over its lifetime and is expressed as cents per kWh of storage capacity per hour.

4.2.2.4 Demand side management (DSM)

The DSM in SDS model-II is a rule-based program that manages the loads, the generation, and the storage system based on the day-ahead price signals announced to the customer. Fig. 4.9 shows the flowchart of the rule-based DSM for a T=24-hour period. A 24 -hour period was selected because first, it is the shortest duration that the tasks of the electricity management scheme, such as load shifting (all the delayed loads should be satisfied on the same day they are shifted), can be included independently; and second, the values of each stochastic variable at the same hour of different days have a good

correlation such that a specific probability distribution can be defined for that variable and that hour in the long term [133].

There are two sets of decision rules in this proposed DSM for obtaining the maximum benefit from the available facilities of the customers. The first set of rules manages the overall electricity generation, consumption, and *Task 1* of the storage system. This program starts with obtaining the statistics associated with loads, generation, and electricity rate. Then, the rules are applied to minimize the customer's electricity cost. In this scheme, if the generation is not sufficient to supply the total load ($\delta(t_j) > 0$), the decision is to discharge the battery and/or buy electricity from the grid to supply the remaining load. Otherwise, the surplus generation will eventually be stored or sold back to the grid. The remaining charge of the battery at the end of each period is carried over to the next one.

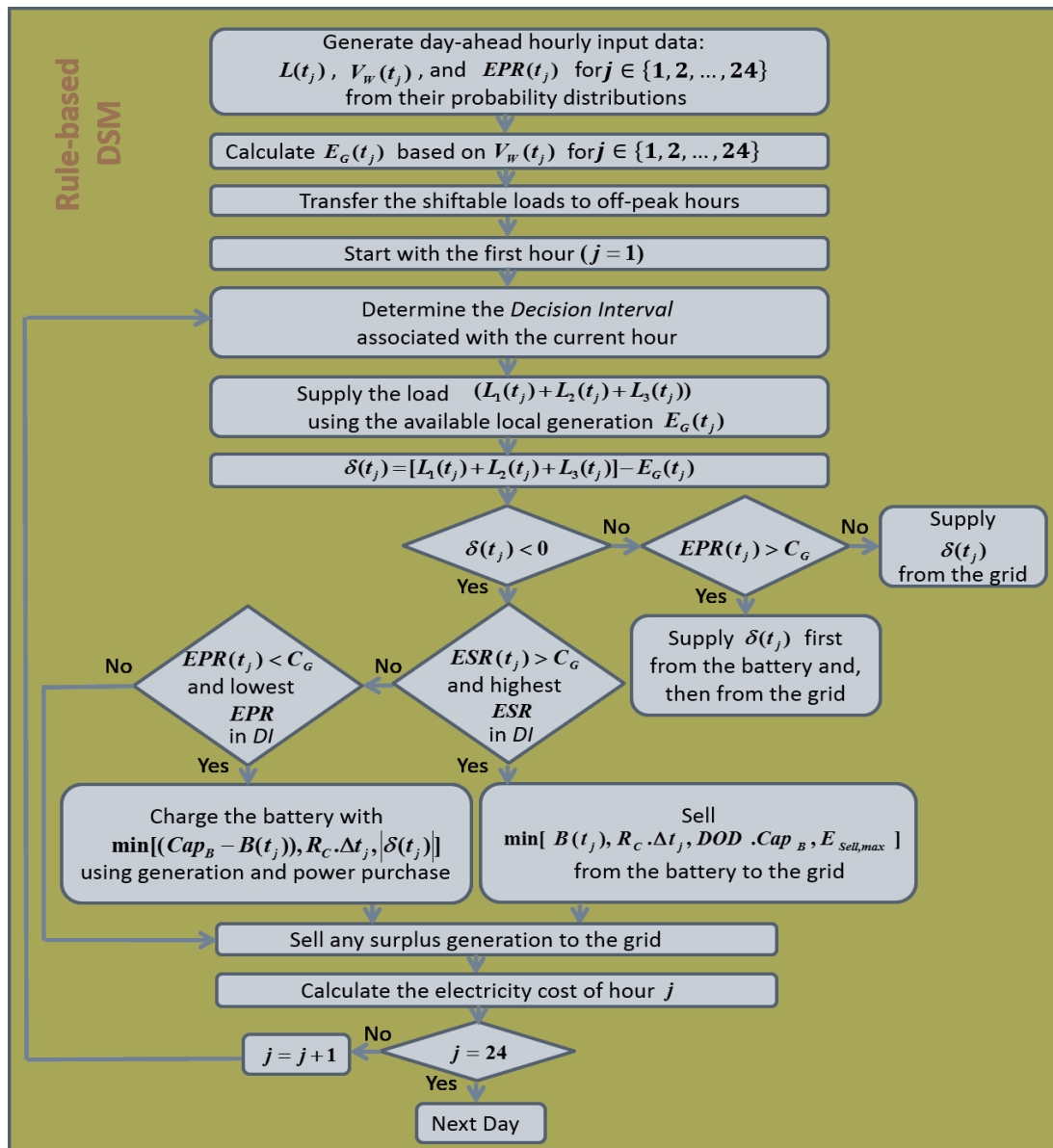


Figure 4.9 Flowchart of the rule-based DSM

The second set of rules mutually affects the battery storage system, along with the first set of rules, to perform *Task 2* of the storage system mentioned earlier. In this study, battery charge/discharge decisions, used for electricity trade-off with the grid, are made at extrema points of some predefined dynamic intervals. These *Task 2* decision intervals (DI) are defined as being between two consecutive intersections of leveled wind generation

cost (C_G) and EPR curves and may be from one to several hours long, as shown in Fig.

4.10. During each *Task 2* DI, the household is only allowed to buy/sell electricity from/to the grid once by charging/discharging its battery. While electricity trade using a battery is a profitable strategy for a customer, the definition of DI in this scheme aims to limit the number of charge/discharge cycles to extend the battery lifetime.

Fig.4.10 shows typical electricity rates, wind generation, battery decisions of *Task 2*, and a typical one-day load schedule.

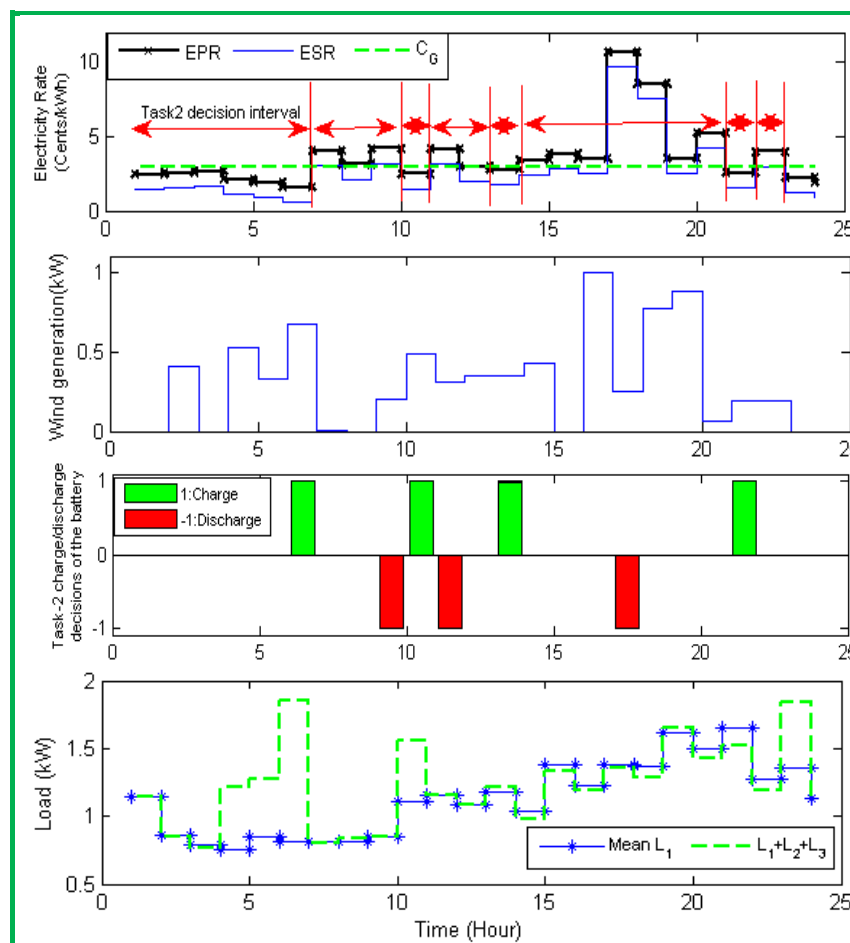


Figure 4.10 Typical variables determined and used by the DSM within a day

The bottom curves show both the mean L_1 load, based on which the load probability distribution is defined for each hour, and the resulting total load for a typical day. Due to stochastic behavior of the load, the actual load may be higher or lower than the mean base load at any hour. According to these determined variables, DSM analyzes the amount of power surplus/deficit of the customer which should be traded with the grid at each hour; and the cost of electricity is calculated accordingly.

4.2.3 SDS model-III

In the previous two models described for a smart distribution system, the main focus was on the customer model and customer initiated DSM, and little emphasis was put on modeling of the grid. However, in SDS model-III the focus is more on modeling the grid side and the customers' behavior and DSM are modeled using load curves.

4.2.3.1 Electrical grid

In SDS model-III we model a power distribution system in detail using the DIgSILENT Power Factory software. This software allows for including power flow required data such as bus rated voltage, power line impedance, load active and reactive power, etc. in our analysis. In addition, we can consider the power flow constraints of such system such as loading limits of power system branch components and operating voltage limit of the system buses.

$$\text{Constraints: } \begin{cases} \text{Loading}_{Line} < \text{Loading}_{Line}(\text{Max}\%) \\ \text{Loading}_{\text{Transfmr}} < \text{Loading}_{\text{Transfmr}}(\text{Max}\%) \\ V_{Min} (p.u) < V_{bus} < V_{Max} (p.u) \end{cases} \quad (4.17)$$

An example of a power distribution system model is provided in Fig.4.11. This system typically includes power lines and cables, transformers, buses, switches, loads, and external connections modeled using external grids.

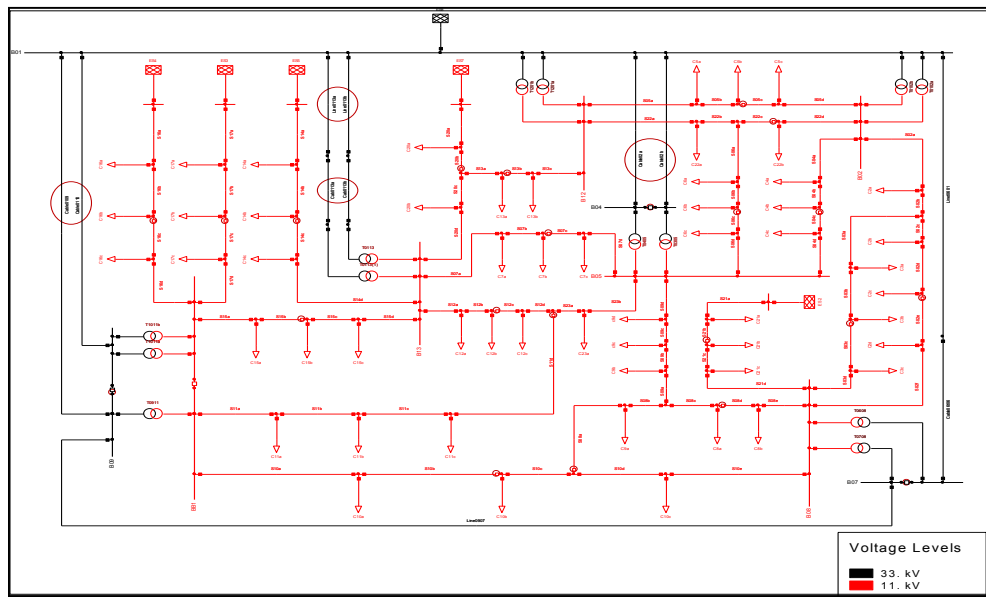


Figure 4.11 One-line diagram of a power distribution system model in DIGSILENT

4.2.3.2 Customers

The customers are modelled using their load curves. In SDS model-III, instead of modelling the renewable generation and storage system for each customer, the aggregated impact of the customers' demand and local generation may be considered using load curves. The load curves represent the hourly power or the percentage of peak load requested by the customers during a 24-hour period, such as the one shown in Fig.4.12. Therefore, the active and reactive power of the distribution system buses change on an hourly basis.

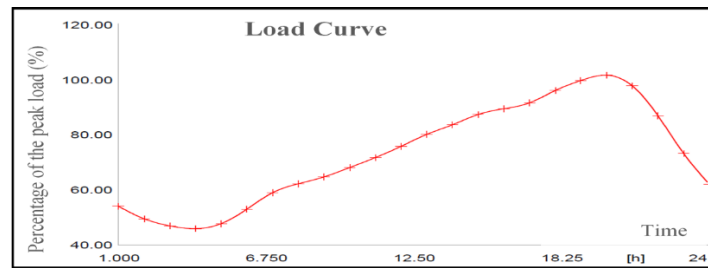


Figure 4.12 A typical load curve in SDS model-III

4.2.3.3 Demand side management (DSM)

As mentioned before, a DSM may adjust the load curves of customers through a variety of programs, such as peak clipping, load shifting, valley filling, energy conservation, etc. [66]. There are two demand side management programs proposed for SDS Model-III; *Energy Conservation*, and *Load shifting* methods.

The *Energy Conservation* method models the incorporation of various energy efficient strategies and equipment at the customer level as well as the system level such that the overall loading of the distribution system decreases.

The load curves for the *Energy Conservation* method are shown in Fig.4.13. Different percentages of load impacts due to the DSM are considered, where the decrease in the system load is uniformly modeled throughout a day using different load scaling factors.

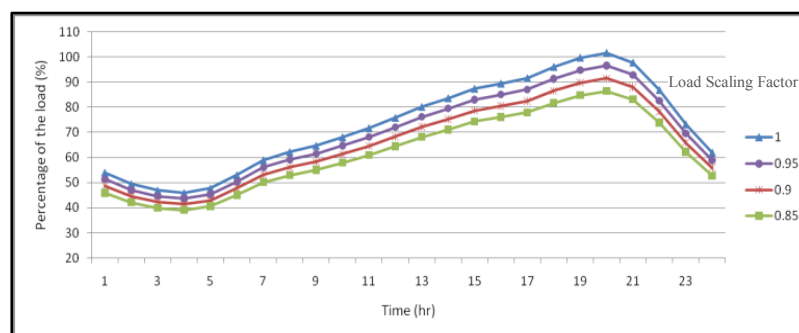


Figure 4.13 Load profiles with different levels of energy conservation.

In the *Load shifting* method, the loads are shifted from high-load to low-load hours. So, the peak load is shaved; and the load curve valley is filled. This scheme is modeled using different percentages of load shifting applied to the load curves in the distribution system, as shown in Fig.4.14. Here, the total demand of the customers is constant.

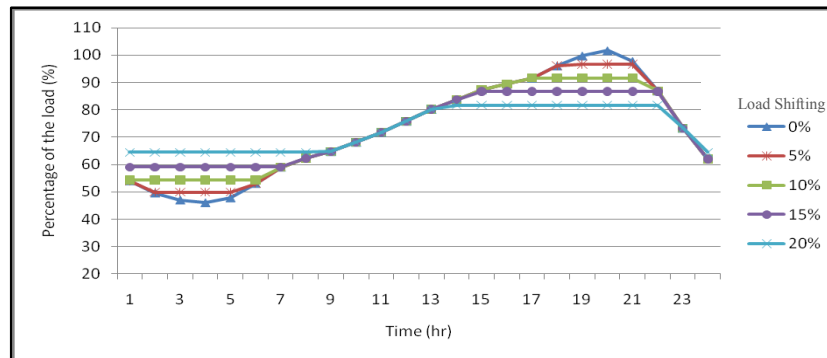


Figure 4.14 Load profiles with different levels of load shifting.

4.3 SDS Reliability with Demand Side Management

The SDS Model-III is used to determine the impact of the DSM on reliability of a smart distribution system. A number of recent research studies have considered the impact of incorporating Distributed Energy Resources, such as electric vehicles [134] and distributed generation-storage systems [135], on DSM and system reliability. The effects of DSM on the adequacy of power generation have been previously studied in the literature [136]. It has been indicated that the highest reliability benefit of DSM in terms of outage cost reduction is associated with the large user sectors rather than small residential and agricultural loads [137]. In [138], the authors have discussed the effect of demand response on distribution system reliability, but their work is a conceptual representation of a framework and does not include case study analysis and results.

Another study evaluates the effectiveness of two DSM schemes on reliability improvement of a distribution system [32]. However, this research is limited by some specific scenarios and does not include load flow analysis for reliability evaluation.

Here, we determine the impact of DSM strategies, such as *Load Shifting* and *Energy Conservation*, on the reliability of the smart distribution systems. Following a contingency in the system, the faulted area of the system is quickly isolated but part of the loads in that area may still be restored automatically. In a normal operation of a distribution system a number of normally open switches are used to separate different feeders and create a radially operated network. These switches may be used to restore the power to the areas disconnected when a failure occurs in the system [139].

There are at least two main reasons why an effective DSM is expected to improve the reliability of the distribution system. First, an effective DSM reduces the loading stress on the system components and, therefore, reduces the probability of failure. Second, applying DSM programs leads to peak load shaving; and, therefore, given a failure and outage of a component in the system, the probability that the grid is still capable of supplying the loads without being overloaded will be increased. In other words, since there is more line capacity available in the system for power restoration when utilizing DSM, fewer loads will be shed. In this research, this aforementioned impact of DSM on the reliability of a distribution system is analyzed using AC load flow, considering the voltage limits of the buses and loading constraints of the branches in the network. We also consider the sequential operational steps after a fault in an automated distribution system.

The reliability evaluation of the distribution system is based on load flow study and state enumeration for failures in an automated distribution system. The reliability data, including failure rate and repair duration of the components, are assumed to be the same when using DSM schemes in different case studies. The active and reactive power of the bus loads change on hourly basis and are modeled using daily load curves.

Each contingency initiates a scenario handled by simulating the system's automated sequential reactions. The post-fault operational steps include [139]:

- Fault clearance using the protection components of the system.
- Fault isolation by opening separating switches.
- Power restoration by closing normally open switches of the system.
- Load flow study of the restored distribution system.
- Load shedding for overload elimination.
- Load shedding in case of voltage constraint violations.
- Taking the system back to the pre-fault configuration after the completion of the repair.

Throughout performing these steps a number of loads may be interrupted for certain durations. After performing contingency analysis and calculating pre- and post-contingency AC power flow, the reliability metrics may be calculated and compared for different case studies. The common reliability indices for distribution systems used in this study are SAIFI, SAIDI, CAIDI, ENS, and ASAI whose definition and calculation

formulas have been provided in Chapter 2 of this dissertation. Therefore, the reliability assessment will be more accurate and applicable to future power distribution systems by considering DSM, automated switching, load shedding, and protection system.

4.4 SDS Reliability with Energy Storage System

Considered as one of the essential distributed energy resources for the future power networks, electricity storage systems are generally used to smooth out the volatilities of renewable generation. In addition, they may be employed to shift the peak load, trade electricity in a dynamic pricing scheme, provide ancillary services, etc. [140]. However, the electricity stored can also be used as an online backup resource in case of a failure to avoid the interruption of the critical loads of the system. In fact, uninterruptable power supplies (UPS) have been used for a long time in sensitive and high priority facilities, such as data centers [141]. Here, using SDS Model-III, we increase the primary storage capacity of a distributed generation-storage system determined in the planning phase and allocate the excess capacity for standby electricity storage. It is assumed that the standby electricity storage can take over the load in a case of a contingency. The goal is to determine the optimum allocation of the standby electricity storage from a reliability perspective considering load interruption costs.

Optimal placement of DER in distribution power systems has been extensively studied in the literature [142], [143]. In addition, many researchers have studied the optimum sizing of energy storage for distributed generation, such as wind power [144] and photovoltaic systems [145]. Therefore, rather than focusing on the optimal placement

of distribution resources, we concentrate on determining the additional electricity storage capacity of a DER system, whose optimum location and primary capacity have been determined in a smart grid, in order to determine the impact of energy storage and improve network reliability. When a contingency occurs, standby stored electricity prevents the interruption of a larger number of customers at the installation load point. In addition, the stored electricity can reduce system loading even with a contingency on its neighboring feeders; and relieving the power line loading could improve power restoration. Using cost/benefit analysis, the condition upon which the standby storage becomes beneficial is specified; and subsequently, the optimum capacity of such energy storage is determined using particle swarm optimization (PSO) method.

A method for determining the optimum size of backup storage from a reliability perspective has been reported in [146]. However, this study does not include the network topology and the costs incurred due to interruptions in the system. Xu et al. [147] have evaluated the impact on reliability and the economics of energy storage with different control strategies using the Monte Carlo simulation approach. They, however, neither considers the power flow constraints of a distribution system nor the load point reliability indices.

In the approach presented here, the reliability evaluation of distribution systems with standby electricity storage is based on power flow study and state enumeration. The failure probabilities of the distribution system components are used to generate simulation contingencies. Each contingency is handled through the scenario including fault clearance, fault isolation, power restoration, system overload detection, load

shedding, etc. Notably, load profiles and customer interruption costs are considered in the analysis. Then, the optimum standby storage capacities are calculated at the DER integration points of the distribution system using the PSO method [148].

In case of a failure affecting the feeder with an integrated DER, the standby resource quickly switches in and saves part of the load from being interrupted. The standby stored electricity may also be used when a contingency has occurred at the neighboring feeders in order to alleviate the loading on the lines and prevent load shedding. Each load modeled has a load profile and an interruption incremental cost curve known as the Sector Customer Damage Function (SCDF). When a load is interrupted due to a contingency or a load is shed because of an overload/voltage violation during power restoration, the expected interruption cost is calculated based on the interrupted power, duration of the interruption, and the SCDF, as denoted by Eq. 4.18.

$$LPIC = \sum_{i=1}^I m_i \cdot SCDF(d_i) \quad (4.18)$$

where m_i and d_i are the interrupted power and the duration of the interruption i , respectively; I is the total number of interruptions at the load point, and $LPIC$ is the Load Point Interruption Cost in dollars per year. Some of the other reliability indices calculated in this study are $LPIF$, $LPID$, and $LPENS$ for the DER-connected load points, and, EIC , $SAIDI$, and $SAIFI$, as the system reliability indices. The definition and calculation formulas for these indices have been provided in Chapter 2 of this dissertation.

For reliability and failure cost evaluation, all failures associated with power lines, transformers, and load connections should be considered. The summation of the system EIC and the levelized cost of standby energy storage represent the system incurred Total Cost, which may be compared over different scenarios. Figure 4.15 shows the flowchart of this study [148].



Figure 4.15 Flowchart of the study to determine the optimum storage capacity

The optimum capacities of the standby storage systems are determined by using sensitivity analysis and the PSO method. In fact, in each iteration and for each particle of

the PSO, reliability of the distribution system is evaluated in order to find the set of standby storage capacities which minimizes the Total Cost as the objective function.

$$\text{minimize: Total Cost} = EIC + \sum_{k=1}^N C_{store}(Cap_{L_k}) \quad (4.19)$$

where C_{store} represents the cost of the standby electricity storage as a function of its capacity Cap_{L_k} at the load point L_k , and N is the total number of DER-connected load points.

4.5 Optimum DER Capacity for Reliable SDS

While it is critical to supply the electric loads of the smart power distribution system reliably, it is also important to minimize the costs of the resources and operation of the equipment. The challenge in minimizing the electricity costs of a customer of a SDS is determining the optimum capacities of the renewable generation-battery system best suited to that customer's electricity management system. The optimum capacities depend on various factors, such as electricity rates, stochastic behavior of renewable resources, load profile, and grid connection policies.

Here, we aim to obtain the optimum capacity of DER such as a renewable generation and storage system for the residential customers of the future power system. It should be noted that determining the optimum capacity for the renewable generator and the battery is a planning problem which should include the behavior of the customers in the optimization process. Hence, we use the SDS model-II explained in Section 4.2.2 of this dissertation.

An optimization approach has been proposed to solve the planning problem of determining the optimum capacities of the battery storage and renewable generation of the smart household incorporating the DSM while considering the probabilistic behavior of loads, renewable energy resources, and electricity rates.

The study method is based on a Monte Carlo simulation process and particle swarm optimization, which is denoted by MCS-PSO method. The iterations in the MCS are used to capture the long-term stochastic behavior of a smart household given the expected probability distributions of load, wind generation, and electricity rates; and, at the same time, those iterations are employed by the PSO particles [149] to efficiently solve the optimization model.

Operation of a smart household in the long run is simulated by providing load, generation, and electricity rates, at each hour of the day, as inputs to the DSM program. The electricity cost of the household at the end of the j th time interval of the day, t_j , can be calculated by Eq. 4.20. The duration of each interval is one hour in this study.

$$C_H(t_j) = C_G \cdot E_G(t_j) + C_B \cdot Cap_B \cdot \Delta t + E_{Buy}(t_j) \times EPR(t_j) - E_{Sell}(t_j) \times ESR(t_j) \quad (4.20)$$

$E_{Buy}(t_j)$ and $E_{Sell}(t_j)$ represent the amount of electricity bought/sold from/to the grid during Δt_j , which are calculated within operation of the DSM and are functions of the renewable generation and battery capacities of the household. C_G and C_B are the levelized costs of the renewable generation and battery for the residential customer.

There are cost-benefit trade-offs involved in optimum capacity calculations. Higher-capacity generators are costlier but contribute more to supplying load and reducing dependency on grid power. The surplus generation can also be sold back to the grid. In the same way, paying more for a higher-capacity battery could be compensated for by additional energy storage and energy trade capability.

Therefore, the objective function to be minimized is the total electricity cost of the household, as expressed by Eq. 4.21.

$$F = \sum_{j=1}^N C_H(t_j) \quad (4.21)$$

subject to the system load flow, generation and battery operation constraints mentioned in the modeling section by Eq.4.12 and Eq.4.16.

Since the electricity cost of the household depends on DSM and the inputs to the DSM are stochastic variables obtained from their probability distributions, this cost can be generally represented by an implicit function of the following variables and parameters.

$$C_H = f(L_1, L_2, L_3, V_W, B_{init}, ESR, EPR, C_G, C_B, Cap_G, Cap_B) \quad (4.22)$$

The expected electricity cost of the household in the long run, with certain generation and battery capacities, can be calculated through a sequential Monte Carlo simulation (MCS). In the Monte Carlo scheme, samples from individual probability distributions of load, generation, and electricity rates are taken at each hour of the day. Using the process described in Section 4.2.2.4 for the DSM, $C_H(t_j)$ is calculated and

accumulated to find the total electricity cost of the day. By repeating the whole process, the expected electricity cost of the household is calculated.

Subsequently, particle swarm optimization (PSO) is used to calculate the optimum Cap_G and Cap_B by minimizing the objective function given in Eq. 4.21. The goal of the objective function (fitness function) is to minimize the total expected electricity cost of the household calculated by MCS over the duration of the study. In the PSO method, initial capacities for the generation and battery are selected; and then, a population of M particles is generated to evolve toward the optimum capacities of battery and renewable generation for the household. This method has been demonstrated to be more robust and faster in finding the global solution compared with other heuristic optimization methods, such as genetic algorithms [150].

To improve the efficiency of the optimization process, an iterative procedure combining MCS and PSO methods is proposed. Using the hybrid MCS-PSO method, the input to each iteration of the PSO is stochastic and originates from the variables' probability distribution functions. Therefore, in the long run, it inherently incorporates the MCS method while it is searching for the optimum solution. Fig.4.16 shows the optimization process using the rule-based DSM introduced for SDS model-II.

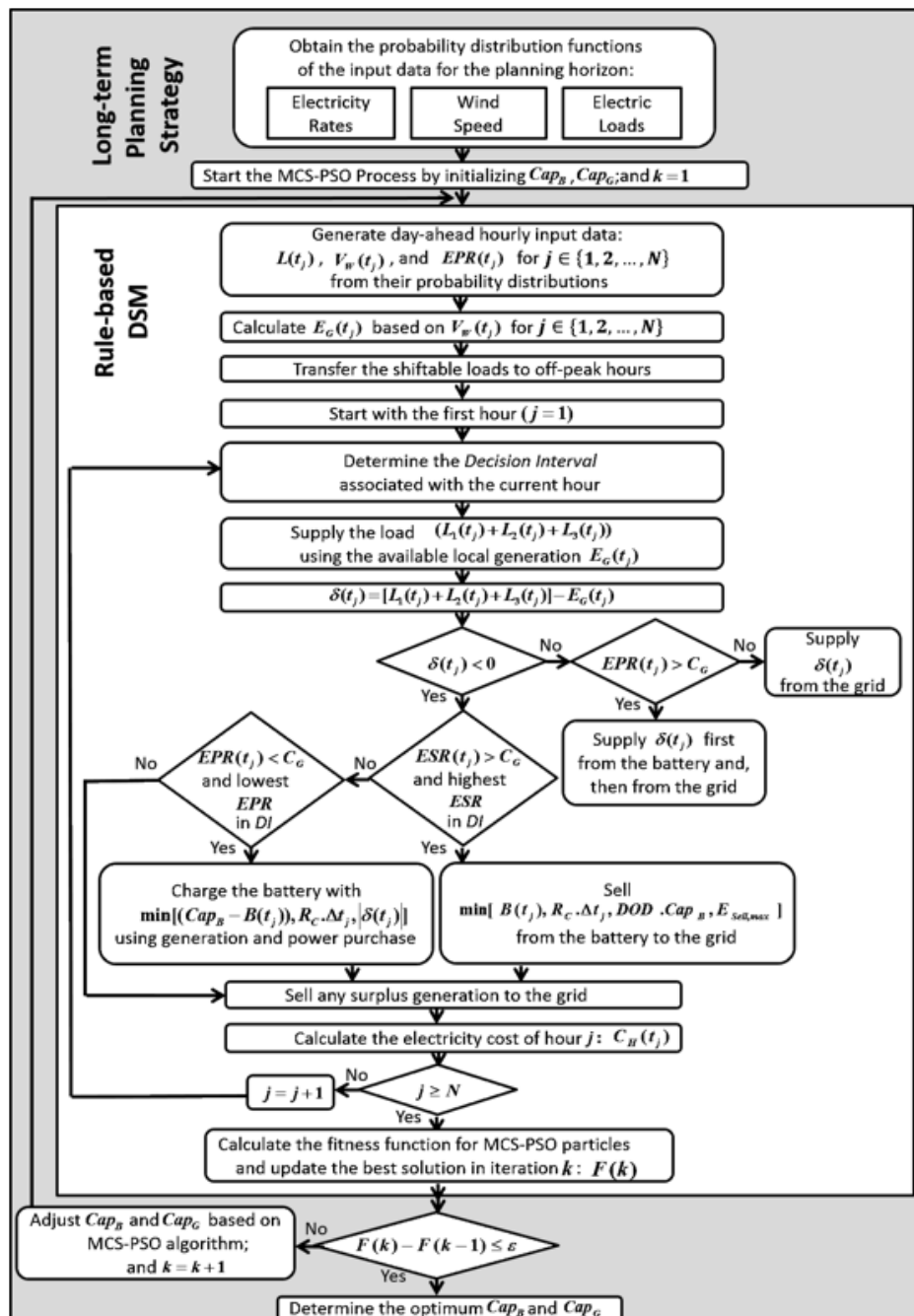


Figure 4.16 The optimization process incorporating the rule-based DSM of SDS model-II

The procedure can be expressed by the following steps [121].

- Determine N individual probability distribution functions for different variables, such as wind speed, load, and electricity rate, according to historical data. Each function

represents the probability distribution of a variable for a time step of t_j in the MCS-PSO where $j \in \{1, 2, \dots, N\}$.

- B. Obtain C_G, C_B , and the parameters of the MCS-PSO method, such as stop criterion based on maximum number of iterations or minimum error, and the number of particles, M , in the PSO.
- C. Initialize each particle by assigning two dimensional position and velocity vectors according to Eq.4.23, and also initialize $\mathbf{x}_{pbest}^i, \mathbf{x}_{gbest}$, and the battery charge $B_{init}^i(k)$ for the iteration $k = 1$.

$$\begin{cases} \mathbf{x}^i(k) = [Cap_G^i(k) & Cap_B^i(k)] \\ \mathbf{v}^i(k) = [v_{Cap_G}^i(k) & v_{Cap_B}^i(k)] \end{cases} \quad (4.23)$$

where, $i \in \{1, 2, \dots, M\}$; \mathbf{x}_{pbest}^i , and \mathbf{x}_{gbest} are best position vector of individual particle i , and best position vector of all particles in MCS-PSO study, respectively; \mathbf{x} and \mathbf{v} are position and velocity vectors of particles in MCS-PSO analysis, respectively.

- D. For iteration k and every particle i of the population, given the current $Cap_G^i(k)$, and $Cap_B^i(k)$, do the following:
- a. Calculate the values of the loads, $L_1^i(k, t_j)$, $L_2^i(k, t_j)$, and $L_3^i(k, t_j)$, wind speed, $V_W^i(k, t_j)$, and electricity rates, $EPR^i(k, t_j)$ and $ESR^i(k, t_j)$, based on their N distinct probability distribution functions.

- b. Run the HEMS process for a duration of $T = N \cdot \Delta t$, and compute the value of the fitness function.

$$F(\mathbf{x}^i(k)) = \sum_{j=1}^N C_H^i(k, \Delta t_j) \quad (4.24)$$

- E. If $F(\mathbf{x}^i(k)) < F(\mathbf{x}_{pbest}^i)$, then update the values for the local optimum capacities:

$\mathbf{x}_{pbest}^i = \mathbf{x}^i(k)$; and if $F(\mathbf{x}^i(k)) < F(\mathbf{x}_{gbest})$, then update the global best capacities:

$$\mathbf{x}_{gbest} = \mathbf{x}^i(k).$$

The minimum of the cost function $F(\mathbf{x}_{gbest})$ in each iteration k has been denoted by $F(k)$ in Fig. 4.16.

- F. If the stop criterion is not satisfied, update the position and velocity vectors according to Eq.4.25, increase iteration k by one, and go to Step D.

$$\begin{cases} \mathbf{x}^i(k+1) = \mathbf{x}^i(k) + \mathbf{v}^i(k+1) \\ \mathbf{v}^i(k+1) = w(k) \cdot \mathbf{v}^i(k) + c_1 \phi_1 (\mathbf{x}_{pbest}^i - \mathbf{x}^i(k)) \\ \quad \quad \quad + c_2 \phi_2 (\mathbf{x}_{gbest} - \mathbf{x}^i(k)) \\ B_{init}^i(k+1) = B^i(k, \Delta t_N) \end{cases} \quad (4.25)$$

where, ϕ_1 and ϕ_2 are cognitive and social random numbers of the algorithm between 0 and 1; and, c_1 and c_2 are cognitive and social parameters of PSO algorithm, respectively.

In this equation, B represents the available battery charge.

- G. Determine the optimum capacities associated with the minimum objective function.

$$\begin{cases} [Cap_G^* \ Cap_B^*] = \mathbf{x}_{gbest} \\ \{Min \{C_H(T)\} = F(\mathbf{x}_{gbest}) \end{cases} \quad (4.26)$$

4.6 SDS Reliability with Active Customer Interactions

As previously highlighted, it is essential to evaluate the reliability of future power distribution systems considering its new features and corresponding equipment. The reliability study objectives may include:

- 1) Investigation of the impact of a variety of factors, such as customer diversity (residential, commercial, and industrial) and type of distributed generation (wind, PV), on the reliability of an SDS and its active customers;
- 2) Study the effect of a DSM program, through active customer decisions and trading power within the neighboring customers, on providing reliable electricity; and
- 3) Assessment of the impact of the size of wind and PV renewable generation and storage systems on SDS reliability.

In order to evaluate the reliability of a smart distribution system, the SDS model-I is used. This model includes a variety of customers with wind and PV renewable generation and storage systems. The infrastructure allows for communication and power flow between neighboring customers which would affect system reliability. Using the reliability evaluation module developed, it is possible to constitute probabilistic failures in an SDS with a diverse range of impacted customers.

Fig.4.17 shows a schematic of the model used for reliability evaluation, including electric utility, different types of customers, neighborhood zones, and instances of the areas impacted by different contingencies.

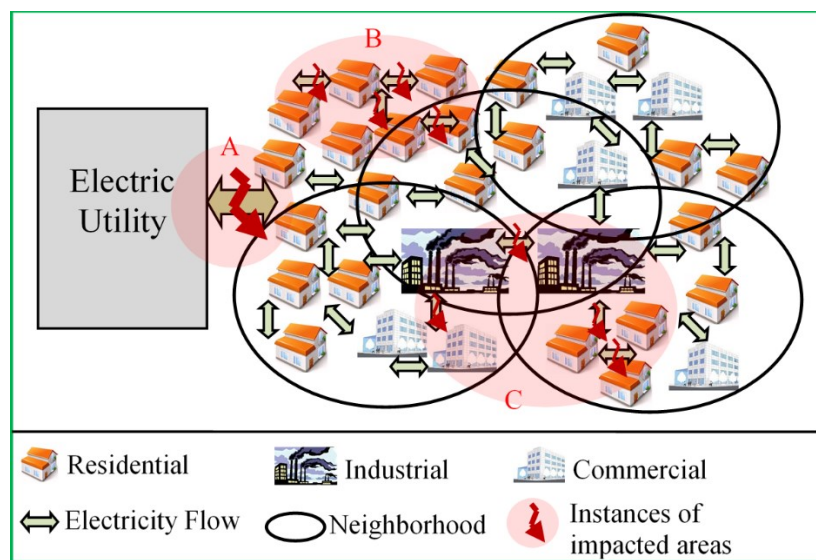


Figure 4.17 Main entities of an SDS model used for reliability evaluation impacted by instances of contingencies A, B, and C.

Since the SDS model-I utilizes multiagent system modeling and a graph theoretic representation of a power distribution system, instead of simulating individual contingencies, the consequences of these contingencies are modeled as impacted areas. An impacted area is modeled by suspending power transactions among the grid and all of the customers within a neighborhood around the center of the contingency.

4.6.1 Outage Response

In the case of an outage and when Customer Agent x needs power for a specific hour, x sequentially sends a Request-To-Buy (RTB) message to its neighbors, who may be able to deliver part of the required power until either x manages to fulfill its demand, or there are no other neighbors left to ask. On the other hand, Customer Agent i receives a request and responds if it has excess power generated that hour or it has extra electricity stored. Fig.4.18 illustrates a customer's interaction with M_x number of neighboring agents and shows an outage area caused by a contingency. Customer Agent x affected by

an outage starts to respond by recalling the following *sequential outage response* algorithm for each time step t_j (e.g., one hour) of the reliability assessment MCS process.

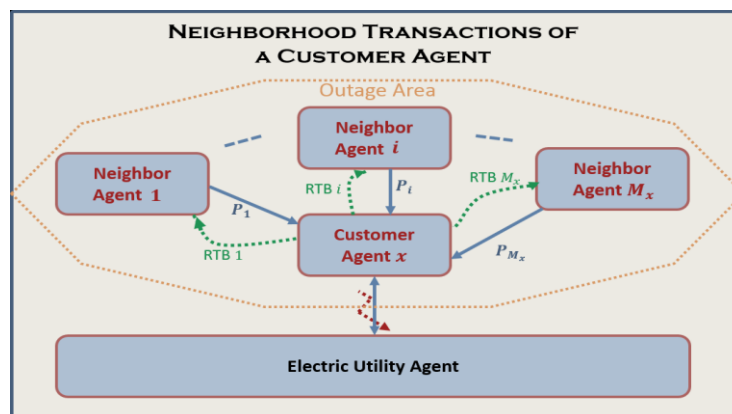


Figure 4.18 Potential sequential requests of a customer agent from its neighbors during an outage.

Algorithm *Sequential Outage Response*

- I. If there is a non-zero demand for customer x at time step t_j , $d_x(t_j) > 0$, then try to supply the load first from the generation ($g_x(t_j)$) and next from the battery storage up to $(\min\{b_x(t_j), DR_x\})$, where DR_x is the maximum allowable battery discharge rate for customer x in % of battery capacity per t_j .
- II. If the residual demand is nil ($d'_x(t_j) = 0$), then a) there is no loss of load ($LOL_x(t_j) = 0$), and b) exit algorithm.
- III. Start to communicate with a neighbor ($i = 1$).
- IV. Send an RTB to the neighbor (i) asking for power in the amount of $d'_x(t_j)$.
- V. Use the power received from the neighbor ($P_i(t_j)$), if any, to supply $d'_x(t_j)$ and update the residual demand: $d'_x(t_j) = d'_x(t_j) - P_i(t_j)$.

- VI. Run the condition described in Step II of this algorithm.
- VII. If $d'_x(t_j) > 0$ and the customer is the last neighbor asked (M_x), then a) $LOL_x(t_j) = d'_x(t_j)$ and b) exit the algorithm.
- VIII. $i = i + 1$; go to Step IV.

End Algorithm

In the above algorithm, we define $LOL_x(t_j)$ to represent the amount of customer x 's loss of load power at time step t_j . We further define the index of interruption, $IOI_x(t_j)$, as:

$$IOI_x(t_j) = \begin{cases} 1 & LOL_x(t_j) > 0 \\ 0 & \text{Otherwise} \end{cases} \quad (4.27)$$

Subsequently, we also define the index of interruption frequency, $IOIF_{x,k}$, by taking the union of IOI for each customer x affected by the outage k , as expressed by Eq.4.28, where T_k is a set of all time steps during outage k .

$$IOIF_{x,k} = \bigcup_{t_j \in T_k} IOI_x(t_j) \quad (4.28)$$

Eq. 4.28 indicates that if a customer cannot meet the load for one or more time steps during an outage, then the customer is counted as interrupted due to that outage (i.e., $IOIF_{x,k} = 1$).

Similarly, since each time step is assumed to be one hour, the duration of interruption can directly be calculated by adding up the multiples of the hours (i.e. IOI).

The index of interruption duration, $IOID_{x,k}$, is defined by Eq.4.29 which represents the duration of interruption per outage k , for each customer x .

$$IOID_{x,k} = \sum_{t_j \in T_k} IOI_x(t_j) \quad (4.29)$$

4.6.2 Reliability Assessment Method

The reliability for each customer of a specific load sector and for the total system is assessed using a sequential MCS approach. In this method, the time to the next failure and the duration of that failure in the system are determined by sampling the associated failure and repair probability distributions, respectively. During a failure, each agent attempts to avoid its load interruption using the available resources at each time step.

Process Sequential MCS

- I. Determine the load and renewable generation profiles for each customer and the outage occurrence schedule, duration, and impacted areas based on the associated probability distributions.
- II. Start the simulation at the first time step (t_1).
- III. For the customers in a normal operation mode (not disconnected), run the DSM to supply the loads.
- IV. For the customers in an outage operation mode (disconnected due to a contingency), recall the *Sequential Outage Response* Algorithm, described earlier in this Section.
- V. Go to the next time step ($j = j + 1$).

- VI. Run Steps III and IV of this simulation for the total number of simulation steps (J).
- VII. Collect the data on frequency and duration of interruptions as well as the unsupplied energy per customer sector, based on Eq. 4.27- 4.29.
- VIII. Evaluate the reliability indices defined for customer sectors and the whole system, as described in Section 4.6.3.

End Process

4.6.3 Reliability Evaluation Indices

Reliability of an SDS is evaluated using commonly used system indices, such as System Average Interruption Frequency Index (SAIFI) and System Average Interruption Duration Index (SAIDI). Reliability is also assessed from the customer point of view using a number of proposed indices, such as Value of Lost Load (VOLLs), Energy Not Supplied (ENSs), and Customer Interruption Cost (CICs), for a customer in each sector. The customer-side reliability indices are defined to account for the smart grid features and aim to capture the influence of active customers' behavior on the reliability of future power systems.

In fact, the perception of reliability may vary among various types of customer sectors as their load profiles and interruption damage functions are different. From the system's perspective, *SAIFI* and *SAIDI* are defined as:

$$SAIFI = \frac{\sum_{x=1}^N \sum_{k=1}^{N_{con}} IOIF_{x,k}}{N \times J/8760} \quad (4.30)$$

$$SAIDI = \frac{\sum_{x=1}^N \sum_{k=1}^{N_{con}} IOID_{x,k}}{N \times J/8760} \quad (4.31)$$

where N and N_{con} are the number of customers and the number of outages during J simulation hours, respectively.

The units for the customer-side reliability indices, ENS_s , $VOLL_s$, and CIC_s , may be expressed in $\frac{kWh}{customer, year}$, $\frac{\$}{kWh}$, and $\frac{\$}{year}$ for each customer sector s , respectively; e.g., for the residential customers:

$$ENS_R = \frac{\sum_{xr=1}^{N_R} \sum_{j=1}^J LOL_{xr}(t_j)}{N_R \times J/8760} \quad (4.32)$$

$$VOLL_R = \frac{\sum_{xr=1}^{N_R} \sum_{k=1}^{N_{con}} \frac{CDF_R(IOID_{x,k})}{IOID_{x,k}}}{N_R \times N_{con}} \quad (4.33)$$

$$CIC_R = ENS_R \times VOLL_R \quad (4.34)$$

where N_R represents the number of residential customers and CDF is the customer sector damage function in $\$/kW$ which is a function of interruption duration. Eq. 4.32- 4.34 may be revised for commercial and industrial customer sectors by replacing “ xr ” with “ xc ” and “ xi ”, and “ R ” with “ C ” and “ I ” subscripts, respectively.

4.7 Summary of the models and proposed studies

The next table provides a list of the models developed for smart power distribution systems and the analysis planned based on each model, as discussed in this section. Section 5 provides case studies and results of these analyses.

Table 4.1 Models developed and their features for different types of SDS studies

MODELE	FEATURES					STUDY SECTION
	DSM	Renewable Generation	Energy Storage	Dynamic Electricity Rate	Neighborhood Power Transaction	
SDS MODEL-I	Utility-based Method	√	√	√	√	Section 4.6
	Average Deficit Method					
SDS MODEL-II	Rule-based Method	√	√	√		Section 4.5
SDS MODEL-III	Load Shifting Method	√	√			Section 4.4
	Energy Conservation					Section 4.3

CHAPTER 5

SYSTEM STUDIES

5.1 Reliability of Distributed Energy Resources

(Case study: wind turbines)

5.1.1. Fault Tree Analysis

5.1.2. Failure Mode, Effect, and Criticality Analysis

5.1.3. Markov processes

5.1.4. Monte Carlo Simulation

5.1.5. Hybrid Analytical-Simulation Approach

5.2 Reliability of Smart Power Distribution System

5.2.1. SDS Reliability with Demand Side Management

5.2.2. SDS Reliability with Energy Storage System

5.2.3. Optimum DER Capacity for Reliable SDS

5.2.4. SDS Reliability with Active Customer Interactions

This section includes different case studies, results of the reliability assessment and a number of sensitivity analysis based on the models provided in the previous chapters. The first part of this chapter presents the result of reliability evaluation for wind turbines as examples of distributed energy resources. In the second part of this chapter, we describe different smart distribution system reliability studies and discuss the results.

5.1 Reliability of Distributed Energy Resources (Case study: wind turbines)

The methods described in Chapter 3 are used to evaluate the reliability of individual wind turbines as well as wind farms in this section.

5.1.1 Fault Tree Analysis

In order to calculate the reliability and availability of a wind turbine, typical failure rate of the components, whose failure stops the wind turbine operation, were obtained [15], [78]. The failure rates of the main parts of the wind turbine, used for the study, are shown in the next table.

Table 5.1 Failure rates for main subassemblies of a wind turbine

Main subassemblies of the wind turbine	Failure rate per year
Rotor	0.15
Drive Train	0.08
Gearbox and Lube	0.12
Generator and Cooling system	0.17
Brakes and Hydraulics	0.2
Yaw system	0.13
Control system	0.32
Electrical system and Grid connection	0.45
Miscellaneous	0.08

This will result in an overall failure rate of $\lambda = 1.94 \times 10^{-4}$ per hour, per turbine. The average repair rate is also chosen to be $\mu = 2.94 \times 10^{-3}$ per hour, per turbine. Based on these values and Eq. 3.1 and 3.2, the average availability and the reliability of the wind turbine is calculated.

$$\begin{cases} A_{Turbine} = \frac{\mu}{\mu + \lambda} = \frac{2.94 \times 10^{-3}}{2.94 \times 10^{-3} + 1.94 \times 10^{-4}} = 0.938 \\ R_{Turbine}(t) = e^{-\sum_{i=1}^n \lambda_i t} = e^{-1.94 \times 10^{-4} t} \end{cases} \quad (5.1)$$

Fig.5.1 estimates the reliability of the wind turbine within a week assuming that it is initially 100% reliable.

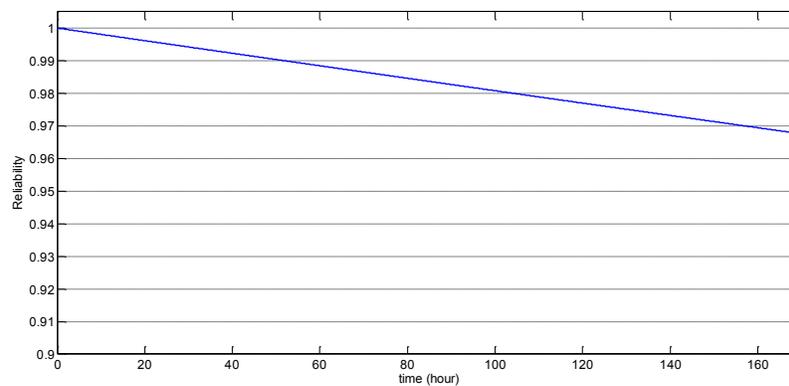


Figure 5.1 Change in reliability of the wind turbine within a week

5.1.2 Failure Mode, Effect, and Criticality Analysis (FMECA)

The proposed RB-FMEA method is applied to a 3MW direct drive wind turbine. Based on the model described, the study required failure probabilities, vulnerabilities, costs, and durations which are estimated based on different resources reported in [77]. A spreadsheet was set up using Microsoft Excel, and the result parameters were derived for the wind turbine parts as shown in Fig. 5.2.

	A	B	C	D	E	F	G	H	I	J	K	L	M	N
2	Type of Study	Scale of Occurrence	Scale of Severity	Scale of Detection	RPN	Probability of Failure	Probability of Not Detection	Effect and Severity per failure						
3	Item Name							P_F	P_{ND}	D_F (Hours)	C_P (\$)	C_S (\$)	C_L (\$)	C_O (\$)
4	Electrical System	5	3	4	60	0.23	0.6	100	10275	6450	1000	6000	23725	3274.05
5	Gearbox	--	--	--	--	--	--	--	--	--	--	--	--	--
6	Hydraulic System	3	3	4	36	0.088	0.8	60	1500	4050	600	3600	9750	686.4
7	Control System	5	2	7	70	0.101	0.9	48	2775	900	480	2880	7035	639.4815
8	Blades	3	4	4	48	0.065	0.7	96	30750	18375	960	5760	55845	2540.9475
9	Pitch Mechanism	3	2	7	42	0.041	0.9	72	4800	1800	720	4320	11640	429.516
10	Generator	5	4	4	80	0.198	0.7	180	61500	29325	180	10800	101805	14110.173
11	Yaw System	3	2	4	24	0.065	0.8	55	1950	5475	550	3300	11275	586.3
12	Mechanical Brake	3	3	7	63	0.06	0.9	72	1725	4575	720	4320	11340	612.36
13	Converter	5	3	4	60	0.129	0.8	48	13650	1800	480	2880	18810	1941.192
14	Main Shaft	2	3	7	42	0.009	0.9	120	6150	14700	120	7200	28170	228.177
15	Tower and Structure	2	4	7	56	0.009	0.9	96	27300	22050	960	5760	56070	454.167
16	Other Parts	2	2	10	40	0.005	1	86	3450	900	860	5160	10370	51.85

Figure 5.2 Snapshot of the spreadsheet for RB-FMEA Analysis

For the base condition, it is assumed that for the duration of the failures, the Capacity Factor (CF) of the wind turbine and the EPR have been 0.4 and 5¢/kWh respectively. The resulted CPN (cost priority number) column shows that, the generator is ranked the most critical part of the studied direct drive wind turbine followed by electrical system, blades and converter. This analysis can be conducted for any other types of wind turbine and for any operation condition. In addition, by summing up the CPN of all the parts of a turbine, one can estimate the overall CPN of that wind turbine. This number can then be compared with the overall CPNs of other types of wind turbine in order to rank them from criticality perspective. For our study, the overall CPN adds up to \$25.5k.

The calculation of RPN was also included in Fig. 5.2 for evaluation, and the required parameters were determined using rating scheme of [151]. Fig 5.3 compares the results of RPN and CPN for our study case.

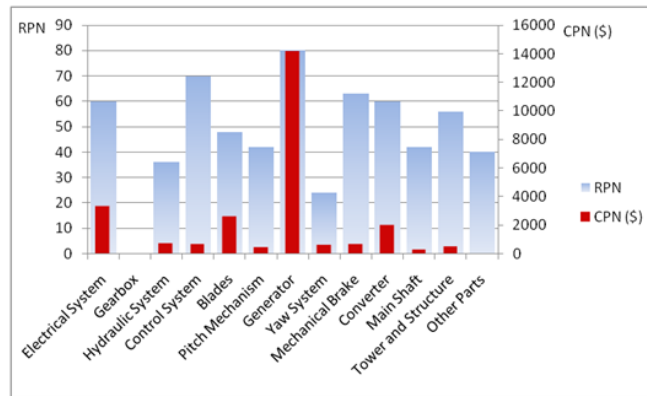


Figure 5.3 RPN and CPN for major parts of the study wind turbine

While two methods are in agreement about the generator being the most critical part of the direct drive wind turbine, the building blocks of RPN are discrete and qualitative, and therefore, cannot represent the strength of criticality, effectively. Nevertheless, CPN is calculated based on the actual costs, and, so, is more rational to be looked up to for making adjustments on design, operation and maintenance of wind turbines. The Annual Failure Cost of this direct drive wind turbine, is shown in Fig. 5.4.

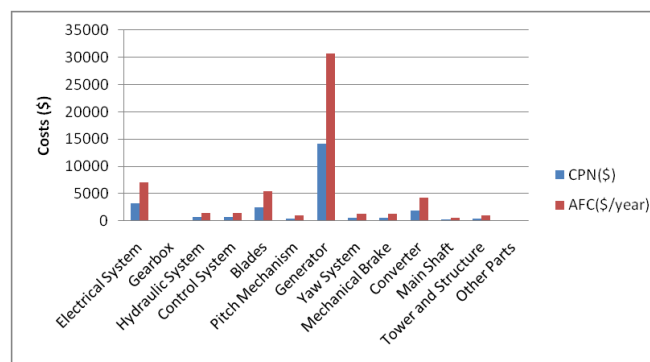


Figure 5.4 AFC and CPN for major parts of the wind turbine

In fact, each part's CPN has been multiplied by its Failure Vulnerability as a weighting factor. Failure Vulnerability specifies how many times per year each of the wind turbine parts has been detected with a risk of failure or has actually failed. Based on

the results, the total AFC of the wind turbine is \$55.5k, which implies an overall failure vulnerability of 2.17 per year for our study wind turbine.

5.1.2.1 Sensitivity Analysis

One of the key parameters affecting the total cost of failure is the duration of failure. Generally, the repair of a wind turbine may be delayed due to lack of parts in the inventory, unavailability of the required facility, adverse weather condition, or human error. As a sensitivity analysis, the annual failure cost has been determined by increasing the imposed delay of repair as shown in Fig. 5.5.

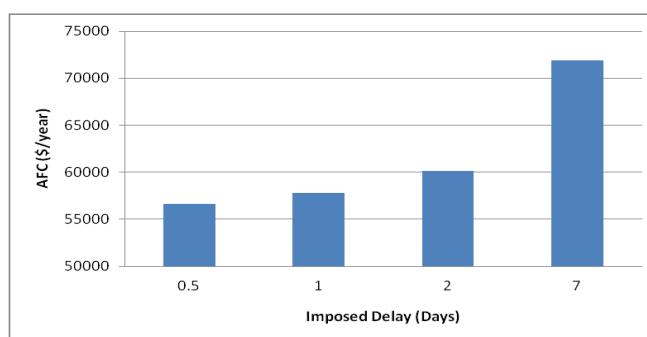


Figure 5.5 Sensitivity of the turbine AFC to the additional imposed delay

The results of this study may suggest the reasonable amount of money to be spent in order to avoid these types of delays. For example, one week of delay in repairs escalates the initial annual failure cost of \$55.5k to more than \$70k. Hence, any solution for delay prevention, such as recruiting more labor or providing extra tools, will be beneficial as long as its cost is less than \$14.5k per year.

The above results are derived based on the previously selected base values for EPR and CF. In fact, CF and EPR are two major parameters which vary due to the wind speed and the location of the site, and therefore, alter the cost of opportunity during the

downtime of the turbine. Fig. 5.6 displays the effect of these two parameters on the annual failure cost of the wind turbine in our case study.

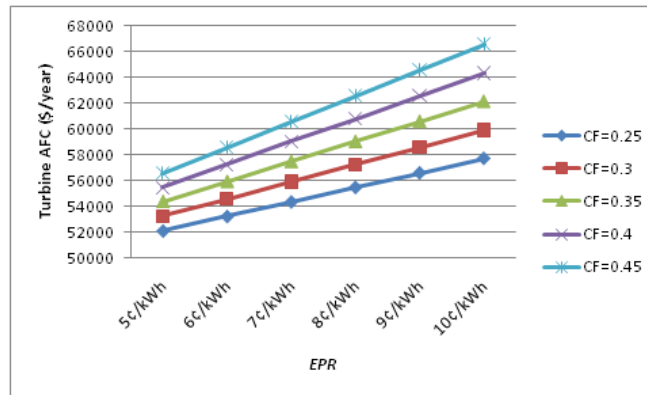


Figure 5.6 Sensitivity of the turbine AFC to the EPR and CF

According to these results, annual cost of failure may vary more than 25%, due to the change in the energy price and the wind speed. One effective approach to reduce the failure cost is by improving the failure detection system (e.g. through condition monitoring). Fig. 5.7 illustrates the total savings in turbine’s AFC, by 10 percent improvement in the generator fault detection system. The total savings are approximately \$3000 per year with the capacity factor of 0.4 and EPR of 5cents/kWh.

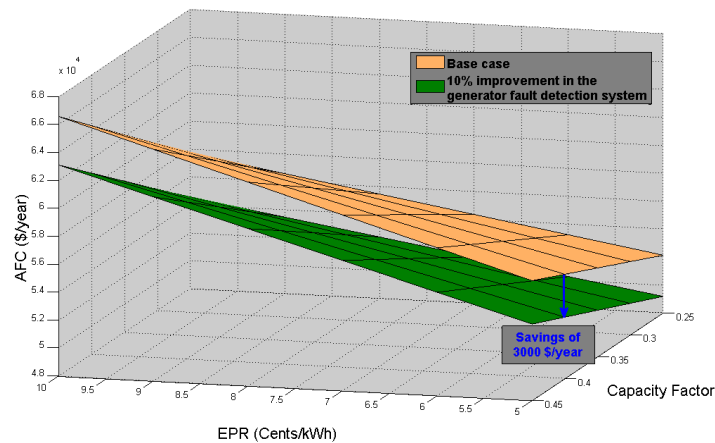


Figure 5.7 Failure cost with 10% improvement in the turbine’s fault detection

5.1.3 Markov Processes

The procedure given in Fig.3.9 has been applied to a wind farm in western Nebraska located at Kimball and is owned by Municipal Energy Agency of Nebraska (MEAN). This 10.5 megawatt wind farm consists of 7 turbines whose power curve provided by the manufacturer for each turbine was shown in Fig. 3.7.

5.1.3.1 Short-term study

Suppose that availability and reliability of this wind farm for duration of one week is of interest. The data used for this site are the average failure and repair rates of turbines as: $\lambda = 1.94 \times 10^{-4}$, $\mu = 2.94 \times 10^{-3}$ per hour and turbine [15]. Table 5.2 provides results obtained from calculation of the wind farm availability, based on initial number of working wind turbines at different times. Obviously, the initial working condition of the turbines impact the wind farm availability in short-term

Table 5.2 Wind farm availability with respect to initial conditions and time

Time	Beginning of the week	Middle of the week	End of the week
Initial Number of working turbines			
0	0	0.0333	0.0662
1	0.1429	0.1740	0.2047
2	0.2857	0.3147	0.3431
3	0.4286	0.4553	0.4816
4	0.5714	0.5960	0.6199
5	0.7143	0.7364	0.7569
6	0.8571	0.8739	0.8852
7	1	0.9862	0.9753

Wind speed data of Kimball within one week were used to incorporate output power variations to this model. The effect of initial conditions on short-term generation of wind farm can be observed where Fig.5.8 illustrate the difference in capability to meet the demand between having 7 and 3 initial available turbines.

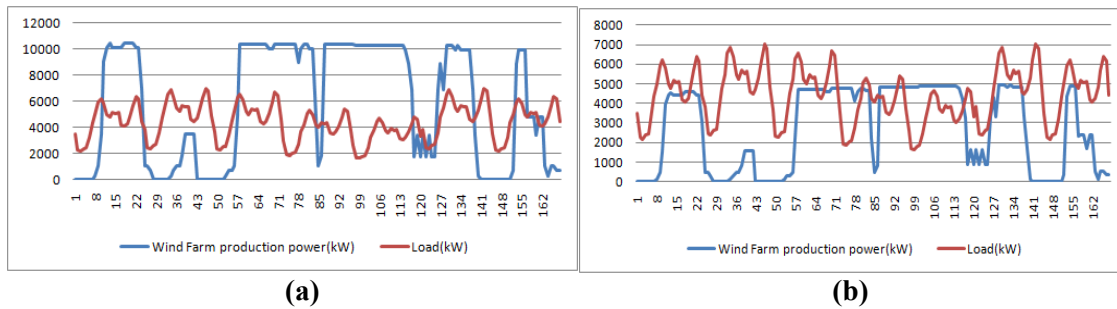


Figure 5.8 Hourly wind farm power production vs. load demand with 7 (a) and 3 (b) initially available wind turbines

Apparently, this wind farm without any connection to an external grid or energy storage system cannot be operated stand alone to supply the load. Using the Eq. 3.14 and 3.15, Table 5.3 provides wind farm's LOLP, LOEE and ESWE for a week starting at different number of working wind turbines.

Table 5.3 LOLP, LOEE and ESWE within a week

Initial Number of working turbines	LOLE (hours/week)	ESWE (MWh/week)	LOEE (MWh/week)
0	168	0	705.8
1	164	0.7	567.3
2	152	14.9	442.3
3	124	57.2	345.4
4	93	145.4	294.4
5	80	265.7	276
6	76	388.3	263.4
7	75	489.5	254.7

5.1.3.2 Long-term study

For the long-term study, Eq. 3.17 and 3.18 have been used to derive the steady state probabilities as follows:

Table 5.4 Steady state probabilities of the wind farm model

Steady state probability	π_0	π_1	π_2	π_3	π_4	π_5	π_6	π_7
Value	0	0.0003	0.0019	0.0092	0.035	0.106	0.2678	0.5798

According to Eq. 3.19, the expected availability of the wind farm in long-term is calculated.

$$A_{Farm} = \frac{\sum_{j=0}^{j=7} (\pi_j \times j)}{7} = 0.9096 \quad (5.2)$$

Alternatively, the same availability can be reached through time domain study. Fig.5.9 shows that if enough time elapses, wind farm availability will converge to a single value regardless of the initial available number of wind turbines.

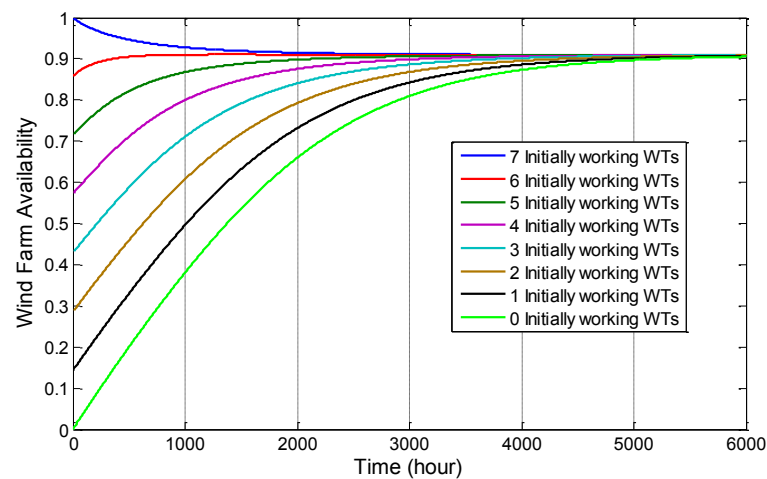


Figure 5.9 Long-run availability of the wind farm

Figure 11 captures the probability distribution of output power states (P_{q_i}), based on the statistical data of hourly wind speed for one year.

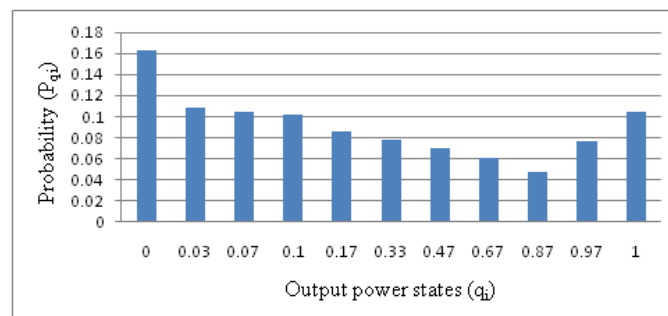


Figure 5.10 Probability distribution of the wind turbine output power states

The wind farm energy production within that year is calculated to be 29.26GWh, based on Eq. 3.21. The estimated generation has roughly 3% error compared to the actual energy production of the wind farm [152].

Additional repair crew could improve the availability due to increase in the number of parallel repair crew (S) and/or decrease in average repair time ($1/\mu$) in the Markov model of Fig. 3.6. In our case, doubling the repair crew if they work in parallel, would increase the wind farm's availability by 0.025;

Using probability distributions for wind farm power production of Fig.5.10 and the annual load demand, reliability indices of the wind farm are calculated.

Table 5.5 LOLP, LOEE and ESWE for one year

study Period	LOLE (hours/year)	ESWE (GWh/year)	LOEE (GWh/year)
one year	5860	9.9	20.5

According to table 5.5 and from planning point of view, an external power grid needs to supply an estimated annual energy of 20.5GWh to compensate the lack of wind and turbines' availability. On the other hand, this wind farm can export an estimated annual energy of 9.9GWh to the grid when its power production exceeds load demand.

5.1.4 Monte Carlo simulation

Similar to the previous section, the wind speed data of Kimball was has been used which are best fitted to an Erlang distribution with shape parameter of 2.57, and rate parameter of 3. At any point in time, a wind speed is generated based on its distribution, and the decision block of our model in Fig.3.10 determines how much power will be

generated due to the power curve of the wind turbine. The simulation was run for 1000 iterations and the average expected power generated by the wind turbine is calculated to be 572.25kW with a 90% confidence interval of [543.25, 600.9].

Next, in order to consider the failures on different subassemblies of wind turbine, the model of Fig. 3.11 has been used where the time between failures is based on exponential distribution, and the mean time to repair is assumed to follow the Log-normal distribution [86]. Table 5.6 presents the expected outage durations based on the simulation. Adding all the outage durations, the total unavailable duration of a single wind turbine will be 494.95 hours per year.

Table 5.6 Average outage duration of a wind turbine's subassemblies

Turbine subassemblies	Rotor	Drive Train	Gearbox and Lube	Generator and Cooling system	Brakes and Hydraulics	Yaw system	Control system	Electrical system and Grid connection	Miscell.
Average outage duration (hours/year)	48.49	24.27	31.5	46.11	62.62	42.95	82.42	128.28	28.28

The availability of this wind turbine can be calculated as the total available hours divided by the total simulation hours.

$$A_{Turbine} = \frac{\text{Available hours}}{\text{Total hours}} = \frac{8760 - 494.95}{8760} = 0.943 \quad (5.3)$$

On the other hand, there are more wind turbines and vulnerable parts in a wind farm. Therefore, there may be some components which need to wait in a queue to be repaired in case of simultaneous incidents. This will definitely add to the total outage time of that part and decrease the overall availability of the wind farm.

The results for our case study wind farm with 7 turbines are provided in Table 5.7 which represent the average expected outage duration of wind turbines' subassemblies.

Table 5.7 Average outage duration of 7turbines' subassemblies

Average outage duration (hours/year)	Turbine 1	Turbine 2	Turbine 3	Turbine 4	Turbine 5	Turbine 6	Turbine 7
Rotor	63.5246	59.9877	59.5584	59.908	62.985	63.1532	61.7618
Drive Train	31.3439	34.5249	40.2679	32.572	39.5224	40.4409	30.6156
Gearbox and Lube	51.0125	46.1707	44.4766	38.9964	59.6583	49.5643	42.9627
Generator and Cooling system	74.1599	61.5122	61.2925	69.9683	64.3959	63.3315	59.1052
Brakes and Hydraulics	91.5364	75.2734	85.3813	80.397	88.6469	83.1478	83.5085
Yaw system	56.6079	56.9755	49.8854	51.2551	45.908	55.157	52.9629
Control system	116.02	121.76	126.29	126.33	137.88	133.45	115.32
Electrical system and Grid connection	156.86	181.36	160.31	156.2	157.62	156.99	170.35
Miscellaneous	39.3361	23.5451	33.4664	36.3336	25.295	33.4188	35.3504
Sum	680.401	661.109	660.928	651.960	681.911	678.653	651.937

As expected, the comparison between Table 5.6 and 5.7 suggests more outage duration per components of a turbine with higher number of wind turbines. The average availability of the wind farm in this case is 0.923.

5.1.5 Hybrid analytical-simulation approach

The models described in Section 3.2.5 are employed to study wind turbine reliability. The following tables present the parameters used in the model based on the data for a typical 3 MW direct drive wind turbine [77], and they are considered as the base case for the rest of this section.

Table 5.8 provides the expected reward/penalty of being in each state where negative values correspond to the costs of repair and maintenance. In this table, it is assumed that as the turbine deteriorates, its capacity factor decreases; and as a result, the reward from being in D_i is reduced as i increases. With the same reasoning, the cost of maintenance slightly decreases over time because of lower opportunity costs for an aged turbine. Table 5.9 contains the transition probabilities from the maintenance states back to the working states. It is assumed that major maintenance is more effective than minor maintenance; and a small probability of 1% is included to account for human error.

Table 5.8 Expected reward/penalty of being in each state

State	Expected Reward/Penalty	State	Expected Reward/Penalty
D_1	210,500	m_1	-9,000
D_2	184,000	m_2	-9,000
D_3	131,500	m_3	-8,500
M_1	-23,000	F_0	-37,000
M_2	-21,500	F_1	-1,400,000
M_3	-20,500		

Table 5.9 Transition probabilities after maintenance

From	To	Probability	From	To	Probability
M_1	D_1	0.99	m_1	D_1	0.99
M_1	D_2	0.01	m_1	D_2	0.01
M_2	D_1	0.89	m_2	D_1	0.4
M_2	D_2	0.1	m_2	D_2	0.59
M_2	D_3	0.01	m_2	D_3	0.01
M_3	D_2	0.9	m_3	D_2	0.35
M_3	D_3	0.1	m_3	D_3	0.65

The transition rates used to calculate the remaining transition probabilities are presented in Table 5.10. To consider the vulnerability of aged equipment, it is assumed

that the rate of random failure increases with deterioration. For the base case study, the durations for major and minor maintenance are 6 and 3 days, respectively, and the duration of repairs after deterioration and random failures are 14 and 3.5 days, respectively.

Table 5.10 Transition rates among the states

Parameter	Rate (day ⁻¹)	Parameter	Rate (day ⁻¹)
λ_{12}	1/730	λ_3	1/122
λ_{23}	1/365	μ_0	1/3.5
λ_{3f}	1/365	μ_1	1/14
λ_1	1/243	μ_M	1/6
λ_2	1/183	μ_m	1/3

The results for availability assessment of wind turbines are derived using SMDP and MCS as analytical and simulation methods, respectively.

5.1.5.1 Analytical approach

The analytical approach is based on SMDP model using MATLAB software. The goal is to determine the optimum maintenance policy where the availability of the wind turbine is within an acceptable limit. The optimum policy depends on decision frequency (λ_d); and as the time between these decisions becomes longer (less frequent maintenance), a more extensive type of maintenance will be required. Fig. 5.11.a, b, and c show the optimum maintenance strategies obtained for each operating state of the wind turbine with different maintenance frequencies.

The most efficient decision in D_1 is always to do nothing since the wind turbine is in its best operating condition; however, in D_2 and D_3 , the optimum decision may vary. Performing too many maintenance functions is not efficient; and that is reflected in the optimization results with a do nothing decision if the maintenance frequency goes beyond 1.6 and 3.65 times per year for D_2 and D_3 , respectively. On the other hand, if the maintenance is performed less frequently, the optimum decision will shift toward performing a major maintenance.

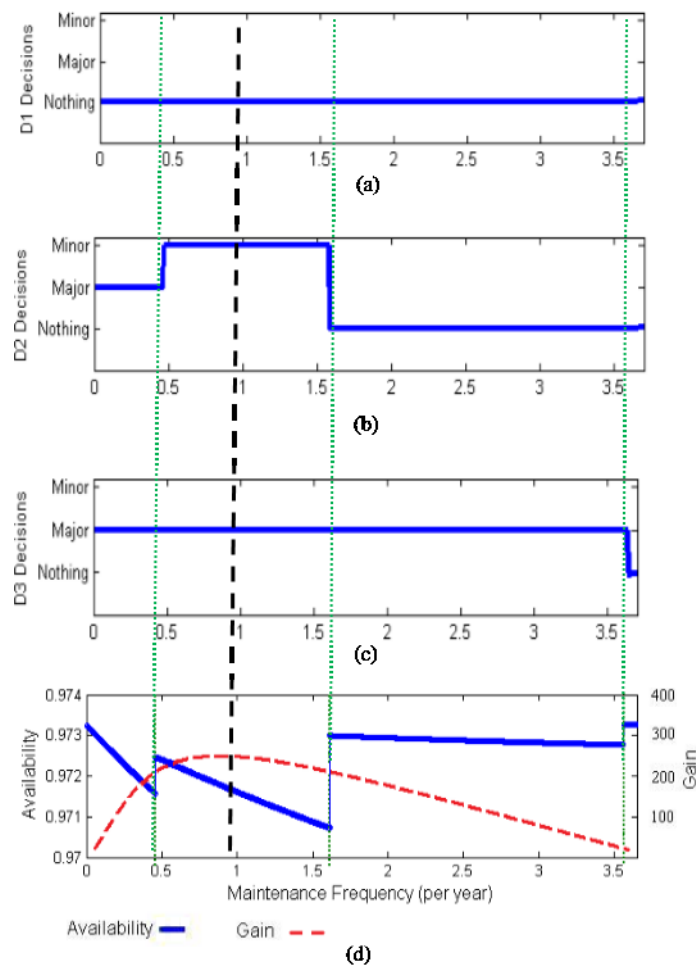


Figure 5.11 Optimum maintenance decisions at different operating states: a) D_1 , b) D_2 and c) D_3 using SMDP. d) Wind turbine availability and total system gain with various maintenance frequencies

Based on the optimum maintenance decisions at each working state, the availability of the wind turbine can be determined as shown in Fig. 5.11.d. The discontinuity in the availability curve occurs due to a change in the optimum maintenance strategy which modifies the transition probability matrix of the model. According to this figure, availability of the wind turbine is decreasing as the maintenance frequency increases. However, changes in optimum maintenance policy create sudden desirable availability rises at the corresponding points in maintenance frequency. In addition, Fig. 5.11.d. shows the gain of the system based on the SMDP model for different maintenance frequencies. Among these decisions, a maintenance rate of nearly once per year results in the highest calculated gain for which the optimum maintenance decisions are *do nothing*, *do minor maintenance*, and *do major maintenance* in D_1 , D_2 , and D_3 , respectively.

5.1.5.2 Simulation approach

The MCS-based model developed is employed to analyze the effect of maintenance and repair resource constraints on the availability and cost of the wind turbines, through different case studies.

First, the optimum maintenance policy is analyzed using MCS, and the results are compared with those from the SMDP method. Therefore, with the previously determined optimum maintenance frequency of once per year, we have run the MCS model (Fig. 3.13) for all 27 combinations of possible maintenance policies (d_1 , d_2 , d_3) in D_1 , D_2 , D_3 , and determine the policy which results in the highest gain (optimum policy). The simulation duration in this study is 20 years, and 5,000 is selected as the number of

iterations in order to have less than one percent error in the expected results with significance level of 0.05.

Fig. 5.12 shows the expected gains and the confidence intervals for all of the cases studied. *do nothing*, *do minor maintenance*, and *do major maintenance* are denoted by “1,” “2,” and “3” in this figure, respectively. The maintenance policy corresponding to the highest gain is “123” which is in agreement with the result of the SMDP method.

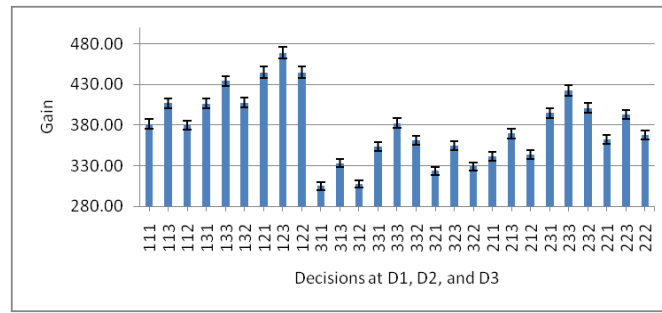


Figure 5.12 Expected gain of the wind turbine with different maintenance policies.

Fig. 5.13 displays the availability of the wind turbine with different policies. The availability corresponding to the optimum maintenance policy (about 0.972) is not the highest in this figure. This availability value is the same as the one derived from SMDP (Fig. 5.11) with a maintenance frequency of once per year.

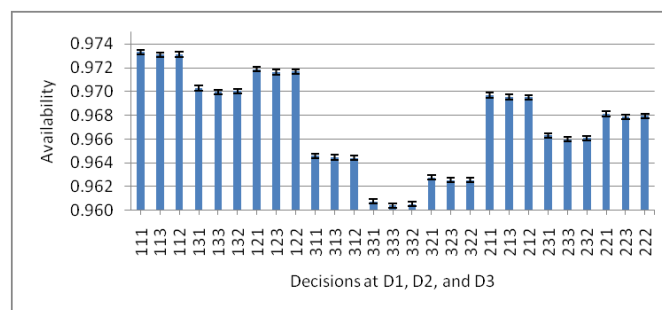


Figure 5.13 Expected availability of the wind turbine with different maintenance policies.

Next, if the duration of the maintenance or repair is increased, due to unavailability of the parts to be replaced or the ambient condition, the reliability of the wind turbine will decline and that impacts the increases the opportunity cost (OC) of the turbine (Eq. 3.27), as well. Fig. 5.14 shows the expected availability of the wind turbine with different duration of the maintenance compared to the base case. Three different profit rate (PR) of 2, 3, and 4 cents/kWh have been considered in these figures; and capacity factor is assumed to be 0.35 for all of the cases.

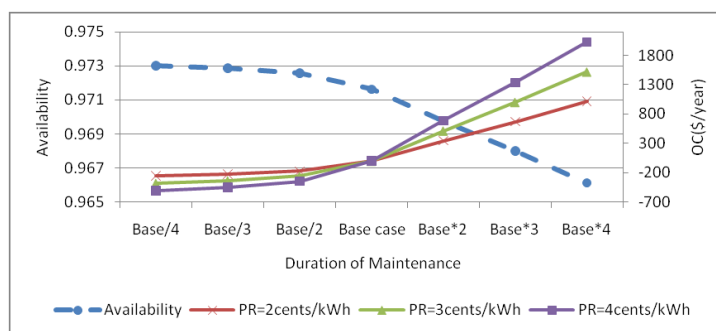


Figure 5.14 Expected availability of the wind turbine with different durations of maintenance.

The reliability of a group of wind turbines in a wind farm is affected by unavailability of the repair crew. Maintenance of a fleet of equipment can usually be planned ahead to minimize delay and lead time. However, equipment failures are random; in a wind farm, for example, simultaneous failures may occur on different wind turbines. Then, a turbine repair may be delayed due to already-scheduled repairs to other turbines.

This condition is modeled by simultaneous simulation of 20 wind turbines representing a wind farm using the MCS model. Assuming that the wind turbines are repaired one at a time, Fig. 5.15 depicts the expected wait time before repair, on average,

in both F_0 and F_1 failure states. As expected, the situation is aggravated in a wind farm with more wind turbines.

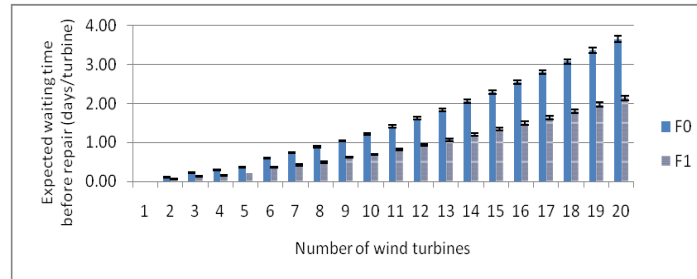


Figure 5.15 Expected wait time before repair with different numbers of turbines on a wind farm.

Fig. 5.16 shows the average availability of the wind turbines on this wind farm. Although the availability does not change considerably with a small number of wind turbines, this effect becomes increasingly significant to the long-term operation of large wind farms.

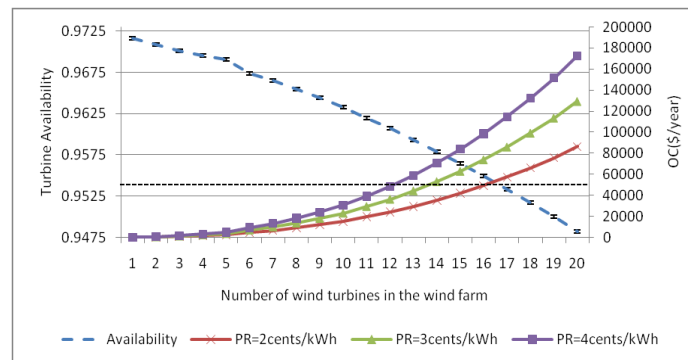


Figure 5.16 Expected availability of the wind turbine based on the number of turbines on the wind farm.

Fig. 5.16 also presents the opportunity costs the wind farm incurred because of the delay in repair of the wind turbines, with different expected rates of profit. A comparison of this cost with the cost of hiring an additional repair technician may be used to determine a cost-effective option. For our case study, it is assumed that a second

technician can be hired at a rate of \$50,000 per year [153]. Therefore, according to Fig. 5.16, the second repair technician becomes profitable with more than 12, 14, and 16 wind turbines on a wind farm with a \overline{PR} of 4, 3, and 2 cents/kWh, respectively.

5.2 Reliability of Smart Power Distribution System

In order to assess the reliability of a smart power distribution system, three different models, SDS model-I, SDS model-II, and SDS model-III, have been developed and described in Section 4.2. In addition, a number of studies have been proposed to evaluate the reliability of an SDS considering a variety of features of such system in the future. This section provides the results and discussion for these case studies and different sensitivity analyses.

5.2.1 *SDS reliability with demand side management*

The distribution system used for the case studies is an 86-bus system with a mesh topology based on SDS model-III. The one-line diagram of the system is shown in Fig. 4.10. A number of normally open switches are used to separate different feeders and create a radial-operated network during normal conditions. These switches are used to restore the power to the areas disconnected due to a failure. The main bus of this distribution system is a 33kV swing bus, and the loads are distributed on the 11kV buses.

The overall system data is given in Table 5.11. The input data used for the failure rates and repair durations of the system lines, transformers, and buses are given in Table 5.12.

Table 5.11 Distribution System Components

No. of busbars	86
No. of lines	92
No. of transformers	13
No. of loads	56
Avg. No. of customers per load point	186
Total peak load	52.08 MW
Total grid power losses	130 kW

Table 5.12 Input failure and repair data for the reliability analysis

Component	Failure rate	Mean Repair duration
Underground Cables	0.01/(km, year)	72 hrs
Overhead Lines	0.015/(km, year)	50 hrs
Power Transformers	0.008/year	96 hrs
11kV Busbar	0.008/year for terminal; 0.015/year per connection	7 hrs
33kV Busbar	0.005/year for terminal; 0.015/year per connection	10 hrs

The load values are diversified at different buses of the distribution system, and they represent different number of customers. However, loads are assumed to be from the same sector; and, therefore, the hourly change of all the loads follow the same pattern.

This section is comprised of different case studies. First, the base case without a DSM is studied; and the reliability indices are calculated. The effectiveness of a DSM strategy depends on both the scheme chosen and characteristics of the distribution system. Next, the impact of two DSM schemes presented in Section 4.2.3, *Energy Conservation* and *Load Shifting*, on the distribution system reliability is obtained. Finally, a sensitivity analysis is performed where the impact of different percentage of load shifting and system branch capacities on system reliability is determined.

5.2.1.1 Base case reliability

In this case, no DSM strategy is employed; and the load curve of Fig. 4.11 is applied to the loads. The results of the reliability indices are provided in Table 5.13. The total Energy Not Supplied of the distribution system is almost 76MWh per year; and each customer, on average, experiences 0.25 failures and an interruption duration of 1.9 hours per year.

Table 5.13 Reliability indices for the base case study

SAIFI 1/(Customer, Year)	SAIDI Hr./(Customer, Year)	CAIDI (Hr.)	ENS (MWh/Year)	ASAI
0.245187	1.904	7.767	76.369	0.9997826

5.2.1.2 Reliability with energy conservation

As described in section 4.2.3 the energy conservation is modeled using scaling factors. The reliability indices have been calculated for different load scaling factors and are shown in Table 5.14. The load scaling of “1” means there is no DSM in this scheme (base case). It is observed that as the system bus loads decrease, the reliability of the system improves. In this case, as a result of a 10% load reduction, SAIFI and SAIDI decrease by almost 20%.

Table 5.14 Reliability indices with different load scaling factors

Scaling Factor	SAIFI 1/(Customer, Year)	SAIDI Hr./(Customer, Year)	CAIDI (Hr.)	ENS (MWh/Year)	ASAI
1	0.245	1.904	7.767	76.369	0.99978
0.95	0.242	1.813	7.485	69.982	0.99979
0.9	0.240	1.47	6.118	51.986	0.99983
0.85	0.231	0.997	4.321	30.045	0.99989

5.2.1.3 Reliability with load shifting

The results for the reliability indices with different percentages of load shifting are given in Table 5.15.

Table 5.15 Reliability indices with different percentages of load shifting

Load Shifting	SAIFI 1/(Customer, Year)	SAIDI Hr./ (Customer, Year)	CAIDI (Hr.)	ENS (MWh/Year)	ASAI
0%	0.245	1.904	7.767	76.369	0.99978
5%	0.258	2.349	9.113	98.161	0.99973
10%	0.267	2.541	9.506	105.433	0.99971
15%	0.273	2.631	9.64	105.263	0.9997
20%	0.246	2.056	8.343	82.025	0.99976

Unlike what was expected, the results show that the customers, on average, experience higher failure frequency and duration as the loads are shifted by 5, 10, and 15%. Then, these indices decline with a 20% load shifting. In other words, the reliability of the distribution system may get worse with the load shifting DSM.

In fact, the reason is that one of the main factors affecting the reliability of a distribution network, in this case, is the loading of system components. If the system is highly loaded and lines and transformers are operating close to their maximum limit, there is a higher chance that peak load shaving does little in preventing load interruptions compared to valley filling at off-peak hours, in case of a failure. The next case study aims to justify the results and discussion provided with a sensitivity analysis.

5.2.1.4 Sensitivity analysis

This section evaluates the reliability of distribution systems with different levels of loadings and the load shifting DSM. In order to perform sensitivity analysis, the

capacities of the lines and the transformers of the system are increased to generate the network cases with lower levels of component loadings compared to the base case. Fig. 5.17 shows the loadings of the lines and transformers with different capacities at peak load, and as the capacities increase, the loading values decrease in the system.

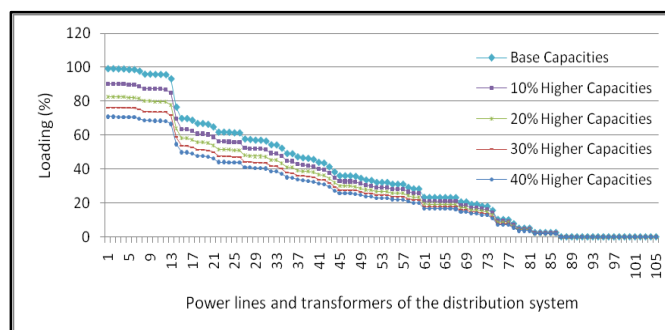


Figure 5.17 Loadings of power lines and transformers with different capacities at the peak load.

Figures 5.18 and 5.19 show the results for SAIFI and SAIDI, respectively. There are a number of important points to discuss in these case studies. First, the reliability of distribution system with higher capacities of branch components (while other system parameters are kept unchanged) is generally higher. Second, in a highly loaded distribution system, SAIFI and SAIDI usually rise with higher load shifting. However, there is a turning point where these indices start to decline. As indicated in the figures, this turning point approaches faster and in lower percentages of the load shifting if the distribution system components have higher capacities (i.e., lower system loadings). Third, the degree to which DSM impacts the reliability of a distribution system depends on the system capacity. For example, in the base case, the reliability of the system does not improve even with a 20% load shifting compared with the case where no DSM is applied.

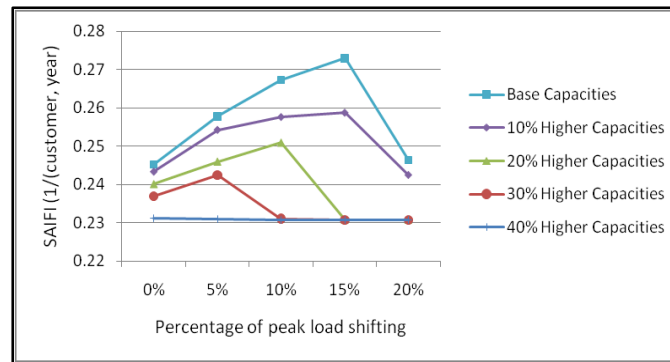


Figure 5.18 SAIFI with different percentage of load shifting and system capacity increments.

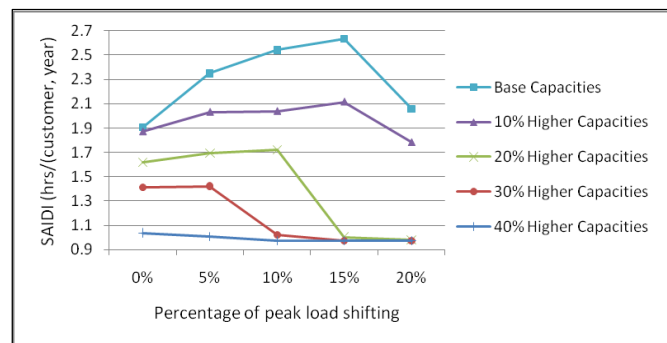


Figure 5.19 SAIDI with different percentage of load shifting and system capacity increments.

On the other hand, in certain loading levels of the system, the reliability may be improved with DSM. For example, in a case in which the capacity of a distribution system is 20% or 30% higher than our base case capacity, SAIFI and SAIDI may be improved if enough load shifting is applied. This impact is more dominant in interruption duration than in frequency.

In addition, the results indicate that if the capacity of the system is high enough (40% higher capacities than the base case), the load shifting has almost no impact on the reliability of the system. This implies that the loading level of the distribution system, in

this case, is much lower than a threshold where the shape of the load curve could influence the reliability.

5.2.2 SDS reliability with energy storage system

This study is performed based on SDS model-III. The single line diagram of the distribution system is shown in Fig. 5.20 where four DER systems are connected at the load points, LP1, LP2, LP3, and LP4, to generate the base case study. The statistics of the distribution system components are provided by Table 5.16.

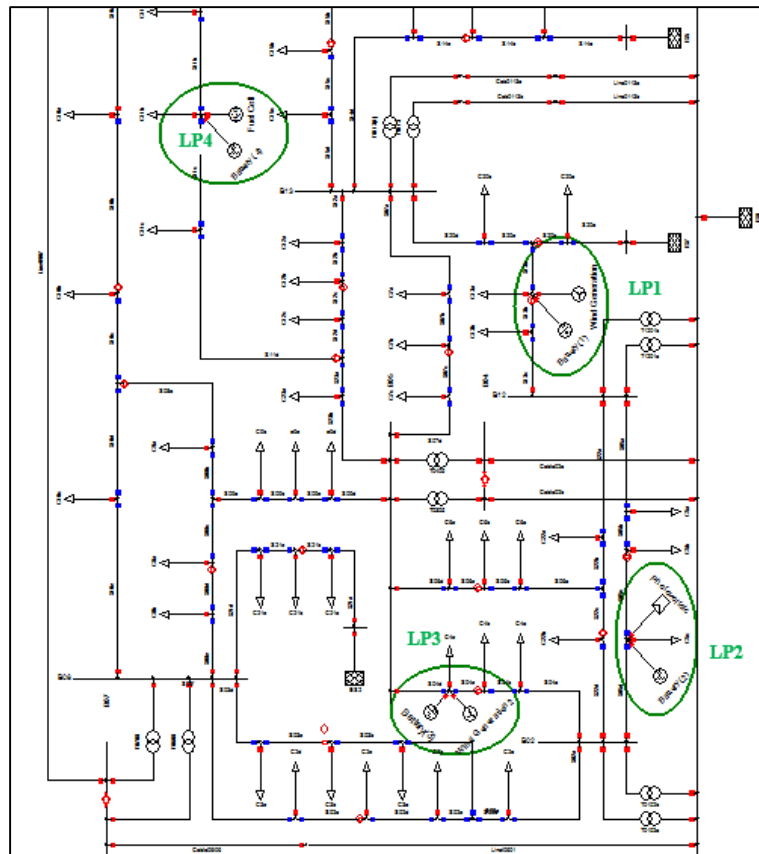


Figure 5.20 Single line diagram of the case study with four integrated DERs

Table 5.16 Distribution system statistics

No. of busbars	86
No. of lines	92
No. of transformers	13
No. of loads	56
No. of customers at LP1	440
No. of customers at LP2	460
No. of customers at LP3	320
No. of customers at LP4	60

The load curves at different load points are binned and represented by load state probabilities for the reliability study. As an example, Fig. 5.21 shows the load distribution for LP1 which includes the impact of DER in peak shaving, as well. This base case is used for reliability study and also for analyzing the effect of additional standby electric storage capacities on system reliability.

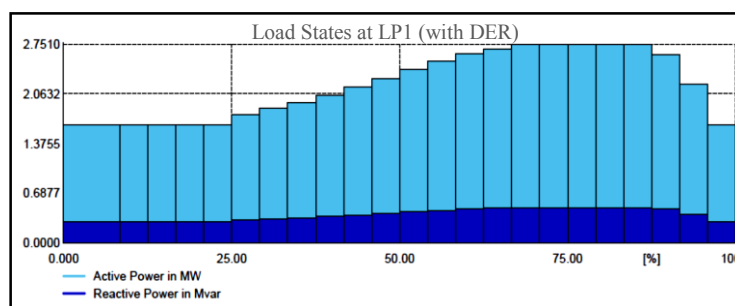


Figure 5.21 Cumulative percentage of LP1 active and reactive power binned to define load states, with DER in the system (base case).

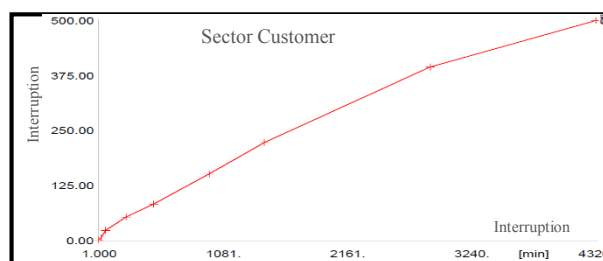
Table 5.17 provides the load flow information on the load points and the total system with and without DER integration. In addition, the input data for reliability analysis include the components' failure rates and repair duration as well as the load interruption cost function. These data are provided by Table 5.18 and Fig. 5.22, respectively.

Table 5.17 Load flow results of the distribution system

Parameters	Without DER	With DER (Base Case)
Peak Load at LP1	4.32 MW	2.75 MW
Peak Load at LP2	3.98 MW	2.53 MW
Peak Load at LP3	2.77 MW	1.76 MW
Peak Load at LP4	0.52 MW	0.33 MW
Total System Peak Load	53.4 MW	48.4 MW
Total System Power Loss	1.4 MW	1.15 MW

Table 5.18 Input data for the reliability analysis

Component	Failure Rate	Mean Repair Duration
Underground Cables	0.01/(km, year)	128 hrs
Overhead Lines	0.015/(km, year)	54 hrs
Power Transformers	0.006/year	116 hrs
11kV Busbar	0.009/year for terminal; 0.015/year per connection	7 hrs
33kV Busbar	0.006/year for terminal; 0.015/year per connection	12 hrs

**Figure 5.22 Load interruption cost function for the customers.**

Since the cost of interruption may vary for different types of customers, the curve provided in Fig. 5.22 is used as the base load interruption cost function in the study; and each load adopts this cost curve with an specific scaling factor. Furthermore, each feeder of the distribution system is equipped with a protection device which is used to clear the fault defined by the contingencies during the reliability evaluation.

5.2.2.1 Base case reliability

As previously described, four DER are connected at the specified load points, LP1 to LP4, but no standby storage capacity for reliability improvement is available in this case. The results of the system reliability indices are provided in Table 5.19. The total Energy Not Supplied of the distribution system is 145.5 MWh per year, and each customer, on average, experiences 0.46 failures and interruption duration of 4.02 hours per year.

Table 5.19 System reliability results for the base case study

System Reliability Indices (Base Case)				
SAIFI 1/(customer, year)	SAIDI hrs/(customer, year)	ASAI	EENS (MWh/year)	EIC (k\$/year)
0.46	4.02	0.99954	145.5	184

Table 5.20 provides the reliability results at the DER-integrated load points. The interruption costs are different at these load points due to variation of their loads, damage costs, and location in the distribution system. The LPENS and LPIC are highest at LP1 and lowest at LP4.

Table 5.20 Load point reliability results for the base case

Location	Load Point Reliability Indices (Base Case)			
	LPIF (1/year)	LPIT (hrs/year)	LPIC (k\$/year)	LPENS (MWh /year)
LP1	0.47	3.39	30	8.9
LP2	0.34	3.11	16.2	7.5
LP3	0.36	2.63	7.78	4.3
LP4	0.58	5.24	0.5	1.8

5.2.2.2 Sensitivity Analysis

Different sizes of standby electricity storage is added to the LP1 to LP4 nodes in the distribution system to improve reliability, and Total Cost of the system is analyzed for each case based on Eq. 4.19. Fig. 5.23 shows the system Total Cost comprised of expected interruption cost (EIC), as a representative of reliability cost, and levelized costs of different standby storage capacities at LP1. The levelized cost of standby storage is assumed to be 0.3 cents per kWh of capacity, per hour [132]. According to the results, a standby storage of 500 kWh is optimal at LP1. With this standby capacity added to the primary energy storage, the system Total Cost decreases by 2.7%; and the LPIC at LP1 is reduced by almost 30%, compared with the base case.

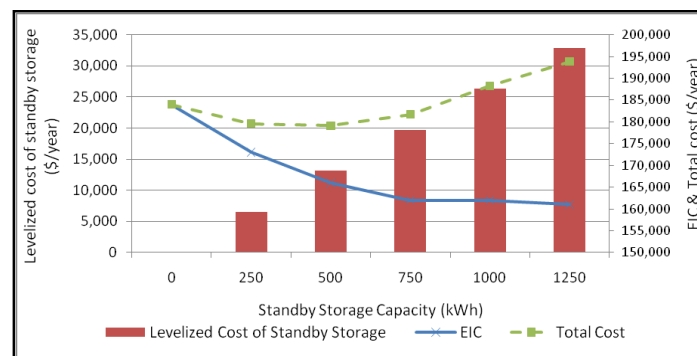


Figure 5.23 Cost analysis with different capacities of standby storage at LP1.

Figure 5.24 shows the results for all four DER-integrated load points. The total costs for each load point is derived by changing the storage capacity at that node while there is no standby storage capacity available at the other load points. This way, the results for each individual load point are compared independent of the changes in the other load points. For each load point, the increment steps of the storage capacity are defined by the percentages of that load point's peak load.

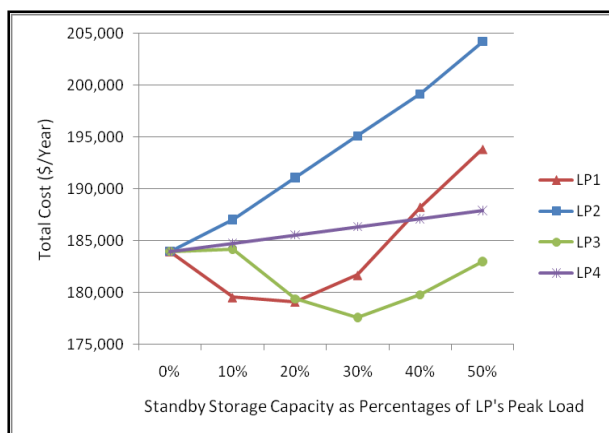


Figure 5.24 Cost analysis with different capacities of standby storage at all the DER-integrated load points.

According to this figure, standby storage is cost effective only at LP1 and LP3 where the Total Cost can be lower than the base case scenario.

5.2.2.3 Reliability-based sizing of energy storage system

In the previous section, the impact of the standby storage capacities on the system reliability was included independently using EIC at each load point. However, in order to size the energy storage system, their mutual effect on a distribution system should also be taken into consideration.

Due to the nonlinearity of the system, the study requires a sequential iterative process (Fig. 4.14) for reliability evaluation and determining the optimum standby storage capacities at all four DER-integrated load points.

Fig. 5.25 shows the results of the optimum standby capacities. The PSO study indicates that no standby storage is beneficial at LP2; but it is optimum to have standby electricity available at LP1, LP3, and LP4. The EIC of the system with these optimum

capacities is \$134,000 per year, and the Total Cost adds up to \$159,000 per year, which is less than the Total Costs in the previous section presented in Fig. 5.24.

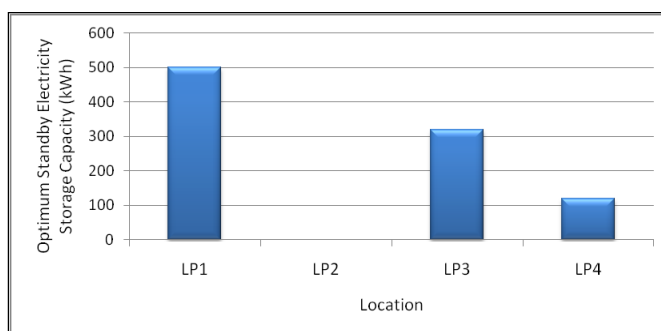


Figure 5.25 Optimum standby storage capacities at all of the DER-integrated load points.

The load point reliability indices provided by Table 5.21 indicate reliability improvement compared with the base case results in Table 5.20. In addition, SAIFI and SAIDI indices are slightly improved by 1% and 3% in this case, respectively.

Table 5.21 Load point reliability results with integration of the optimum standby energy storage systems

Location	Load Point Reliability Indices (With Optimum Standby Storage Capacities)			
	LPIF (1/year)	LPIT (hrs/year)	LPIC (k\$/year)	LPENS (MWh /year)
LP1	0.47	3.1	20	5.8
LP2	0.34	3.05	16.1	7.35
LP3	0.36	2.62	5.4	3.1
LP4	0.53	4	0.2	0.6

The reliability improvement is more considerable at LP1 which has the highest optimum standby storage capacity.

5.2.3 Optimum DER capacity for reliable SDS

This study aims to achieve a reliable and cost-effective demand supply for residential customers of smart power distribution system by determining the optimum sizes of distributed generation and storage system that best fit into the DSM used by the customers.

The study is based on the described SDS model-II according to which three types of loads have been introduced. L_1 has previously been defined using Eq.4.14. The demand considered for the schedulable L_2 group of loads is shown in Table 5.22. These loads are randomly distributed throughout the week in a way that complies with their usage frequency. Electric vehicle, for example, is one of the schedulable loads in this case study and consumes 4 kWh with an average commute of 15 miles/day [154]. It is also assumed that all L_2 loads are scheduled to be accomplished during 24 hours. In addition, during each hour, there are some expected L_3 loads, including TV, personal computer, some lighting, etc., which randomly change based on the uniform distribution, not exceeding 5% of the L_1 .

Table 5.22 L_2 Loads considered for the case study

Device	Total Energy (kWh)	Usage Frequency	Duration (Hours)
Washing machine	0.5	Twice a week	1
Clothes dryer	1.1	Twice a week	1
Dishwasher	1.2	Every day	2
Electric oven	2	Once a week	1
Electric vehicle	4	Every day	4
Iron	1	Once a week	1

The study parameters chosen for the base case are provided in Table 5.23 based on typical data from [132], [155]. The results of the base case indicate that a wind turbine of 3 kW and a battery of 4.5 kWh are the optimum choices for this residential customer to reliably supply all its electrical demand where the electricity cost of the household will be 65.4 cents per day. In addition, the results for this case show that the optimum plan would save an average of 25 percent compared to a conventional home with the same average load without battery and generation.

Table 5.23 Input parameters of the base case study

Parameter	C_G	C_B	R_c	DOD	ΔR	$E_{sell}(\max)$
Value	3.5	0.3	2	85	1.5	15
Unit	$\frac{\text{cents}}{\text{kWh}}$	$\frac{\text{cents/kWh of capacity}}{\text{Hour}}$	$\frac{\text{kWh}}{\text{Hour}}$	%	$\frac{\text{cents}}{\text{kWh}}$	$\frac{\text{kWh}}{\text{day}}$

5.2.3.1 Sensitivity to the cost of DER

The impact of renewable generation and battery cost (C_G and C_B) on the optimum capacities is studied and the results are shown in Fig. 5.26. As C_B decreases, the optimum point is shifted toward higher battery capacities (from 0 to about 7 kWh). In addition, as the cost of wind generation increases, larger batteries become relatively more efficient than wind generators. It is observed that the optimization process prefers to choose the highest battery capacity when the battery cost is at its minimum and the wind generation cost is at its maximum value. Contrary to Fig. 5.26(a), the cost of battery in Fig. 5.26(b) does not show a considerable impact on the generator capacity.

On the other hand, as the cost of generation decreases, higher-capacity wind turbines become more beneficial. In this graph, the generation cost of about 3.5 cents/kWh acts like a turning point at which there is a high slope toward higher wind generation capacities. This is possibly because the average EPR of this case study is 3.2 cents/kWh; and, therefore, generation costs less than this rate become exceedingly appealing.

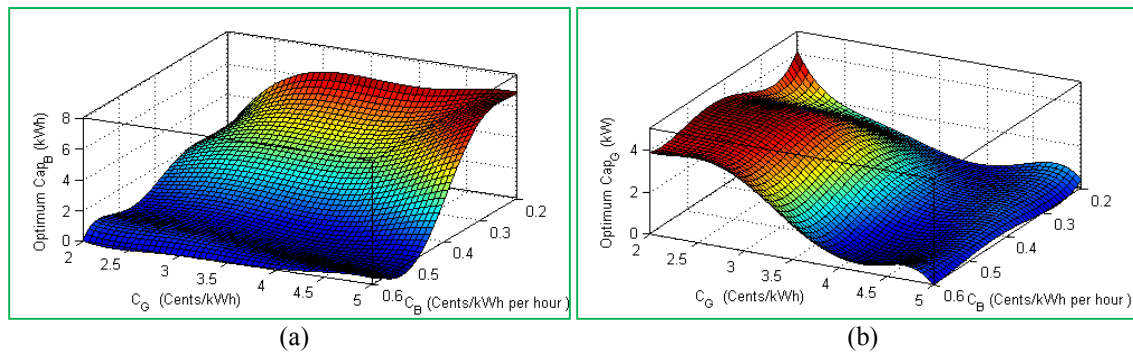


Figure 5.26 Optimum size of battery (a) and wind generation (b), with different leveled costs of wind generation and battery.

As a result of this study, the minimum household electricity costs are computed and plotted in Fig. 5.27. As expected, the electricity cost of the home is highest when both C_G and C_B are at their maximum values.

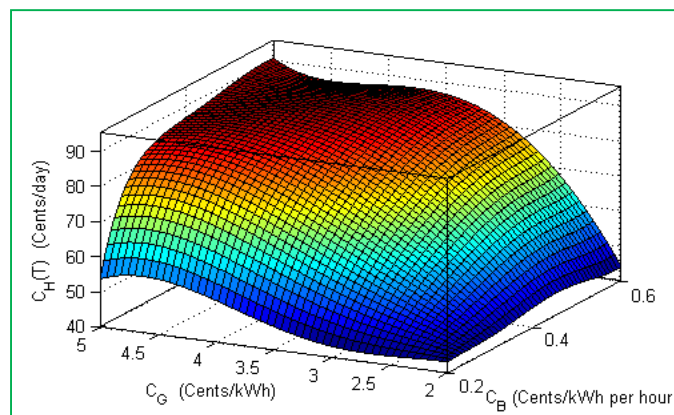


Figure 5.27 Minimum electricity cost of the household with different leveled costs of wind generation and battery.

An interesting result is achieved by comparing the electricity cost in this figure with one of a conventional home without a generation-storage system. In the case of a conventional household, the electricity cost is 92 cents/day, which is close to the $C_H(T)$ value of the household with a C_G of 5 cents/kWh and a C_B of 0.6 cents/kWh per hour. Therefore, it is expected that beyond this operating point, no additional savings can be achieved by investing in a wind generator and battery, indicating the corresponding optimum capacity of the wind generator and battery should be almost zero, as justified by the results shown in Fig. 5.26.

5.2.3.2 Sensitivity to electricity purchase rate

In this case, the sensitivity of the capacities and electricity cost of the household for the base case with different electricity rates (EPR) have been studied; according to the results shown in Fig. 5.28, as EPR rises, an increasing trend toward higher generation-battery capacities is observable.

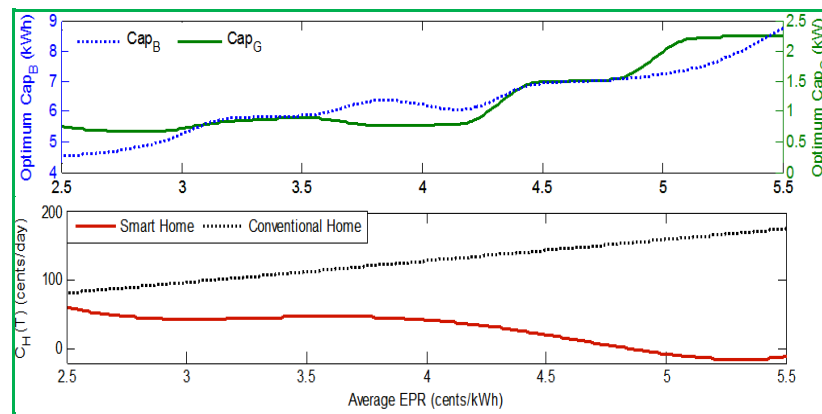


Figure 5.28 Sensitivity of wind generation-battery capacities (top) and the electricity cost of the home (bottom) to the change of average EPR.

It is notable that as the electricity cost of a conventional household rises with a higher EPR, the electricity cost of the smart home decreases. The difference between these two costs is more noticeable at electricity rates higher than the levelized cost of wind generation where the electricity cost of the smart household has a higher rate of decrease. Residential customers are even able to make a profit from selling their power to the grid at an average EPR of 5 cents/kWh; This could be because beyond this point, the cost of wind generation becomes less than the average ESR (with a ΔR of 1.5 cents/kWh).

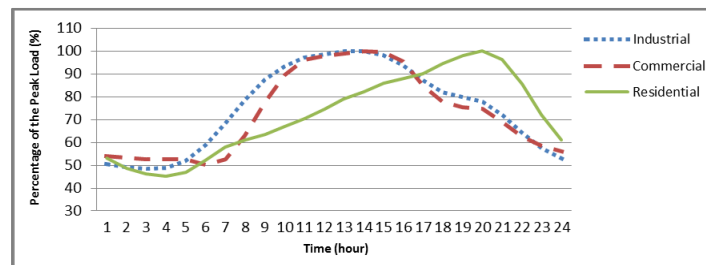
5.2.4 SDS reliability with active customer interactions

A number of case studies are provided for reliability assessment of a smart power distribution system comprised of different types of active customers who may own renewable generation and storage systems. The SDS model-I has been used for the studies. Table 5.24 provides base case information about residential, commercial, and industrial customers denoted by subscripts R, C, and I, respectively. R_{out} represents the radius of the impacted area, and it is used to model the extent of a contingency in the system. This radius is randomly selected between 0 (i.e., no impact) and up to $10 \times d_N$ (i.e., nearly total system outage) where d_N represents the average distance between neighboring customers. $\overline{Cap_B}$ and $\overline{Cap_G}$ denote average battery and renewable generation capacities, respectively; The parameter d is an indicator of the customer demand, and λ and μ are the average rates of outage and system restoration, respectively.

Table 5.24 Parameters used for the case studies.

Parameter	N_R	N_C	N_I	$\overline{Cap_{B,R}}$	$\overline{Cap_{B,C}}$	$\overline{Cap_{B,I}}$	$\overline{Cap_{G,R}}$	$\overline{Cap_{G,C}}$
Value	400	200	20	1.25	2.5	15	0.5	1
Unit	-	-	-	kWh	kWh	kWh	kW	kW
Parameter	$\overline{Cap_{G,I}}$	$d_{R,max}$	$d_{C,max}$	$d_{I,max}$	R_{out}	λ	μ	DR_x
Value	25	1.1	1.6	20	$U(0-10)$	2	2×10^{-4}	20
Unit	kW	kW	kW	kW	d_N	$\frac{1}{Year}$	$\frac{1}{Year}$	%/hour

The impact of different types and capacities of renewable generation as well as customers' interactions on the reliability is studied through various scenarios. The hourly data used for the wind speed, solar radiation, and customer loads are from [156], [157], and [158], respectively, where the average data for three load sectors, wind, and PV generation are depicted in Figs. 5.29 and 5.30, respectively. The customer damage functions used for the loss-of-load cost analysis per customer sector are based on typical data from [159] and [160].

**Figure 5.29 Average load profiles for residential, commercial, and industrial loads.**

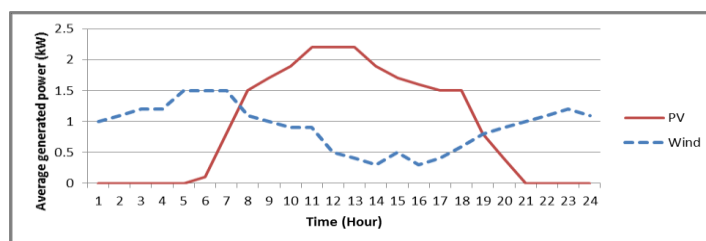


Figure 5.30 Typical average PV and wind generation profiles.

5.2.4.1 Reliability analysis with residential customers

In this study, the agents are all residential customers; and their distributed generation is solely wind power. The objective is to investigate the impact of renewable generation and storage systems, as well as neighborhood electricity trading among the agents, on SDS reliability from the system and customer points of view.

Fig. 5.31 shows the SAIFI and SAIDI parameters of the smart grid, with different percentages of residential customers using battery-wind generation systems, and the neighborhood power trading option (SAIFI and SAIDI are represented in a single diagram to save space). As the percentage of customers with DER increases, both the average duration and frequency of the interruption in the system decrease with different percentages. In fact, by having additional electricity resources in the system, the customers are more likely to be able to satisfy their loads, subject to a contingency in the system. Therefore, a cost analysis may be exercised by the customers to determine whether the cost of the DER is justifiable considering the customers' loss of load costs.

Note also that the reliability of the SDS cannot be improved by having customers of the same sector trade electricity within their neighborhood. As shown in Fig. 5.31,

with no DER available, the reliability indices are similar with or without electricity trading because there is not any extra resource to be shared by the customers. However, in a system where all of the customers have distributed generation and battery systems, reliability degrades with neighborhood trading. Neighborhood trading is not advantageous in this case because all of the residential customers have relatively similar demand profiles, causing the agents to have concurrent deficit/surplus electricity throughout a typical day. In other words, when a residential customer needs power due to a failure in the system, there is a high chance that all other neighbors need power as well.

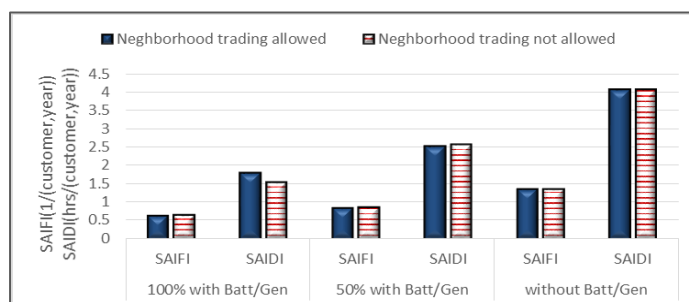


Figure 5.31 SDS-perspective reliability indices with different percentages of residential customers owning generation-battery systems and neighborhood electricity trading option.

Table 5.25 provides the reliability indices from the customer's perspective, for the same study. As a result of using DER, customers' energy not supplied and the interruption costs decrease. In this case, by having 50% and 100% of customers own distributed generation and battery systems, the customer interruption cost drops by 45% and 79%, respectively.

Table 5.25 Customer perspective reliability with different percentages of them owning generation-battery systems, and neighborhood electricity trading option.

Customer Sector	Percentage with Batt/Gen	Neighborhood Trading Option	$VOLL_R$ (\$/kWh)	ENS_R (kWh/customer, year)
Residential	0%	Possible	6.67	2.91
		Off	6.67	2.91
	50%	Possible	6.67	1.6
		Off	6.65	1.6
	100%	Possible	6.6	0.63
		Off	6.5	0.62

5.2.4.2 Reliability analysis with residential, commercial, and industrial customers

In this case, the customers are diversified from residential, commercial, and industrial sectors, with parameters provided in Table 5.24. These customers have different load profiles during an average day, as shown in Fig. 5.29. Similar to the previous diagram, Fig. 5.32 shows how the reliability of the smart grid improves by having higher percentages of the customers own DER. However, unlike the previous case, the smart distribution system benefits from customers cooperation within their neighborhood area.

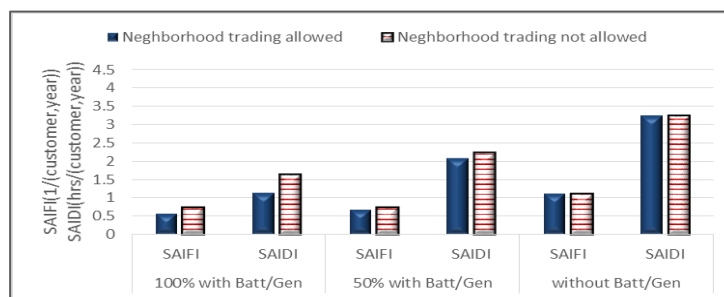


Figure 5.32 SDS-perspective reliability indices with different percentages of residential/commercial/industrial customers owning generation-battery systems and neighborhood electricity trading option.

When a failure occurs in a certain region, it is likely that the agents, randomly distributed in the environment, are from different load categories; and part of the electricity demand of one agent can be supplied by the excess power of its neighbor. By comparing the reliability indices with and without neighborhood electricity trading in Fig. 5.32, it is noted that system reliability improves more as the percentage of customers owning DER increases. For example, in a system where all the customers use renewable generation and storage systems, if neighborhood power trading is allowed, SAIFI and SAIDI can be improved by 24% and 31%, respectively. Table 5.26 provides the values for customer-side reliability indices.

Table 5.26 Reliability of the residential/commercial/industrial customers with varying percentages of owning generation-battery systems, and neighborhood trading options.

Customer Sector	Percentage with Batt/Gen	Neighborhood Trading Option	$VOLL_s$ (\$/kWh)	ENS_s kWh (customer, year)
Residential	0%	Possible	6.62	2.19
		Off	6.62	2.19
	50%	Possible	6.6	1.2
		Off	6.67	1.28
	100%	Possible	5	0.44
		Off	6.36	0.61
Commercial	0%	Possible	33.3	4.38
		Off	33.3	4.38
	50%	Possible	33	2.4
		Off	33	2.56
	100%	Possible	30	0.88
		Off	31.8	1.22
Industrial	0%	Possible	25	43.8
		Off	25	43.8
	50%	Possible	24	24
		Off	24	25.6
	100%	Possible	21	8.8
		Off	22.7	12.2

The diversity of customer sectors makes the power trading option valuable. In a case study where all of the customers own renewable generation and storage systems, the option of electricity trading among the neighbors reduces the interruption cost for residential, commercial, and industrial customers by 43%, 32%, and 33%, respectively. Compared with the previous case, residential customers here experienced less duration of outage and value of lost load, accordingly.

5.2.4.3 Sensitivity analysis with wind and PV generation

The goal of this section is to determine the impact of renewable generation-battery capacities (by scaling the base capacity values provided by Table 5.24), as well as the type of renewable generation (wind, PV), on the reliability of an EDS. In our case study, the capacity factors of wind and PV generation are roughly 30% and 25%, respectively. Therefore, in order to study the impact of these two generation technologies on system reliability, regardless of their total generated electricity, the capacity of the PV system is considered to be 20% higher than that of wind generation. In all of the case studies in this section, the customers own DER and are allowed to trade electricity with their neighbors. Figs. 5.33 and 5.34 provide SAIDI and SAIFI results for three cases, respectively: 1) all of the customers have wind generation systems, 2) half of the customers use wind generation and the other half use PV, and 3) all of the customers have PV systems.

Fig. 5.33 indicates that by increasing the capacities of the generation and storage, the customers' average duration of interruption decreases. In fact, by allocating higher

generation capacity, the customers are able to generate more power during a contingency; and with higher capacities of electricity storage, they are able to survive longer using the stored electricity. Reliability improvement is faster with lower DER capacities, and there is a threshold near the scaling factor of 2, where a DER is capable of providing almost the total demand of its customer independent from the utility. Thus, the reliability improvement is not significant for the capacities larger than this threshold.

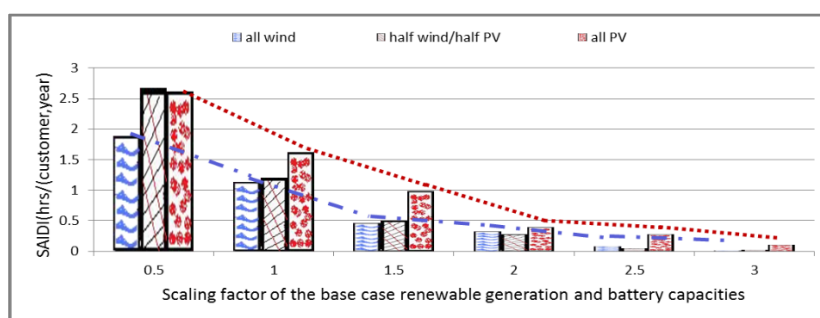


Figure 5.33 SAIDI of the SDS affected by different capacities of renewable generation-storage and generation technologies.

In addition, the trend curve for SAIDI with wind generation lies below that for PV generation; and this generally indicates a lower duration of customer interruption with wind generation. The reason should be related to generation profiles of these two types of renewable generation. The average wind generation varies less than the PV output, which is zero during the night (Fig. 5.30). Therefore, in case of an interruption due to a lack of generation/storage at a certain time of a day, the customers with wind generation are expected to generate power sooner than those with solar panels; and, this causes their duration of interruption to be shorter.

Fig. 5.34 shows the average frequency of the failure per customer for the same case. According to this figure, SAIFI with a PV system drops at lower capacities (scaling factor of ~ 1.5) than with the wind generation.

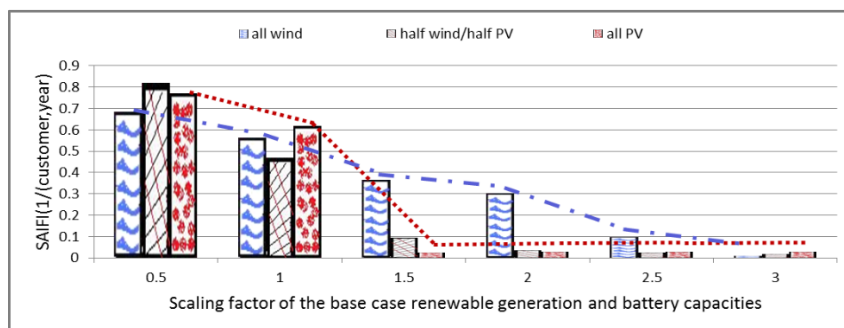


Figure 5.34 SAIFI of the SDS affected by different capacities of renewable generation-storage and generation technologies.

The output power of a solar panel is basically available during the daytime and more correlated with the load (Figs. 5.29 and 5.30) compared with the wind generation which is more diversified throughout a day. Therefore, the PV system would be capable of fully supplying its own loads at lower capacity than wind generation; and it leads to a faster drop of failure frequency of an average customer. Comparison of the results between these two generation technologies indicates that the energy not supplied is almost the same in both cases. On the other hand, Fig. 5.35 compares the value of lost load for all three customer sectors having wind or PV distributed generation systems.

The results indicate that with wind generation, VOLL is 23%, 10%, and 8% lower than with PV system for residential, commercial, and industrial customers, respectively.

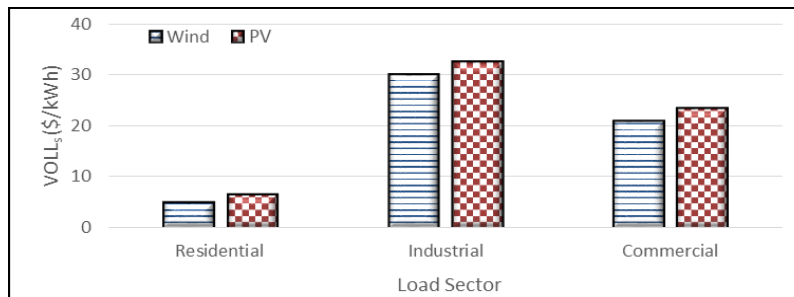


Figure 5.35 Comparison of wind and PV impact on VOLL in load sectors.

Since VOLL is a function of interruption duration (Eq. 4.33), lower VOLL implies less duration of interruption with wind generation, which is a similar result to what is observed in Fig. 5.33.

CHAPTER 6

CONCLUSION AND FUTURE WORK

6.1 Conclusion

6.2 Recommendation for the Future Work

6.1 Conclusion

There are two main goals planned for this dissertation. First, due to the increasing number of distributed and renewable energy resources in the power system and the uncertainties involved regarding their reliable operation and availability of their output generation, the first goal was to model the operation and evaluate the reliability of wind turbines as renewable-based generators. Next, considering the future power system infrastructure accommodating the renewable generation, energy storage, advanced customer initiated demand side management, and the urge for improving the reliability and availability of electricity to the customers, the second goal was to provide corresponding models and methods to evaluate and improve the reliability of future power distribution systems.

A summary of the contribution of this dissertation is provided as follows:

- An improved FMEA method was proposed for reliability evaluation of renewable generation, such as wind turbines. The improvement was required in order to overcome the previous shortcomings including difficulty to determine the failure modes severity with diverse types of wind turbines, and limited and qualitative results. The proposed RB-FMEA method is a cost initiated quantitative approach whose outcome is proportional to the equipment performance. The case study and sensitivity analysis showed the simplicity of the method and its application to determine the failure costs under different restrictions, electricity rates, and fault detection strategies.

- A Markovian model was proposed to evaluate the reliability of wind farms where each state of the model represented the number of similar wind turbines working at a time in order to reduce the computational burden compared with a two-state Markov model. The model was used for both short-term time dependent reliability evaluation, which can be employed for operational planning and maintenance, and long-term reliability assessment, which is suitable for determining the expected loss of load and wind power generation in the long run.
- A hybrid analytical-simulation approach was proposed for reliability assessment and maintenance optimization of renewable generation systems such as wind turbines. The proposed method was based on the Markov decision processes and Monte Carlo simulation methods in order to overcome the limits of each individual method, namely model complexity and large number of iterations, respectively. Using this approach, wind farm maintenance planners and asset managers are able to (1) determine the optimum type and frequency of maintenance for the wind turbines; (2) study the effect of maintenance and repair resource restrictions on the availability and costs of the wind farm; and (3) run cost/benefit studies to allocate the proper number of technicians for maintenance and repair, taking into consideration the costs of wind farm unavailability and additional crew employment.

- Three different models of a smart distribution system, SDS model-I, SDS model-II, SDS model-III, and several demand side management strategies were developed which are applicable for operation, planning and reliability studies of future power systems. The software used for these three models were Repast symphony, MATLAB, and DIgSILENT Power Factory, respectively.
 - The SDS model-I, as a multiagent system based model, included electricity customers with distributed power generation and storage system. The stochastic behavior of renewable generation, loads, and dynamic electricity rate were also taken into account. In addition, customers had the chance to interact with the grid and their neighbors to trade electricity when required. Two demand side management strategies, *Utility-based method*, and *Average Deficit method*, were proposed to direct the customers to buy, store, sell, or consume electricity in order to reliably supply their demands cost-effectively. The study results showed that customers could successfully reduce their electricity costs, and at the same time, help to alleviate the total peak demand from the utility.
 - The SDS model-II was developed for planning purposes. In the first stage, the customer used a rule-based electricity management system which could effectively manage various types of its load, renewable generation, and electricity storage, and trade power with the grid. The

time-variant inputs to this system were wind speed, three categories of load, and electricity rates. In the second stage, an optimization problem was formulated where for planning purposes, the stochastic variables were represented by their individual probability distributions for each hour of a day. Using the proposed hybrid MCS-PSO approach in the third stage, the optimum sizes of the generation and battery system were obtained such that the overall electricity cost of the customer was minimized. Therefore, this model may be used by the customers of future power distribution system to invest in the right capacity of renewable generation and battery considering reliable load supply, renewable resource availability, and electricity rates.

- The SDS model-III provided a more detailed model of the utility side of a distribution system considering power flow constraints, such as loading limits of power system branch components and operating voltage limit of the system buses. This model was used to study the impact of demand side management and energy storage on the reliability of the power distribution system. The results showed that depending on the loading of the system components, peak load alleviation might improve reliability in a distribution system. In addition, according to the optimization study, the allocation of additional storage capacity, as a standby electricity resource, at

specific system buses improved load point and system level reliability, and minimized the total reliability costs.

- A number of simulation approaches for reliability evaluation were proposed which could address different aspects of future power distribution systems. Reliability was assessed from both the system and customer point of view by applying a number of commonly used and newly defined indices. Several case studies were analyzed to determine and improve the reliability of future power systems impacted by various features, such as:
 - Diversity of active customers from different sectors;
 - Different demand side management programs;
 - Communication and power transactions among neighboring customers;
 - Type and capacity of integrated renewable generation and storage systems.

6.2 Recommendation for the Future Work

- *A comprehensive reliability model*: This dissertation provided modeling and reliability analysis of future distribution power systems considering a variety of key factors. However, as previously mentioned, the interdependency of electrical, communication, and control systems in the future smart grid necessitates a comprehensive reliability model which considers the mutual impacts of these systems on one another. The comprehensive reliability model should be modular and flexible in order to include various potential design

configurations and their effect on the overall system reliability. The work in this dissertation could be used as the base for such comprehensive model.

- *MAS-based electricity market model integration*: It is accepted by many power system engineers that retail electricity market is an efficient way of managing the demand and providing reasonable electricity rates to the end customers. The MAS model of the active customers (SDS model I), developed in this dissertation, may be expanded to include a MAS-based retail electricity market which provides dynamic electricity rates based on the system demand, and power flow restrictions.
- *Reliability of smart grids impacted by future protection schemes*: The future power system relies on the latest advances in sensing, computation, and communication technology. For instance, Synchronized Measurement Technology (SMT), including Phasor Measurement Units (PMUs) play a key role in making distributed real-time data available throughout the power system, where all the measurements are synchronized to a reference clock signal from the Global Positioning Systems (GPS). This enables real-time monitoring and control, and more generally wide area monitoring protection and control (WAMPAC), for a fast decision making in case of congestions or disturbances in the system. It is critical to model and study the impact of WAMPAC on reliability of the future power system, including the distribution system, since high reliance on these systems increases the consequence of their malfunction, as well. The smart grid model in this dissertation is a

suitable base for incorporating the distributed protection schemes and analyzing their impact on reliability of the future power systems.

REFERENCE

- [1] "Methods for NERC's 2008-2017 Regional & National Peak Demand and Energy Projection Bandwidths," Load Forecast Working Group, NERC, 2008.
- [2] Litos Strategic Communication, "Smart Grid: an Introduction," U.S Department of Energy.
- [3] K. H. LaCommare and J.H. Eto, "Cost of power interruptions to electricity consumers in the United States," Berkeley National Laboratory, 2006.
- [4] F. Li, W. Qiao, H. Sun, H. Wan, J. Wang, Y. Xia, Z. Xu and P. Zhang, "Smart transmission grid: Vision and framework," *IEEE Trans. Smart Grid*, vol. 1, no. 2, pp. 168-177, 2010.
- [5] T. Basso and R. DeBlasio, "Advancing Smart Grid Interoperability and Implementing NIST's Interoperability Roadmap," in *Grid-Interop Conference*, 2009.
- [6] V. Hamidi, K.S. Smith and R. Wilson, "Smart Grid technology review within the transmission and distribution sector," in *Innovative Smart Grid Technologies (ISGT)*, 2010.
- [7] P. Palensky and D. Dietrich, "Demand Side Management: Demand Response, Intelligent Energy Systems, and Smart Loads," *IEEE Trans. on Industrial Informatics*, vol. 7, no. 3, pp. 381-388, Nov 2011.

- [8] G. T. Heydt, B. H. Chowdhury, M. L. Crow, D. Haughton, B. D. Kiefer, F. Meng and B. R. Sathyanarayana, "Pricing and control in the next generation power distribution system," *IEEE Trans. Smart Grid*, vol. 3, no. 2, pp. 907-914, 2012.
- [9] "Smart Grid System Report," U.S. Department of Energy, 2009.
- [10] "2010 Smart Grid Report," U.S. Department of Energy, Report to Congress, 2012.
- [11] "Grid 2030: A National Vision For Electricity's Second 100 Years," U.S. Department of Energy, 2003.
- [12] E. S. Cheney, "U.S. Energy Resources: Limits and Future Outlook," *American Scientist*, vol. 62, no. 1, pp. 14-22, 1974.
- [13] T. Tezuka, K. Okushima and T. Sawa, "Carbon tax for subsidizing photovoltaic power generation systems and its effect on carbon dioxide emissions," *Applied Energy*, vol. 72, pp. 677-688, 2002.
- [14] J. A. Momoh, *Electric Power Distribution, Automation, protection, and Control*, New York: CRC Press, 2008.
- [15] F. Spinato, P.J. Tavner, G.J.W. van Bussel and E. Koutoulakos, "Reliability of wind turbine subassemblies," *IET Renewable Power Generation*, vol. 3, no. 4, pp. 387-401, 2009.
- [16] P. Denholm and R. M. Margolis, "Evaluating the limits of solar photovoltaics (PV) in traditional electric power systems," *Energy Policy*, vol. 35, pp. 2852-2861, 2007.
- [17] C.E. Ebeling, *An introduction to reliability and maintainability engineering*, New York: McGraw Hill, 1997.

- [18] S. Faulstich, B. Hahn, P. Tavner, R. Gindele, M. Whittle and D. Greenwood, "Study of Effects of Weather & Location on Wind Turbine Failure Rates," in *European Wind Energy Conference and Exhibition (EWEC)*, Warschau, 2010.
- [19] H. Guo, S. Watson, P. Tavner and J. Xiang, "Reliability analysis for wind turbines with incomplete failure data collected from after the date of initial installation," *Reliability Engineering and System Safety*, vol. 94, no. 6, p. 1057–1063, 2009.
- [20] E. L. Meyer and E. E. van Dyk, "Assessing the reliability and degradation of photovoltaic module performance parameters," *IEEE Trans on Reliability*, vol. 53, pp. 83-92, 2004.
- [21] T. E. Hoff and R. Perez, "Modeling PV fleet output variability," *Solar Energy*, vol. 86, pp. 2177-2189, 2012.
- [22] M. A. Eltawil and Z. Zhao, "Grid-connected photovoltaic power systems: Technical and potential problems-A review," *Renewable and Sustainable Energy Reviews*, vol. 14, pp. 112-129, 2010.
- [23] V.V. Tyagi, N.A.A. Rahim, A. Jeyraj and L. Selvaraj, "Progress in solar PV technology: Research and achievement," *Renewable and Sustainable Energy Reviews*, vol. 20, pp. 443-461, 2013.
- [24] P. Nimnuan and S. Janjai, "An approach for estimating average daily global solar radiation from cloud cover in Thailand," *Procedia Engineering*, vol. 32, pp. 399-406, 2012.
- [25] T. Sarver, A. Al-Qaraghuli and L. L. Kazmerski, "A comprehensive review of the

- impact of dust on the use of solar energy: History, investigations, results, literature, and mitigation approaches," *Renewable and Sustainable Energy Reviews*, vol. 22, pp. 698-733, 2013.
- [26] C. Deline, A. Dobos, S. Janzoua, J. Meydbray and M. Donovan, "A simplified model of uniform shading in large photovoltaic arrays," *Solar Energy*, vol. 96, pp. 274-282, 2013.
- [27] K. Moslehi and R. Kumar, "A Reliability Perspective of the Smart Grid," *IEEE Trans. on Smart Grid*, vol. 1, no. 1, pp. 57-64, 2010.
- [28] "Reliability of Electric Utility Distribution Systems: EPRI White Paper," EPRI, Palo Alto, 2000.
- [29] M. G. Lauby, "Reliability considerations for application of Smart Grid technologies," in *IEEE Power & Energy Society GM*, 2010.
- [30] M. Rastegar, M. Fotuhi-Firuzabad and A. Safdarian, "A Novel Method to Assess Distribution System Reliability Considering Smart Solar Cell," in *Second Iranian Conference on Smart Grids (ICSG)*, 2012.
- [31] P. Wang and R. Billinton, "Reliability cost/worth assessment of distribution systems incorporating time-varying weather conditions and restoration resources," *IEEE Trans. Power Delivery*, vol. 17, pp. 260-265, 2002.
- [32] I.S. Ilie, I. Hernando-Gil, A. J. Collin, J.L. Acosta and S. Z. Djokic, "Reliability Performance Assessment in Smart Grids with Demand-side Management," in *2nd ISGT Europe*, 2011.

- [33] G. Celli, E. Ghiani, F. Pilo and G. G. Soma, "Reliability assessment in smart distribution networks," *Electric Power Systems Research*, vol. 104, pp. 164-175, 2013.
- [34] M.A. da Rosa, A. M. L. da Silva and V. Miranda, "Multi-agent systems applied to reliability assessment of power systems," *Electrical Power and Energy Systems*, vol. 42, pp. 367-374, 2012.
- [35] S.M.Spina and J.D.Skees, "Electric utilities and the cybersecurity executive order: anticipating the next year," *The Electricity Journal*, vol. 26, no. 3, 2013.
- [36] Smart Grid Interoperability Panel, "Guidelines for smart grid cyber security: vol.1, smart grid cyber security strategy architecture, and high-level requirements," NIST, 2010.
- [37] D. Niyato, Q. Dong, P. Wang and E. Hossain, "Optimizations of power consumption and supply in the smart grid: analysis of the impact of data communication reliability," *IEEE Trans. Smart Grid*, vol. 4, pp. 21-35, 2013.
- [38] Y. Jun, "Modelling and Analysis on Smart Grid against Smart Attacks," in *Master's Theses*, 2013.
- [39] Anumaka and M. Chukwukadibia, "Fundamentals of reliability of electric power system and equipment," *International Journal of Engineering Science and Technology*, vol. 3, no. 6, 2011.
- [40] R. Ahmad and S. Kamaruddin, "An overview of time-based and condition-based maintenance in industrial application," *Computers and Industrial Engineering*

Journal, vol. 63, pp. 135-149, 2012.

- [41] "Glossary of Terms Used in NERC Reliability Standards," NERC, 2014.
- [42] A.P. Sanghvi, "Cost-benefit analysis of power system reliability: Determination of interruption costs," Bailly Inc., 1990.
- [43] R. Billinton and R. Allan, *Reliability Evaluation of Power Systems*, New York: Plenum Press, 1996.
- [44] I. S. 762, "Standard Definitions for Use in Reporting Electric Generating Unit Reliability, Availability, and Productivity," IEEE, 2006.
- [45] I. S. 859, "IEEE Standard Terms for Reporting and Analyzing Outage Occurrences and Outage States of Electrical Transmission Facilities," 1987.
- [46] I. S. 1366, "IEEE Guide for Electric Power Distribution Reliability Indices," 2012.
- [47] H. L. Willis, *Power Distribution Planning Reference Book*, New York: Marcel Dekker Inc, 1997.
- [48] P. Hu, R. Karki and R. Billinton, "Reliability evaluation of generating systems containing wind power and energy storage," *Generation, Transmission & Distribution, IET*, vol. 3, no. 8, pp. 783-791, 2009.
- [49] M. Stamatelatos, *Fault Tree Handbook with Aerospace Applications*, Washington DC: NASA, 2002.
- [50] W.E. Vesely, F.F. Goldberg, N.H. Roberts and D.F. Haasl, *Fault Tree Handbook*, Washington DC: U.S. Government Printing, 1981.
- [51] D. H. Stamatis, *Failure Mode and Effect Analysis: FMEA from Theory to*

- Execution, Milwaukee: ASQ, 2003.
- [52] R. J. Mikulak, R. McDermott and M. Beauregard., *The Basics of FMEA*, CRC Press, 2008.
- [53] O.C. Ibe, *Markov Processes for Stochastic Modeling*, Elsevier, 2009.
- [54] H. Ge, *Maintenance optimization for substations with aging equipment*, Lincoln: University of Nebraska-Lincoln, 2010.
- [55] Billinton and Allan, *Reliability Assessment of Large Electric Power Systems*, Kluwer Academic Publishers, 1988.
- [56] L. d. M. Carvalho, *Advances on the Sequential Monte Carlo Reliability Assessment of Generation-Transmission Systems using Cross-Entropy and Population-based Methods*, Porto: University of Porto, 2013.
- [57] R. Billinton and W. Li, *Reliability assessment of electric power system using Monte Carlo methods*, New York: Plenum Press, 1994.
- [58] N. Hatziargyriou, H. Asano, R. Iravani and C. Marnay, "Microgrids, an overview of ongoing research, development, and demonstration projects," *IEEE Power and Energy Magazine*, pp. 78-94, 2007.
- [59] "What the Smart Grid Means to Americans," U.S. Department of Energy, 2009.
- [60] Y. M. Atwa, E. F. El-Saadany, M. M. A. Salama and R. Seethapathy, "Optimal Renewable Resources Mix for Distribution System Energy Loss Minimization," *IEEE Trans. on Power Systems*, vol. 25, no. 1, 2010.
- [61] "Decentralised storage: impact on future distribution grids," EURELECTRIC,

Smart Grid Task Force, 2012.

- [62] "The Impact of Control Technology: Control for Renewable Energy and Smart Grids," IEEE Control Systems Society, 2011.
- [63] SGTF, "Reliability Considerations from the Integration of Smart Grid," NERC, 2010.
- [64] A. Nourai, "Installation Of The First Distributed Energy Storage System (DESS) At American Electric Power (AEP)," Sandia National Laboratories, 2007.
- [65] J. Eto, "The Past, Present, and Future of U.S. Utility Demand-Side Management Programs," Ernest Orlando Lawrence Berkeley National Laboratory, 1996.
- [66] C. W. Gellings and W. M. Smith, "Integrating Demand Side Management into Utility Planning," *Proc. of the IEEE invited paper*, vol. 77, no. 6, pp. 908-918, 1989.
- [67] R. Billinton and D. Lakhanpal, "Impacts of demand side management on reliability cost/reliability worth analysis," *IEE Proc. Generation, Transmission, Distribution*, vol. 143, no. 3, pp. 225-231, 1996.
- [68] Tech-wise A/S and DM Energy, "Wind Turbine Grid Connection and Interaction," Deutsches Windenergie-Institut GmbH, 2001.
- [69] T. Manco and A. Tesla, "A Markovian Approach to Model Power Availability of a Wind Turbine," *IEEE Power Tech*, pp. 1256-1261, 2007.
- [70] S. Kahrobaee and S. Asgarpoor, "Short and long-term reliability assessment of wind farms," in *North American Power Symposium*, Arlington, 2010.

- [71] J. A. Andrawus, J. Watson and Mohammed Kishk, "Modelling system failures to optimise wind turbine maintenance," *Wind Energy*, vol. 31, no. 6, pp. 503-522, 2007.
- [72] H. Li and Z. Chen, "Overview of different wind generator systems and their comparisons," *Renewable Power Generation IET*, vol. 2, no. 2, pp. 123-138, 2008.
- [73] J. Peinke, P. Schaumann and S. Barth, *Wind energy: proceedings of the Euromech colloquium*, Springer, 2007.
- [74] P. J. Tavner, A Higgins, H. Arabian, H. Long and Y. Feng, "Using An FMEA Method to Compare Prospective Wind Turbine Design Reliabilities," in *European Wind Energy Conference (EWEC 2010)*, 2010.
- [75] A. Hassan, I. Dayarian, A. Siadat and J. Dantan, "Cost-based FMEA and ABC concepts for manufacturing process plan evaluation," in *IEEE Conference on Cybernetics and Intelligent Systems*, 2008.
- [76] C. M. Spencer and S. J. Rhee, "Cost based failure modes and effects analysis (FMEA) for systems of accelerator magnets," in *Particle Accelerator Conference*, 2003.
- [77] S.Kahrobaee and S.Asgarpoor, "Risk-Based Failure Mode and Effect Analysis for wind turbines (RB-FMEA)," in *North American Power Symposium*, 2011.
- [78] E. Echavarria, B. Hahn, G. J. W. van Bussel and T. Tomiyama, "Reliability of wind turbine technology through time. *Journal of Solar Energy Engineering*," vol. 130, no. 3, 2008.

- [79] J. Ribrant and L. Bertling, "Survey of failures in wind power systems with focus on Swedish wind power plants during 1997-2005," in *IEEE Power Engineering Society General Meeting*, 2007.
- [80] R. E. Abdel-Aal, "Short-Term Hourly Load Forecasting Using Abductive Networks," *IEEE Trans. on Power Systems*, vol. 19, no. 1, pp. 164-173, 2004.
- [81] Z. Yun, Z. Quan, S. Caixin, L. Shaolan and L. Yuming, "RBF Neural Network and ANFIS-Based Short-Term Load Forecasting Approach in Real-Time Price Environment," *IEEE Trans. on Power Systems*, vol. 23, no. 3, pp. 853-858, 2008.
- [82] R.J.Hyndman and Shu Fan, "Density Forecasting for Long-Term Peak Electricity Demand," *IEEE Trans. on Power Systems*, vol. 25, no. 2, pp. 1142-1153, 2010.
- [83] G.J.Anders, *Probability Concepts in Electric Power Systems*, Wiley Interscience Publication, 1989.
- [84] W.L.Winston, *Introduction to Probability Models Vol. 2 : Operations Research*, 2003.
- [85] "Rockwell Arena," [Online]. Available: <http://www.arenasimulation.com>. [Accessed 2014].
- [86] J. S. C. (JSC), "Mean Time to Repair Predictions," [Online]. Available: <http://oce.jpl.nasa.gov/practices/at2.pdf>. [Accessed 2014].
- [87] A. R-Ghahnavie and F-Firusabad, "Application of Markov decision process in generating units maintenance scheduling," in *International Conference on Probabilistic Methods Applied to Power Systems*, 2006.

- [88] T. M. Welte, J. Vatn and J. Heggset, "Markov state model for optimization of maintenance and renewal of hydro power components," in *9th International Conference on Probabilistic Methods Applied to Power Systems*, Stockholm, 2006.
- [89] H. Ge and S. Asgarpoor, "Reliability and maintainability improvement of substations with aging infrastructure," *IEEE Trans. on Power Delivery*, vol. 27, pp. 1868-1876, 2012.
- [90] Y. R. Wu and H. S Zhao, "Optimization maintenance of wind turbines using Markov decision processes," in *International Conference on Power System Technology*, 2010.
- [91] E. Byon, L. Ntamino and Y. Ding, "Optimal maintenance strategies for wind turbine under stochastic weather conditions," *IEEE Transactions on Reliability*, vol. 59, 2010.
- [92] C. L. Tomasevicz and S. Asgarpoor, "Optimum maintenance policy using semi-markov decision process," in *38th North American Power Symp.*, 2006.
- [93] H. Ge, C. L. Tomasevicz and S. Asgarpoor, "Optimum maintenance policy with inspection by semi-Markov decision processes," in *39th North American Power Symp*, 2007.
- [94] S. V. Amari, L. McLaughlin and H. Pham, "Cost-effective condition based maintenance using Markov decision processes," in *Annual Reliability and maintainab. Symp.*, 2006.
- [95] Y. Haung and X. Guo, "Finite horizon semi-Markov decision processes with

- application to maintenance systems," *European Journal of Operational Research*, vol. 212, pp. 131-140, 2011.
- [96] S. G. Gedam, "Optimizing R&M performance of a system using Monte Carlo simulation," in *Annual Reliability and Maintainab. Symp.* , 2012.
- [97] P. Hilber, *Maintenance optimization for power distribution systems*, Stockholm: KTH Royal Institute of Technology, 2008.
- [98] G. Lanza, S. Niggenschmidt and P. Werner, "Behavior of dynamic preventive maintenance optimization for machine tools," in *Annual Reliability and Maintainab. Symp.* , 2009.
- [99] E. Zheng, Y. Li, B. Wang and J. Wu, "Maintenance optimization of generating equipment based on a condition-based maintenance policy for multi-unit systems," in *Chinese Control and Decision Conference*, 2009.
- [100] G. J. Anders and A. M. L. Silva, "Cost related reliability measures for power system equipment," *IEEE Trans. on Power Systems* , vol. 15, pp. 654-660, 2000.
- [101] R. A. Howard, *Dynamic probabilistic systems, semi-Markov and decision processes*, vol. 2, John Wiley & Sons, 1971.
- [102] A. Mohsenian-Rad and A. Leon-Garcia, "Optimal Residential Load Control With Price Prediction in Real-Time Electricity Pricing En-vironments," *IEEE Trans. on Smart Grid*, vol. 1, no. 3, pp. 120-133, 2010.
- [103] A. Mohsenian-Rad, V.W.S. Wong, J. Jatskevich, R. Schober and A. Leon-Garcia, "Autonomous Demand-Side Management Based on Game-Theoretic Energy

- Consumption Scheduling for the Future Smart Grid," *IEEE Trans. on Smart Grid*, vol. 1, no. 3, pp. 320-331, 2010.
- [104] G. Xiong, C. Chen and S. Kishore, "Smart (In-home) Power Scheduling for Demand Response on the Smart Grid," in *IEEE Innovative Smart Grid Technologies (ISGT)*, 2011.
- [105] S. Shao, M. Pipattanasomporn and S. Rahman, "An Approach for Demand Response to Alleviate Power System Stress Conditions," in *IEEE Power & Energy Society General Meeting*, 2011.
- [106] A.J. Conejo, J.M. Morales and L. Baringo, "Real-Time Demand Response Model," *IEEE Trans. on Smart Grid*, vol. 1, no. 3, pp. 236-242, 2010.
- [107] S. Ramchurn, P. Vytelingum, A. Rogers and N. Rjennings, "Putting the Smarts into the Smart Grid: A Grand Challenge for Artificial Intelligence," *Communications of the ACM*, vol. 55, no. 4, pp. 86-97, 2012.
- [108] M. Rahimiyan and H.R. Mashhadi, "An adaptive Q-learning developed for agent-based computational modeling of electricity market," *IEEE Trans. Syst, Man, Cybern. C, Appl. Rev.*, vol. 40, pp. 547-556, 2010.
- [109] Z. Zhou, F. Zhao and J. Wang, "Agent-Based Electricity Market Simulation With Demand Response From Commercial Buildings," *IEEE Transactions on Smart Grid*, vol. 2, no. 4, pp. 580-588, 2011.
- [110] A.A. Aquino-Lugo, Ray Klump and T.J. Overbye, "A Control Framework for the Smart Grid for Voltage Support Using Agent-Based Technologies," *IEEE*

- Transactions on Smart Grid*, vol. 2, no. 1, pp. 173-180, 2011.
- [111] Y. Xu and W. Liu, "Novel Multiagent Based Load Restoration Algorithm for Microgrids," *IEEE Transactions on Smart Grid*, vol. 2, no. 1, pp. 152-161, 2011.
- [112] Y. Xu, W. Liu and J. Gong, "Stable Multi-Agent-Based Load Shedding Algorithm for Power Systems," *IEEE Transactions on Power Systems*, vol. 26, no. 4, 2011.
- [113] M. Pipattanasomporn, H. Feroze and S. Rahman, "Multi-Agent Systems in a Distributed Smart Grid: Design and Implementation," in *IEEE Power Systems Conference and Exposition*, 2009.
- [114] S. Ramchurn, P. Vytelingum, A. Rogers and N.R. Jennings, "Agent-based homeostatic control for green energy in the smart grid," *ACM Transactions on Intelligent Systems and Technology*, 2011.
- [115] R. Roche, B. Blunier, A. Miraoui, V. Hilaire and A. Koukam, "Multi-Agent Systems For Grid Energy Management: A Short Review," in *36th Annual Conference on IEEE Industrial Electronics Society*, 2010.
- [116] S.D. Ramchurn, P. Vytelingum, A. Rogers and N.R. Jennings, "Agent-based control for decentralized demand side management in the smart grid," in *10th Intl. Conf. on Autonomous Agents and Multiagent Systems*, 2011.
- [117] "Repast Symphony," [Online]. Available: <http://repast.sourceforge.net/>. [Accessed 2014].
- [118] C. M. Macal and M. J. North, "Agent-based Modeling and Simulation," in *Proceedings of the 2009 Winter Simulation Conference*, Austin, 2009.

- [119] P. Vytelingum, T.D. Voice, S.D. Ramchurn, A. Rogers and N.R. Jennings, "Agent-Based Micro-Storage Management for the Smart Grid," in *Autonomous Agents and Multiagent Systems (AAMAS)*, 2010.
- [120] S.Kahrobaee, R.A.Rajabzadeh, L.K.Soh and S.Asgarpoor, "Multiagent study of smart grid customers with neighborhood electricity trading," *Electric power System Research*, vol. 111, p. 123–132, 2014.
- [121] S. Kahrobaee, S. Asgarpoor and W. Qiao, "Optimum Sizing of Distributed Generation and Storage Capacity in Smart Households," *IEEE Trans. on Smart Grid*, vol. 4, pp. 1791-1801, 2013.
- [122] W. R. Powell, "An analytical expression for the average output power of a wind machine," *Solar Energy*, vol. 26, pp. 77-80, 1981.
- [123] B.Parida, S.Iniyan and R.Goic, "A review of solar photovoltaic technologies," *Renewable & Sustain. Energy Reviews*, vol. 15, pp. 1625-1636, 2011.
- [124] J. Park, W. Liang, J. Choi, A. A. El-Keib, M. Shahidehpour and R. Billinton, "A Probabilistic Reliability Evaluation of A Power System Including Solar/Photovoltaic Cell Generator," in *IEEE Power & Energy GM*, 2009.
- [125] S. Kahrobaee, R. Rajabzadeh, L.K. Soh and S. Asgarpoor, "A Multiagent Modeling and Investigation of Smart Homes with Power Generation, Storage, and Trading Features," *IEEE Trans. Smart Grid*, vol. 4, pp. 659-668, 2013.
- [126] M. Roozbehani, M. A. Dahleh and S.K. Mitter, "Volatility of power grids under real-time pricing," *IEEE Trans. Power Systems*, vol. 27, no. 4, pp. 1926-1940,

2012.

- [127] J. Wiedman, T. Culley, S. Chapman, R. Jackson, L. Varnado and J. Rose, "Freeing the Grid: Best and Worst Practices in State Net Metering Policies and Interconnection Procedures," The Vote Solar Initiative, and Network for New Energy Choices, 2011.
- [128] "Small Wind Guidebook, Wind for Homeowners, Farmers, and Businesses," U.S. Department of Energy, [Online]. Available: http://www.windpoweringamerica.gov/small_wind.asp. [Accessed 2014].
- [129] "Electricity rates provided by Ameren Illinois for Zone1 customers," Ameren Illinois, [Online]. Available: <http://www.ameren.com/Pages/JumpPage.aspx>. [Accessed 2012].
- [130] U. E. I. Administration, "Residential consumption of electricity by end use," 2001. [Online]. Available: <http://www.eia.gov>. [Accessed 2012].
- [131] E. Consultants, "The Impact of Commercial and Residential Sectors' EEIs on Electricity Demand," Sustainable Energy Authority of Victoria, 2004.
- [132] S. Schoenung, "Energy storage systems cost update, A study for the DOE energy storage systems program," Sandia National Laboratories, 2011.
- [133] M. M. Armstronga, M. C. Swintona, H. Ribberinkb, I.B. Morrisonc and J. Milletted, "Synthetically Derived Profiles for Representing Occupant-Driven Electric Loads in Canadian Housing," *Journal of Building Performance Simulation*, vol. 2, no. 1, 2009.

- [134] C. Pang, M. Kezunovic and M. Ehsani, "Demand Side Management by using Electric Vehicles as Distributed Energy Resource," in *IEEE International Electric Vehicle Conference (IEVC)*, 2012.
- [135] I. Hernando-Gil, I.S. Ilie and S. Z. Djokic, "Reliability Performance of Smart Grids with Demand-side Management and Distributed Generation/Storage Technologies," in *IEEE PES Innovative Smart Grid Technologies Europe (ISGT Europe)*, 2012.
- [136] D. Huang, R. Billinton and W. Wangdee, "Effects of Demand Side Management on Bulk System Adequacy Evaluation," in *International Conference on Probabilistic Methods Applied to Power Systems (PMAPS)*, 2010.
- [137] D. Huang and R. Billinton, "Effects of Load Sector Demand Side Management Applications in Generating Capacity Adequacy Assessment," *IEEE Trans. on Power Systems*, vol. 27, no. 1, 2012.
- [138] S. Mohagheghi, F. Yang and B. Falahati, "Impact of Demand Response on Distribution System Reliability," in *IEEE PES General Meeting*, 2011.
- [139] S. Kahrobaee and S. Asgarpoor, "The effect of demand side management on reliability of automated distribution systems," in *Sustech conference*, 2013.
- [140] R. Angelino, G. Carpinelli, D. Proto and A. Bracale, "Dispersed Generation and Storage Systems for Providing Ancillary Services in Distribution Systems," in *IEEE International Symposium on Power Electronics Electrical Drives Automation and Motion*, 2010.
- [141] A. Karpati, G. Zsigmond, M. Voros and M. Lendvay, "Uninterruptible Power

- Supplies (UPS) for Data Center," in *IEEE 10th Jubilee International Symposium on Intelligent Systems and Informatics*, 2012.
- [142] I. Hussain and A. K. Roy, "Optimal Size and Location of Distributed Generations using Differential Evolution (DE)," in *CISP2012*, 2012.
- [143] J.M. Gantz, S. Massoud-Amin and A.M. Giacomoni, "Optimal Mix and Placement of Energy Storage Systems in Power Distribution Networks for Reduced Outage Costs," in *IEEE Energy Conversion Congress and Exposition*, 2012.
- [144] H. Zhang, J. Liu and W. Li, "Optimized Design of Energy Storage Capacity for Wind Power Generating," in *Power and Energy Engineering Conference (APPEEC)*, 2012.
- [145] Y. Ru, J. Kleissl and S. Martinez, "Storage Size Determination for Grid-Connected Photovoltaic Systems," *IEEE Trans. on Sustainable Energy*, vol. 4, no. 1, 2013.
- [146] J. Mitra, "Reliability-Based Sizing of Backup Storage," *IEEE Trans. on Power Systems*, vol. 25, no. 2, 2010.
- [147] Y. Xu and C. Singh, "Distribution Systems Reliability and Economic Improvement with Different Electric Energy Storage Control Strategies," in *IEEE Power and Energy Society General Meeting*, 2011.
- [148] S. Kahrobaee and S. Asgarpoor, "Reliability-driven optimum standby electric storage allocation for power distribution systems," in *Sustech*, 2013.
- [149] R.C. Eberhart and Y. Shi, "particle swarm optimization: developments, applications and resources," in *Congress on Evolutionary Computation*, 2001.

- [150] D. Sedighzadeh and E. Masehian, "Particle swarm optimization methods, taxonomy and applications," *International Journal of Computer Theory and Engineering*, vol. 1, no. 5, pp. 486-502, 2009.
- [151] H. A. Hoseynabadi, H. Oraee and P.J. Tavner, "Failure modes and effects analysis (FMEA) for wind turbines," *International Journal of Electrical Power & Energy Systems*, vol. 32, no. 7, p. 817, 2010.
- [152] "Mean Wind Project at Kimball," [Online]. Available: <http://www.neo.ne.gov/statshtml/89.htm>. [Accessed 2014].
- [153] R. Poore and C. Walford, "Development of an Operations and Maintenance Cost Model to Identify Cost of Energy Savings for Low Wind Speed Turbines," NREL/SR-500-40581, 2008.
- [154] D. Anair and A. Mahmassani, "State of charge, Electric Vehicles' Global Warming Emissions and Fuel-Cost Savings across the United States," Union of Concerned Scientists, 2012.
- [155] K. Cory and P. Schwabe, "Wind leveled cost of energy: A comparison of technical and financing input variables," NREL/TP-6A2-46671, 2009.
- [156] "Historical data of hourly wind speed measured by Kimball (KIBM) airport weather station," [Online]. Available: www.wunderground.com.
- [157] W.B. Wan, M.Z. Ibrahim, K.B. Samo and A.M. Muzathik, "Monthly mean hourly global solar radiation estimation," *Solar Energy*, p. 379–387, 2012.
- [158] "Southern California Edison Load Profiles, Regulatory Information," [Online].

Available: www.sce.com/AboutSCE/Regulatory/loadprofiles/loadprofiles.htm.

- [159] M. J. Sullivan, M. Mercurio and J. Schellenberg, "Estimated Value of Service Reliability for Electric Utility Customers in the United States," Ernest Orlando Lawrence Berkeley National Laboratory, 2009.
- [160] J. Giraldez, S. Booth, K. Anderson and K. Massey, "Valuing Energy Security: Customer Damage Function Methodology and Case Studies at DoD Installations," NREL/TP-7A30-55913, 2012.